UNIVERSIDADE FEDERAL DE SANTA CATARINA
CENTRO DE CIÊNCIAS DA SAÚDE
PROGRAMA DE PÓS-GRADUAÇÃO EM FARMÁCIA

NANOCARREADORES LIPÍDICOS CONTENDO QUERCETINA: DESENVOLVIMENTO, CARACTERIZAÇÃO FÍSICO-QUÍMICA E AVALIAÇÃO BIOLÓGICA *IN VIVO*

CRISTIANA LIMA DORA

Florianópolis
2010

UNIVERSIDADE FEDERAL DE SANTA CATARINA
CENTRO DE CIÊNCIAS DA SAÚDE
PROGRAMA DE PÓS-GRADUAÇÃO EM FARMÁCIA

NANOCARREADORES LIPÍDICOS CONTENDO QUERCETINA: DESENVOLVIMENTO, CARACTERIZAÇÃO FÍSICO-QUÍMICA E AVALIAÇÃO BIOLÓGICA *IN VIVO*

Tese apresentada ao Programa de Pós-Graduação em Farmácia como requisito parcial à obtenção do grau de DOUTOR em Farmácia

Orientação:
Profa. Dra. Elenara Lemos Senna (Brasil)
Prof. Dr. Redouane Borsali (França)

CRISTIANA LIMA DORA

Florianópolis
2010

Catalogação na fonte pela Biblioteca Universitária
da
Universidade Federal de Santa Catarina

D693n Dora, Cristiana Lima
Nanocarreadores lipídicos contendo quercetina [tese] : desenvolvimento, caracterização físico-química e avaliação biológica in vivo / Cristiana Lima Dora ; orientadores, Elenara Maria Teixeira Lemos Senna, Redouane Borsali. – Florianópolis, SC, 2010.
231 p.: il., grafs., tabs.

Tese (doutorado) - Universidade Federal de Santa Catarina, Centro de Ciências da Saúde. Programa de Pós-Graduação em Farmácia.

Inclui referências

1. Farmácia. 2. Quercetina. 3. Microemulsão. 4. Asma. 5. Melanoma. I. Senna, Elenara Maria Teixeira Lemos. II. Borsali, Redouane. III. Universidade Federal de Santa Catarina. Programa de Pós-Graduação em Farmácia. IV. Título.

CDU 615.12

DEDICATÓRIA

Para meus queridos irmãos, Adriana e Luiz Francisco,
pelo incentivo, apoio e amizade
e por me ajudarem a vencer os momentos difíceis
através do seu carinho, seu exemplo e sua coragem
Amo vocês!

"...todas as substâncias são
venenos, não existe nenhuma que
não seja. A dose correta diferencia
um remédio de um veneno".
Paracelsus

AGRADECIMENTOS

À Prof. Dra. Elenara Lemos Senna pela orientação, amizade, dedicação, oportunidades e compreensão em todos os momentos.

Ao Prof. Dr. Redouane Borsali pela orientação, amizade e apoio durante a estadia na França.

Ao Prof. Dr. Jean Luc Putaux pela amizade, apoio e pela grande ajuda prestada para realização dos experimentos na França.

À Isabelle e Sonia pela colaboração e amizade.

Ao Prof. Dr. Jamil Assreuy, Profa. Dra. Maria Claudia Santos Silva e Prof. Dr. Valdir Soldi pelos ensinamentos, contribuições e disponibilidade para realização deste trabalho.

Aos funcionários do Departamento de Ciências Farmacêuticas, em especial a Sandra, Nilson e Solange pela ajuda fornecida durante a realização dos ensaios.

Aos amigos e colegas do curso, Daia, Taty, Geci, Dani, Ju, Carine, Le, Mari, Bianca, Georgia, Alexandre, Jarbas, Daniel, Letícia, Juliana e Mariana pelo companheirismo, colaboração e pelos bons momentos compartilhados durante o desenvolvimento deste trabalho. Um agradecimento especial ao Luis, meu braço direito e esquerdo, por toda ajuda e dedicação e por estar sempre disposto a colaborar.

Aos meus amigos de toda vida, que me acompanham onde quer que eu esteja e se fizeram presentes em algum momento desta caminhada e especialmente as minhas amigas de coração Vanessa B., Karen, Va, Paula, Ligia, Dani, Roberta, Kaká, Carol e Kika.

A minha família francesa, Didi, Rachinha, Karol, Eltinho e Windson por terem tornado a minha estadia na França um dos momentos mais importantes da minha vida.

Aos meus pais, que mesmo não estando mais presentes, me ensinaram a lutar pelos meus sonhos.

À minha família e meus sobrinhos lindos, Lilica, Gabidu, Lucas e Henrique pelo amor e incentivo.

Aos meus padrinhos, Cely e Fuscaldo, por tudo, meus exemplos de vida.

Ao órgão Financiador CAPES.

A todos que mesmo não citados, colaboraram para a realização deste trabalho.

MUITO OBRIGADA!

RESUMO

A quercetina (QU) é um polifenol pertencente à classe dos flavonóides, presente na dieta humana. Esta substância tem demonstrado inúmeras atividades farmacológicas incluindo antitumoral, antiinflamatória, antioxidante, entre outras. Entretanto, a biodisponibilidade oral desta substância é limitada, em decorrência do seu elevado metabolismo colônico e hepático e da sua baixa solubilidade aquosa. Desta forma, a incorporação da quercetina em sistemas de liberação de fármacos pode ser considerada uma alternativa promissora para administração oral deste composto. Neste trabalho, nanopartículas sólidas lipídicas (NLS), carreadores lipídicos nanoestruturados (NLC), nanoemulsões (NE) e microemulsões (ME) foram preparadas pela técnica de difusão do solvente a quente, variando apenas os componentes da formulação. As características físico-químicas, estruturais e morfológicas dos nanocarreadores foram estudadas e correlacionadas com a capacidade dos mesmos em encapsular e liberar a QU. Além disso, a estabilidade da ME em fluidos gastro-intestinais foi avaliada, assim como a sua atividade antiinflamatória, em modelo de asma alérgica, e antitumoral, em modelo de melanoma subcutâneo B16F10. O tamanho médio das partículas foi aproximadamente de 340, 220, 145 e 20 nm, para as SLNs, NLCs, NEs e MEs, respectivamente. As preparações apresentaram potencial zeta negativo ou carga próxima à zero, no caso da ME, em função da estabilização estérica provocada pelo polietilenoglicol (PEG) presente no surfactante utilizado neste caso. Elevados valores de eficiência de encapsulação foram obtidos para todas as formulações testadas. Entretanto, o teor de QU variou significativamente em função do tipo de nanocarreador e da quantidade de fármaco inicialmente adicionada às formulações. Em especial, a ME apresentou uma maior capacidade de incorporar a QU, aumentando a sua concentração cerca de 1.300 vezes em relação a sua solubilidade aquosa. Os perfis de liberação da QU exibiram uma cinética bifásica, consistindo de uma liberação rápida nas primeiras 8 horas, seguida de uma liberação sustentada durante 24 horas, mas o controle da liberação somente ocorreu em alguns casos. Na análise da avaliação estrutural e morfológica dos nanocarreadores diferentes técnicas foram empregadas, tais como, SAXS, WAXS, DSC, microscopia de luz polarizada, AFM, TEM, e cryo-TEM, dependendo do tipo de nanocarreador estudado. A SLN apresentou formato irregular e angular, na forma de um cristal lamelar. Por outro lado, NLC apresentou um aspecto mais arredondado, mas uma separação de fases

entre o lipídio sólido e líquido foi constatada, indicando que o sistema não é homogêneo. Nestas partículas foi verificada a formação do polimorfo mais estável, β-triestearina. Ambas NE e ME apresentaram formato esférico e foi verificado que a estrutura da partícula da ME é do tipo núcleo-casca. Estudos de avaliação da estabilidade da ME em fluídos gastro-intestinais verificaram que este sistema se mantém estável nos fluidos gástricos e que sua digestão ocorre nos fluidos intestinais quando a enzima lipase está presente. As avaliações da atividade antiinflamatória e antitumoral indicaram que a microemulsão contendo QU inibiu os principais mediadores da resposta inflamatória, assim como o crescimento tumoral, o que não foi observado quando a QU foi administrada na sua forma livre. Além disso, a análise do sangue de ratos tratados com QU livre e QU-ME por HPLC-EM, demonstrou que um íon relacionado a algum metabolito da QU foi detectado somente nas amostras extraídas dos animais tratados com QU-ME. Esses resultados indicam que a incorporação de quercetina nas microemulsões aumentou significantemente a biodisponibilidade oral deste composto e conseqüentemente seu efeito farmacológico pode ser alcançado.

Palavras-chaves: quercetina, sistemas nanocarreadores lipídicos, microemulsão, asma, melanoma.

ABSTRACT

Quercetin (QU) is a polyphenol belonging to the class of flavonoids, present in the human diet. This substance has shown several pharmacological activities, including among others antitumor, anti-inflammatory, and antioxidant. However, the oral bioavailability of this compound is very low due to the high pre-systemic metabolism in the colon and liver and its low water solubility. In this context, the development of quercetin-loaded nanocarriers can be considered an interesting approach to improve the oral bioavailability of QU and to take advantage of its therapeutic properties in the clinical setting. In this work, solid lipid nanoparticles (SLN), nanostrutured lipid carriers (NLC), nanoemulsions (NE) and microemulsions (ME) containing QU were prepared by the hot solvent diffusion method, varying only in formulation composition. The structural, morphological and physic-chemistry characteristics of the nanocarriers were evaluated and correlated with the ability of the colloidal suspensions into incorporate QU, as well as to release this drug. Besides, the gastro-intestinal stability of ME was tested, and the anti-inflammatory and antitumor activity, in allergic asthma and subcutaneous melanoma models, respectively, in mice. The average particle size was 340, 220, 145 e 20 nm for SLNs, NLCs, NEs and MEs, respectively. The formulations displayed negative zeta potential values or charge near zero, in the case of ME, due to the steric stabilization create by the surfactant used in this case. High values of encapsulation efficiency were obtained for all formulations. However, the drug content was significantly varied, depending on the type of the nanocarrier and amount of drug initially added to the formulations. In particular, ME exhibited greater ability to incorporate QU, increasing its concentration around 1,300 times as compared to its aqueous solubility. The release profiles exhibit biphasic kinetics, with a fast release in the first 8 h, followed by a sustained release for 24 h, but the release control only was observed for some cases. In the structural and morphological analysis several techniques were employed, as SAXS, WAXS, DSC, light polarized microscopy, AFM, TEM, and cryo-TEM, depending of the type of nanocarrier evaluated. For SLN a lamellar crystal with irregular and angular shapes was observed. On the other rand, NLC was visualized with shapes more spheroidals, but a phase separation between both lipids, solid and liquid was observed, and therefore this system was not homogeneous. In addition, in SLN and NLC was detected the formation of the more stable β-triestearin polymorph. In the analysis of NE and ME, spheroidal

particles were observed and a core-shell structure was determined for ME. The results of the stability studies in gastro-intestinal fluids indicated that ME is stable in gastric medium and that the nanocarrier digestion occurs in the intestinal medium with the presence of the enzyme lipase. The evaluation of the anti-inflammatory and antitumor activity indicated that QU-ME was able to inhibit the mediators of inflammatory response, as well as the tumor growth, and these results were not observed when free QU was tested. Besides, the blood analysis of rats treated with free QU and QU-ME asses by HPLC-MS, showed the presence of an ion related to a QU metabolite only when the blood extracted from rats treat with QU-ME was assayed. These results indicate that the incorporation of quercetin in microemulsions enhances significantly the oral bioavailability of this compound and therefore its pharmacological effect could be achieved.

Keywords: quercetin, lipid-based nanocarriers, microemulsion, asthma, melanoma.

LISTA DE FIGURAS

Capítulo 1. Revisão da literatura

Capítulo 2. Desenvolvimento dos nanocarreadores lipídicos e avaliação da sua capacidade de incorporação de quercetina

Capítulo 3. Caracterização estrutural e físico-química dos nanocarreadores lipídicos

Publicação 2. Poly (ethylene glycol) hydroxystearate-based nanosized emulsions: Effect of surfactant concentration on their formation and ability to solubilize quercetin

Publicação 3. Structural investigations of lipid-based nanostructured drug delivery systems

Capítulo 4. Investigação da atividade farmacológica da quercetina microemulsionada e da estabilidade da formulação após administração oral

Publicação 6. Poly (ethylene glycol) hydroxystearate/lecithin/castor oil-based microemulsion: investigation of the effect of the gastrointestinal fluids on the droplet size by dynamic light scattering

LISTA DE TABELAS

Capítulo 2. Desenvolvimento dos nanocarreadores lipídicos e avaliação da sua capacidade de incorporação de quercetina

Capítulo 3. Caracterização estrutural e físico-química dos nanocarreadores lipídicos

Publicação 2. Poly (ethylene glycol) hydroxystearate-based nanosized emulsions: Effect of surfactant concentration on their formation and ability to solubilize quercetin

Publicação 3. Structural investigations of lipid-based nanostructured drug delivery systems

Capítulo 4. Investigação da atividade farmacológica da quercetina microemulsionada e da estabilidade da formulação após administração oral

Publicação 6. Poly (ethylene glycol) hydroxystearate/lecithin/castor oil-based microemulsion: investigation of the effect of the gastrointestinal fluids on the droplet size by dynamic light scattering

LISTA DE ABREVIATURAS E SIGLAS

ADN – ácido desoxirribonucléico
AGs – ácidos graxos
ANOVA – análise da variância
ARN – ácido ribonucléico
ASC- área sob a curva
β-CD – Beta-ciclodextrina
CLAE – cromatografia líquida de alta eficiência
CLN – carreadores lipídicos nanoestruturados
CMC-Na – carboxilmetil celulose sódica
CO – óleo de rícino/castor oil
COMT– catecol-*O*-metil transferase
DLS – dinamic light scaterring
DP – desvio padrão
DPPH – difenilpicrilhidrazil
DSC – Calorimetria exploratória diferencial
EE – eficiência de encapsulação
EU – Eudragit
EROS – espécies reativas de oxigênio
GLUT2– tipo transportador de glicose isoforma 2
GMS – monoestearato de glicerila
GSH – glutadiona
HPLC – High Performance Liquid Chromatography
HP-β-CD - hidroxipropril-β-ciclodextrina
HOCl – ácido hipocloroso
HSP 70 – proteína de choque térmico 70
ICH – International Conference on Harmonization
IL– Interleucinas
LOD – limite de detecção
Log P – coeficiente de partição
LOQ – limite de quantificação
ME – microemulsão
MGs – monoglicerídeos
MRP2 – proteína de resistência a múltiplos fármacos 2
NaCl – cloreto de sódio
NE – nanoemulsão
NF-κB – fator nuclear kappa B
NLC – Nanostructured lipid nanocarriers
NLS– nanopartícula lipídica sólida

ONO^-_2 – peroxinitrito
PDI – índice de polidispersão
PEG – polietilenoglicol
PLGA – ácido lático-co-glicólico
QU - quercetina
QU-Glic – quercetina glicosídica
QU-ME – microemulsão contendo quercetina
RSD – relative standard deviation
SAXS – Espalhamento de raios-x a baixos ângulos
SBE-β-CD – sulfobutil éter-β- ciclodextrina
SbPc – hydrogenated soybean phosphatidylcholine
SGLT-1– transportador de glicose dependente de sódio
SLN– Solid Lipid Nanoparticle
ST – sulfotransferase
TEM – transmission electronic microscopy
TG – triglicerídeos
TGI – trato gastro-intestinal
TNFα - fator α de necrose tumoral
TS – triestearina
UGT – uridina-difosfato glicuronosil trasferase
UV – ultravioleta
VCR – vinccristina
WAXS – Espalhamento de raios-x a altos ângulos

SUMÁRIO

Introdução e Objetivos

1.1 Introdução

Compostos polifenólicos naturais e seus análogos constituem um grupo heterogêneo de metabólitos secundários vegetais conhecidos por apresentar várias atividades biológicas. Estes compostos são classificados quimicamente em ácido fenólicos e análogos, estilbenos, flavonóides e um quarto grupo que inclui as cumarinas, lignanos e taninos (FRESCO *et al*., 2006). A quercetina (QU) é o flavonóide polifenólico mais abundante na subclasse dos flavonóis e apresenta a propriedade de formar quelatos sendo, portanto, um potente agente antioxidante no combate de espécies reativas de oxigênio. Além disso, este composto tem sido extensivamente estudado quanto aos seus efeitos farmacológicos, tais como hepatoprotetor, antiinflamatório, antitumoral e antiasmático (INAL e KAHRAMAN, 2000; LEE *et al.,* 2003; COMALADA *et al.,* 2005; ROGÉRIO *et al.,* 2009).

No entanto, um fator importante que influencia a efetividade da interação dos polifenóis com os parâmetros celulares é a sua biodisponibilidade. Muitos estudos mostraram que os compostos fenólicos são extensivamente metabolizados *in vivo*, pela microflora colônica, durante sua passagem pelo intestino, e pelo fígado, resultando na alteração significativa das espécies encontradas na circulação sistêmica (WALLLE *et al.,* 2005; SOOBRATTEE *et al*., 2005). Em particular, a quercetina sofre intensa reação de conjugação, formando compostos glicoronatos e sulfatos que diferem dos seus parentes em tamanho, polaridade e forma iônica (WENZEL e SOMOZA, 2005; KROON *et al.*, 2006). Do ponto de vista biológico, tais reações de conjugação resultam numa mistura de compostos apresentando diferenças significantes no seu potencial redox. Por exemplo, a atividade antioxidante de conjugados de quercetina é, em média, metade daquela da correspondente forma aglicona, e variações existem de acordo com a posição onde ocorre a reação, visto que dois de seus principais metabólitos, quercetina-3'-sulfato e 3'-metil-quercetina-3-glicurônico demonstraram serem completamente ineficazes (JANISCH *et al*., 2004). Além disso, a baixa solubilidade aquosa da quercetina é um fator que limita a absorção. Portanto, estudos realizados *in vitro* não refletem necessariamente o efeito da quercetina *in vivo*.

Atualmente, tem se tornado cada vez mais evidente que a descoberta de novos fármacos não é suficiente para assegurar o sucesso do tratamento de muitas doenças. Problemas relacionados à baixa solubilidade e permeabilidade, rápido metabolismo e eliminação,

distribuição inadequada e toxicidade de muitas substâncias candidatas a fármacos têm levado ao desenvolvimento de sistemas de liberação capazes de contornar tais limitações. Dentre eles destacam-se os sistemas de liberação nanoestruturados (MÄDER e MEHNERT, 2001). Tais sistemas podem ser produzidos com diferentes tipos de materiais, mas possuem como característica comum, seu tamanho submicrométrico (< 1 μm).

Vários materiais poliméricos têm sido usados para a preparação de suspensões coloidais de nanopartículas. Entretanto, em meados dos anos 90, a atenção de diferentes grupos de pesquisa voltou-se à obtenção de nanocarreadores lipídicos, como alternativa frente às desvantagens apresentadas pelas nanopartículas poliméricas. Suas principais vantagens frente aos nanocarreadores poliméricos são a excelente biocompatibilidade e tolerabilidade, além de não apresentarem problemas relacionados à produção em larga escala e à esterilização (WANG *et al*., 2002; WISSING *et al.,* 2004; MANJUNATH *et al*., 2005).

Os nanocarreadores lipídicos são constituídos por lipídios sólidos ou líquidos, ou mistura destes, podendo ser classificados em sistemas matriciais ou reservatórios e obtidos em diferentes faixas de tamanhos de partícula, de cerca de alguns nanômetros até algumas centenas de nanômetros, dependendo da composição da formulação e da técnica de preparação. Tais sistemas se caracterizam pela capacidade em carrear compostos ativos, protegendo-os da degradação após administração, fazendo com que maiores concentrações de fármacos alcancem o sítio de ação, além de permitir o controle da liberação e a redução dos efeitos colaterais indesejáveis. Esses sistemas ainda melhoram a solubilidade de fármacos lipofílicos em água e os protegem contra hidrólise enzimática, além de aumentar o potencial de absorção devido à presença de tensoativos na formulação (PURI *et al.,* 2009).

Nas últimas décadas, a utilização de nanocarreadores lipídicos tem emergido como uma importante estratégia para o aumento da biodisponibilidade oral de fármacos hidrofóbicos. Os mecanismos de aumento da biodisponibilidade envolvem a solubilização dos mesmos em espécies coloidais, que possuem a vantagem de apresentar os fármacos em uma forma dissolvida com uma elevada superfície de contato para absorção. Além disso, o tamanho reduzido das partículas oferece elevada área superficial para a hidrólise dos lipídios pela lípase pancreática, além de proporcionar o aumento da velocidade de liberação

de fármacos e/ou da geração de micelas mistas contendo o mesmo (CHAKRABORTY *et al.,* 2009).

Dentro deste contexto, o presente trabalho teve como objetivo desenvolver nanocarreadores lipídicos contendo quercetina, na busca do aproveitamento do seu potencial terapêutico, quando a via oral é utilizada. Nanocarreadores lipídicos constituídos de nanopartículas lipídicas sólidas, carreadores lipídicos nanoestruturados, nanoemulsões e microemulsões contendo quercetina foram preparados e caracterizados. Igualmente, o efeito da associação da quercetina a nanocarreadores lipídicos sobre a atividade antiasmática e antitumoral *in vivo* foi avaliado.

1.2 Objetivos

Geral:

Desenvolver nanocarreadores lipídicos contendo quercetina, na busca da melhoria das suas propriedades biofarmacêuticas e da sua eficácia terapêutica, após administração oral.

Específicos:

- Preparar sistemas nanocarreadores lipídicos contendo quercetina e caracterizar estes sistemas quanto à estrutura, tamanho, morfologia, eficiência de encapsulação e teor de fármaco.
- Desenvolver e validar métodos de cromatografia líquida de alta eficiência (CLAE) e espectroscopia ultra-violeta (UV) para doseamento da quercetina.
- Estudar o efeito da composição das formulações sobre as características estruturais das partículas e sobre o potencial para incorporação da quercetina.
- Avaliar os perfis de liberação da quercetina a partir dos nanocarreadores.
- Avaliar o efeito da incorporação da quercetina em microemulsões sobre a atividade antiinflamatória *in vivo* em modelo de asma alérgica em camundongos.
- Avaliar o efeito da incorporação da quercetina em microemulsões sobre a atividade antitumoral *in vivo* em modelo de melanoma murino B16F10 subcutâneo.

- Avaliar a estabilidade *in vitro* da microemulsão de quercetina em meios gastro-intestinais simulados e biorrelevantes pela técnica de espalhamento de luz dinâmico.

Capítulo 1

2.1 Quercetina

2.1.1 Características químicas e físico-químicas

Os flavonóides (flavonas, flavonóis, isoflavonas, catequinas, flavanonas e chalconas) constituem uma importante classe de polifenóis, presentes em abundância entre os metabólitos secundários vegetais. Apresentam um núcleo fundamental com 15 átomos de carbono, formado por dois anéis aromáticos ligados entre si por uma cadeia de três átomos de carbono (C_2-C_3-C_4) (Figura 1). Estes compostos, em geral, diferem entre si pelo número e pela posição dos grupos substituintes nos anéis A, B e C, e pela presença ou não de ligação dupla e carbonila no anel C (ZUANAZZI e MONTANHA, 2003).

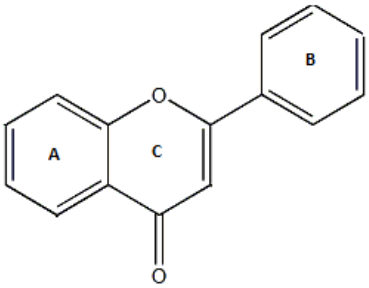

Figura 1. Estrutura geral dos flavonóides.

Em especial, a quercetina (3, 3´, 4', 5, 7-pentahidroxi-flavona) (Figura 2A) é o principal flavonol encontrado na nossa dieta e em função do seu interesse químico e propriedades biológicas, é um dos flavonóides mais estudados. Ela encontra-se principalmente na forma de glicosídeo (Figura 1B) em uma ampla variedade de plantas e alimentos, como cebolas roxa, uvas, maçãs, cerejas, brócolis, frutas cítricas, alcaparras, e produtos derivados destes como sucos, chás e vinhos (HERTOG *et al*., 1995; BOOTS *et al.,* 2008).

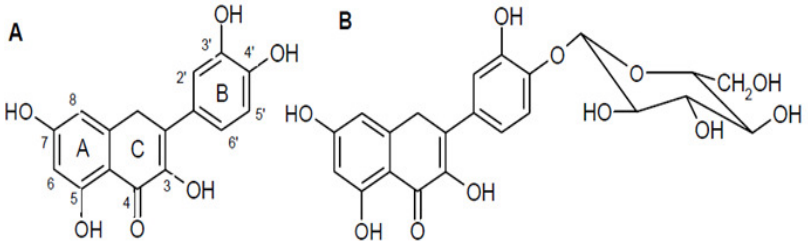

Figura 2. Estrutura química da quercetina (A) e da quercetina 4´-β-D-Glucosídeo (B).

A quercetina apresenta-se como um pó amarelo-alaranjado, com fórmula molecular $C_{15}H_{10}O_7$ e peso molecular de 302,24 g/mol para a forma anidra e de 338,27g/mol para a forma diidratada. Ela torna-se anidra na faixa de temperatura de 93 a 97°C e decompõe-se a 314°C. Em relação à solubilidade, este composto é praticamente insolúvel em água (cerca de 0,30-0,70 µg/mL), sendo mais solúvel em etanol a frio (3,45 µg/mL) e a quente (43,48 µg/mL) (BUDAVARI, 1996). Além disso, estudos realizados por Borghetti e colaboradores (2006), de caracterização física química e morfológica de quatro amostras comerciais de quercetina, demonstraram propriedades diferentes dependendo da origem de cada amostra, indicando a ocorrência de polimorfismo.

A quercetina sofre autoxidação em soluções orgânicas ou em meio aquoso. A autoxidação é dependente do pH e da solução tampão, assim como da presença de oxidantes e está relacionada a dissociação dos grupos OH da molécula, que ocorre com o aumento do pH da solução. De acordo com seu diagrama de formas iônicas, a quercetina encontra-se na forma neutra ou catiônica em pH menores que 5, neutra ou de monovalente a pH 5 e na forma de mono ou bivalentes a pH 7,5. Comparando os valores de pKa (5,5; 7,1; 8,0; 9,6 e 11,4), a ordem preferencial para a desprotonação dos grupos OH seria a seguinte: 5-OH<3-OH<3´-OH<7-OH<4´-OH, indicando que como os grupos hidroxilas em C3 e C5 possuem valores de pKa acima do pH fisiológico, apenas os grupos nas outras posições podem ser deprotonados em meio fisiológico (MOMIC *et al.,* 2007).

Além disso, este composto, assim como outros flavonóides, apresenta sensibilidade à luz. O efeito da irradiação sobre a estabilidade da quercetina em solução aquosa foi avaliada em pH 5, 7,5 e 10 a 25°C

por Momic e colaboradores (2007). Os espectros de absorção de quercetina das amostras irradiadas e não irradiadas a pH 10 e os das amostras irradiadas a pH 5 e 7,5 mostraram uma diminuição dos picos de absorção de quercetina nas faixas de 260-273 e 385-409 nm, dependendo do pH e simultâneo aparecimento de um pico a 321-327 nm, típico da formação de produtos de oxidação, indicando que a irradiação pode iniciar ou aumentar a transferência de elétrons mesmo quando a quercetina se encontra na forma neutra (pH 5) e que ela acelera a taxa de degradação a pH 10.

2.1.2. Propriedades Farmacológicas

A quercetina tem sido estudada como potencial agente terapêutico contra uma série de doenças, tais como, câncer, doenças neurodegenerativas, diabetes, disfunções cardiovasculares, doenças inflamatórias, entre outros, assim como agente no combate do envelhecimento (GALVEZ *et al.,* 1993; FORMICA e REGELSON, 1995; SHOSKES, 1998; MIDDLETON, *et al*., 2000; BOOTS *et al*., 2008). As propriedades medicinais desse composto são principalmente atribuídas a sua capacidade antioxidante, anti-radicais livres, modulação da expressão gênica e interação com as vias de sinalização celulares, tais como, supressão da proliferação celular, indução da parada no ciclo celular e apoptose, inibição de várias quinases, promoção de diferenciação celular e inibição da glicoproteina P, a qual é responsável pela resistência a múltiplos fármacos das células tumorais (IKEGAWA *et al*., 2002; CIPAK *et al*., 2003; SOOBRATTEE *et al*., 2005).

Em um grande número de estudos *in vitro* a quercetina foi caracterizada com um potente antioxidante com capacidade de seqüestrar espécies reativas de oxigênio, oxigênio singleto e radicais de diferentes origens (RICE-EVANS *et al.*, 1996; VAN ACKER *et al.*, 1996; CAO *et al*., 1997; AHERNE e O'BRIEN, 1999; YAMAMOTO *et al.*, 1999). Um estudo de relação estrutura- atividade identificou os elementos estruturais na estrutura dos flavonóides que contribuem para a sua atividade antioxidante. A quercetina possui todos esses elementos na sua estrutura, os quais incluem a dupla ligação C2=C3, o grupamento cetona em C4, o grupo hidroxil em C3 e a estrutura orto-difenólica (grupo catecol) no anel B (Figura 2A) (RICE-EVANS *et al.,* 1996).

Existem muitas evidências científicas baseadas em estudos *in vitro* indicando que a quercetina também apresenta efeito protetor contra o câncer. Sua natureza polifenólica torna a quercetina potencial

alvo de oxidantes pró-inflamatórios, tais como o ácido hipocloroso (HOCl) e peroxinitrito (ONO^-_2), os quais são formados durante as reações metabólicas, principalmente no recrutamento de células inflamatórias nos tecidos tumorais onde se observa um aumento exponencial de espécies reativas de oxigênio (EROS). Os EROS podem danificar proteínas, ADN e ARN, bem como oxidar ácidos graxos das membranas celulares, o que pode aumentar o número de mutações (MERTENS-TALCOTT e PERCIVAL, 2005). Desta forma, um dos mecanismos de quimioprevenção da quercetina está associado a sua capacidade de eliminar espécies reativas deletérias, como o ânion superóxido, radical hidroxila, óxido nítrico e peroxinitrito (MERTENS-TALCOTT e PERCIVAL, 2005).

Um segundo possível mecanismo de proteção da QU contra o câncer consiste na capacidade de modulação do metabolismo de carcinógenos, por meio da inibição e/ou indução de enzimas envolvidas no processo de biotransformação destes, tais como a glutationa-transferase e quinona redutase, as quais protegem células e tecidos contra carcinógenos endógenos e exógenos intermediários (ZHANG *et al.*, 1992; TALALAY *et al.*, 1995;). Adicionalmente, a quercetina é conhecida como um potente inibidor de enzimas do sistema citocromo P450 (KUO *et al*., 2004; WALSKY *et al.,* 2005).

A quercetina também apresentou efeito inibitório sobre a proliferação de linhagens de células tumorais *in vitro*, entre elas, células de câncer de estômago, cólon, próstata, mama e pulmões (CSOKAY *et al.*, 1997; KAPISZEWSKA *et al.*, 2007). Muitos mecanismos para este efeito têm sido propostos, entre eles a apoptose e/ou paralisação do ciclo celular na fase G_1 ou na fase G_2/M (CHOI *et al.*, 2003; ONG *et al.*, 2004; YANG *et al.*, 2006; LEE *et al.*, 2003; JEONG *et al.*, 2009). A habilidade da quercetina em modular a atividade de enzimas envolvidas na tradução de sinais, desenvolvimento e crescimento celular, incluindo a fosfatidilinositol-3-quinase, proteína quinase C e a proteína tirosina quinase, também é relacionada à produção deste efeito antiproliferativo, assim como a regulação da expressão da proteína mutante p53 e inibição das proteínas de choque térmico (MATTER *et al.,* 1992; AGULLO *et al.*, 1997; LAMSOM e BRIGNALL, 2000). Outra possível via de indução de processos apoptóticos decorre da ativação de caspases, proteases essenciais na morte celular que também corroboram para a supressão de tumores e a capacidade de ligação com receptores de estrogênios (LAMSOM e BRIGNALL, 2000; YOSHIZUMI *et al.*, 2001).

A atividade antitumoral ainda pode estar relacionada com a inibição da angiogênese. Um estudo realizado em células endoteliais das veias de cordões umbilicais humanos demonstrou que após exposição à quercetina, ocorreu uma diminuição na expressão e atividade da enzima matriz-metaloproteinase-2, relacionada ao processo angiogênico de migração, invasão e formação de vasos (TAN *et al.,* 2003).

O efeito antidiabético deste composto foi testado por Vessal e colaboradores (2003) em modelo de diabetes induzido por estreptozocina. Neste estudo foi verificado que o grupo tratado com quercetina apresentou uma diminuição da concentração de glicose no plasma, de forma dose-dependente e os autores sugerem que este efeito pode estar relacionado à regeneração das ilhotas pancreáticas e conseqüente aumento da liberação de insulina.

A ação antihistamínica e antioxidativa da quercetina também foi verificada em lesões gástricas induzidas por etanol em ratos. O grupo tratado com quercetina apresentou diminuição significativa no número de mastócitos e da área das lesões gástricas, indicando que a quercetina apresenta efeito antiperoxidativo, antioxidante e antihistaminico neste modelo experimental (KAHRAMAN *et al*., 2003).

A quercetina, igualmente apresenta capacidade de reduzir processos inflamatórios agudos, crônicos e sub-clínicos, uma vez que induz a produção de mediadores responsáveis pela diminuição da produção de interleucinas (IL), possui ação anti-histamínica e apresenta potente efeito inibitório na formação de leucotrieno B_4 em leucócitos. Esta substância causa ainda a supressão da produção de TNFα e óxido nítrico nos macrófagos e mastócitos, além de inibir a formação de importantes agentes pró-inflamatórios, reduzindo a ativação e o recrutamento de células inflamatórias (MIN *et al.*, 2007; ROGÉRIO *et al.*, 2007; BISCHOFF, 2008). Rogério e colaboradores (2007) testaram este composto em modelo de asma alérgica e demonstraram que ocorreu uma redução do recrutamento de eosinófilos no grupo tratado com quercetina. Este efeito foi atribuído à propriedade inibitória que este flavonóide exerce sobre alguns mediadores inflamatórios, assim como a regulação da via do NF-κB. A inibição deste fator de necrose é associada com a supressão da expressão de genes decodificadores de quimiocinas como a IL-8 e a adesão molecular, as quais são rotas cruciais para o controle do recrutamento de eosinófilos.

2.1.3. Propriedades Biofarmacêuticas e Farmacocinéticas

O maior obstáculo para o tratamento com a quercetina, por via oral, está relacionado à sua baixa biodisponibilidade. Este composto sofre intensa reação de conjugação, formando compostos glicuronados e sulfatados que diferem dos seus parentes em tamanho, polaridade e forma iônica (Figura 3) (YU *et al.*, 2002; KROON *et al.*, 2004; WENZEL e SOMOZA, 2005). Do ponto de vista biológico, tais reações de conjugação resultam numa mistura de compostos apresentando diferenças significantes no seu potencial redox. Por exemplo, a atividade antioxidante de conjugados de quercetina é, em média, metade daquela da correspondente forma aglicona, e variações existem de acordo com a posição onde ocorre a reação, visto que dois de seus principais metabólitos, quercetina-3'-sulfato e 3'-metil-quercetina-3-glicurônico demonstraram serem completamente inefetivos (JANISCH *et al*., 2005).

Além disso, a sua baixa solubilidade aquosa é um fator que limita sua administração e/ou absorção. Um pró-fármaco derivado da quercetina hidrossolúvel foi sintetizado (QC-12: 3'(N-carboximetil)carbomil-3,4', 5,7- tetrahidroxiflavona) e testado em humanos, no entanto, após administração oral, nem o derivado, nem a QU foram detectados no plasma, indicando que a alteração na molécula não tornou o composto biodisponível por via oral (MULHOLLAND *et al.,* 2001).

A quercetina presente nas plantas, frutas e legumes encontra-se em grande parte, na forma hidrofílica glicosídica (QU-Glic), que não é absorvida diretamente com facilidade (GRAEFE, *et al*., 1999; GRAEFE *et al.*, 2001). A ligação glicosídica é hidrolisada pela enzima β-glicosidase, encontrada no fígado, nos rins, e no intestino. Esta enzima possui alta afinidade por glicosídeos de flavonóides e isoflavonóides quando a glicose está ligada ao carbono nas posições 7 ou 4'. Porém, flavonóides 3'-glicosídicos não são substratos para a enzima, possivelmente devido ao impedimento estérico (DAY *et al.*, 1998; BOOTS *et al*., 2008).

A QU-Glic começa a ser hidrolisada na cavidade oral, por bactérias e/ou enzimas presentes no citosol das células epiteliais, liberando a forma aglicona, biologicamente mais potente, na superfície das células epiteliais (WALLE *et al.*, 2005). No estômago, a forma glicosídica parece não ser absorvida (DAY *et al.*, 2000) e no intestino delgado, a difusão passiva da QU-Glic pelas membranas celulares dos enterócitos é dificultada, em função do caráter hidrofílico deste

composto. Para que ocorra a absorção, as enzimas β-glicosidases deglicosilam o composto, liberando a forma aglicona, que é capaz de atravessar a membrana do enterócito por difussão passiva (DAY *et al.*, 2000).

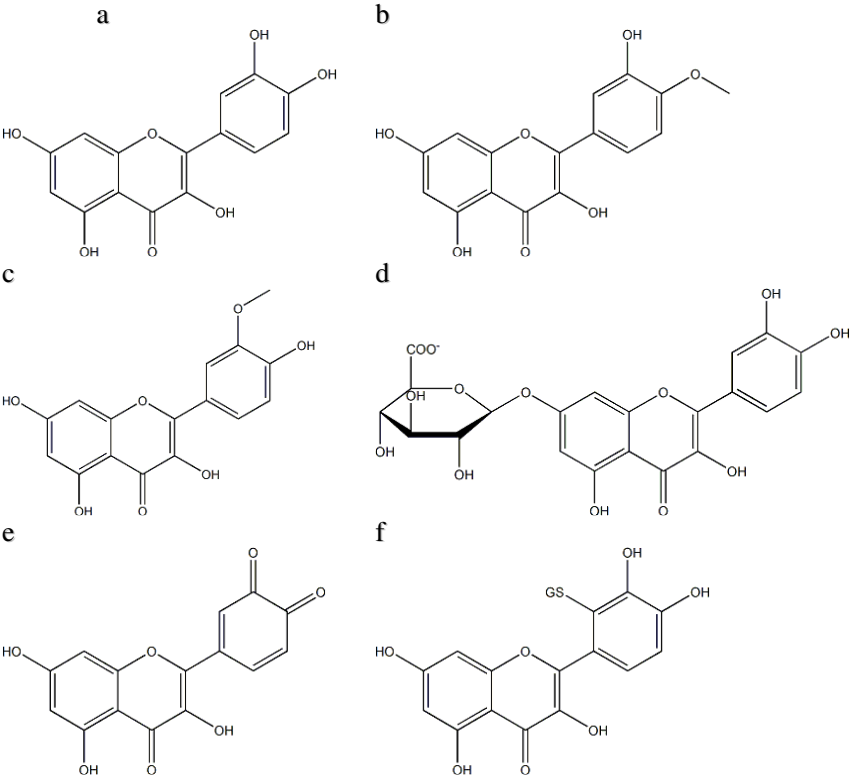

Figura 3. Quercetina (a) e seus principais metabólitos. (b) 4´-*O*-metil-quercetina, (c) 3´-*O*-metil-quercetina, (d) quercetina glicorunizada, (e) quercetina-*O*-quinona e (f) 2´-glutationil-quercetina.

Uma segunda rota para a absorção dos glicosídeos de quercetina envolve o transportador de glicose dependente de sódio (SGLT-1). Estudos em linhagem de células confirmaram que a quercetina- 4´-glicosídeo é transportada pelo SGLT-1 através da membrana apical dos enterócitos, onde posteriormente é hidrolisada pela atividade da enzima citosólica β-glicosidase (DAY *et al.*, 2000; WALGREN *et al.*, 2000;

NEMETH *et al.*, 2003). Outros estudos sugerem que transportadores de proteínas do intestino delgado, tipo transportador de glicose isoforma 2 (GLUT2) e a proteína de resistência a múltiplos fármacos 2 (MRP2) também podem estar envolvidos no processo de absorção (WALGREN *et al.*, 2000b; WOLFFRAM *et al*., 2002; SESINK *et al.*, 2005). Além da atividade da glicosidase presente no intestino delgado, várias bactérias da flora intestinal são capazes de quebrar a estrutura de quercetina e clivá-la em pequenas moléculas como os ácidos fenólicos (KIM *et al.,* 1998; SCHNEIDER *et al.,* 1999; SCHNEIDER; BLAUT, 2000; BOOTS *et al*., 2008).

Seguindo a rota do trato gastro-intestinal (TGI), os glicosídeos que ainda não foram metabolizados e/ou absorvidos no intestino delgado são transportados para o cólon. A microflora colônica expressa as enzimas α,L-ramnosidase e a β-D-glicosidase, o que permite a eficiente deglicosilação da QU-Glic. Além disso, a microflora colônica também é capaz de outras reações metabólicas incluindo a quebra dos anéis A e/ou B da quercetina, levando a formação de moléculas de baixo peso molecular. No cólon, tanto a forma aglicona quanto os produtos de degradação de quercetina podem ser absorvidos para a circulação ou excretados via fezes (RICE-EVANS *et al*., 1996, AURA *et al.*, 2002). Após a absorção pelo intestino delgado ou cólon, a QU passa para a circulação sistêmica alcançando o fígado pela veia porta. O fígado é considerado principal órgão de metabolismo de fármacos, o qual é altamente dependente de enzimas como a catecol-*O*-metil transferase (COMT), a uridina-difosfato glicuronosil transferase (UGT), e a sulfotransferase (ST) (AKSOY *et al*., 1993; COUGHTRIE *et al.,* 1998; KING *et al.,* 2000). Neste órgão, a quercetina é extensivamente metabolizada formando conjugados glicuronizados, metilados e sulfatados (PISKULA e TERAO, 1998; CRESPY *et al.*, 2001; BOERSMA *et al.*, 2002; OLIVEIRA *et al.,* 2002). Após a metabolização, os conjugados passam para a circulação sistêmica onde se ligam a proteínas plasmáticas ou são excretados na bile (O'LEARY *et al.,* 2003). Como β-D-glicuronidase também esta presente na microflora, os glicuronídeos de QU excretados via bile também podem ser deglicuronizados, liberando novamente a forma aglicona e possibilitando o ciclo enterohepático (AURA *et al.*, 2002). As proteínas plasmáticas ligadas à quercetina glicuronizada penetram em tecidos e através da enzima β-glicuronidase, sofrem uma deglicuronização, resultando na liberação da forma aglicona da quercetina, que age na célula como composto bioativo (O´LEARY *et al.,* 2003).

Poucos estudos determinaram a concentração plasmática da forma aglicona de quercetina. GUGLER e colaboradores (1975) administraram 100 mg de QU a humanos por via intravenosa e verificaram que 98% do composto ligou-se a proteínas plasmáticas e 7,4% foi excretado na urina na forma de metabólito conjugado. Por outro lado, quando 4 g de quercetina foi administrado por via oral, a quercetina não foi detectada pela técnica de fluorimetria, nem no plasma, nem na urina. Em um estudo realizado por MOON e colaboradores (2008), 500 mg de QU foi administrada 3 vezes em indivíduos saudáveis durante 7 dias e sua concentração foi determinada no plasma e na urina por HPLC-EM. Os resultados de QU na forma intacta e de seus conjugados foi de 15,4 ng/mL, após 3 horas e de 336 ng/mL, após 4 horas, respectivamente. A recuperação da forma intacta e conjugada na urina variou de 0,05-3,6% e de 0,08-2,6%, respectivamente.

2.1.4. Aspectos Toxicológicos

Durante várias décadas, o efeito genotóxico dos flavonóides, incluindo a quercetina, foi avaliado *in vitro,* pelo teste de AMES, demonstrando potencial mutagênico para bactérias (MACGREGOR e JURD, 1978; SCHIMMER *et al.,* 1988; VRIJSEN *et al.,* 1990), sendo que, neste caso, a atividade mutagênica mostrou ser dependente da presença do grupamento C3-OH, do grupamento cetona em C4 e da presença do grupamento 3´, 4´-dihidroxi no anel B, que permite a formação de metabólitos do tipo quinona (SILVA *et al.,* 2000). No entanto, os aspectos genotóxicos foram menos evidentes em células de mamíferos, decorrentes das diferenças existentes na relação estrutura-atividade da quercetina para efeitos mutagênicos em bactérias e mamíferos. Desta forma, os mecanismos responsáveis pelo efeito mutagênico não são comparáveis, mas alguns dados indicam que a ativação metabólica da quercetina por meio de uma reação de óxido-redução do grupo catecol da molécula, pode levar a formação de produtos tóxicos com atividade pró-oxidante que possuem capacidade de se ligarem irreversivelmente com constituintes celulares, tais como a *o*-semiquinona e a *o*-quinona (CAO *et al.,* 1997; CANADA *et al.,* 1990; METODIEWA *et al.,*1999).

A atividade anti e pró-oxidante da quercetina foi avaliada em um estudo realizado por CHOI e colaboradores (2003). Neste estudo, os autores demonstraram que a administração crônica de quercetina em

ratos causou inibição da peroxidação lipídica e diminuição da concentração de glutationa, assim como da atividade da glutationa redutase, indicando que este composto possui atividade antioxidante, mas igualmente efeitos pró-oxidantes.

Um grande número de estudos sobre a atividade carcinogênica da quercetina foi publicado nos últimos 25 anos, onde foi constatado *(i)* nenhum efeito, *(ii)* efeito protetor ou *(iii)* efeito estimulante da QU no processo de carcinogênese, demonstrando desta forma, que os dados disponíveis são contraditórios, fato que pode relacionado aos diferentes modelos animais e/ou técnicas experimentais utilizadas. Em 1991, o National Toxicology Program (EUA), sob a direção do National Institute for Environmental Health Sciences (NIEHS), publicou um estudo sobre a carcinogenicidade da quercetina. Neste estudo foi constatado "alguma atividade carcinogênica" da quercetina (1900 mg/kg) em ratos machos F344/N, em função no aumento da incidência de adenomas renais, sendo que este efeito não foi observado em ratos fêmeas tratados com a mesma dieta (NATIONAL TOXICOLOGY PROGRAM, 1991; DUNNICK e HAILEY, 1992; STAVRIC, 1994). No entanto, o método utilizado neste estudo foi questionado por muitos pesquisadores e os resultados não foram reprodutíveis. A maioria dos resultados dos estudos *in vivo* indicam que a quercetina não é carcinogênica. Em 1999, a International Agency for Research on Cancer (IARC; EUA) concluiu que a quercetina não é classificada como carcinogênica a humanos (OKAMOTO, 2005). Aparentemente, a relação entre as atividades antioxidante e pró-oxidante deste composto está relacionada à dose administrada (MERTENS-TALCOTT e PERCIVAL, 2005).

2.2 Carreadores coloidais de fármacos

As pesquisas da área farmacêutica tem tornado evidente que somente o desenvolvimento de novas moléculas de fármacos não é suficiente para assegurar o progresso da terapia medicamentosa. Moléculas que exibem baixa solubilidade aquosa e/ou baixa capacidade de permeação através das membranas plasmáticas apresentam biodisponibilidade insuficiente após administração oral, o que pode levar a flutuações da concentração plasmática ou ainda à dependência de alimentos para que ocorra a absorção. Desta forma, muitos esforços têm sido despendidos para desenvolver carreadores de fármacos que possam contornar esses problemas. Para tanto, algumas características são

requeridas, como a ausência de toxicidade aguda e crônica, capacidade de encapsulação suficiente, possibilidade de controle da liberação e direcionamento de fármacos a alvos específicos, estabilidade durante o armazenamento e facilidade de produção em larga escala (COUVEUR *et al.,* 1995; BARRATT, 2000; MEHNERT E MADER, 2001). Os carreadores coloidais têm sido alvo de muito interesse, pois são sistemas promissores que podem cumprir os requisitos descritos acima. Assim, o uso destes sistemas permite carrear fármacos de modo a oferecer a atividade terapêutica máxima, prevenir a degradação ou inativação durante o trânsito até o sítio alvo e proteger o organismo de reações adversas devido à distribuição inapropriada (GUPTA, 1990, BANKER e RHODES,1996).

A característica comum de todos carreadores coloidais é o seu tamanho submicrométrico, havendo consideráveis diferenças em todos outros aspectos, como, estabilidade termodinâmica, estrutura, composição química, capacidade de encapsulação e tipo de aplicação. Os nanocarreadores podem ser utilizados por várias vias de administração para o tratamento de diversas doenças. Os nanocarreadores coloidais mais estudados incluem as nanopartículas e nanocápsulas lipídicas e poliméricas, as nanoemulsões, as microemulsões, os lipossomas e as micelas poliméricas (MADER e MEHNERT, 2005).

Especialmente os nanocarreadores lipídicos têm sido alvo de muitos estudos nos últimos anos, em função da sua alta biocompatibilidade. Estes nanocarreadores podem ser constituídos de lipídios sólidos ou líquidos, ou por misturas destes, levando a produção de sistemas matriciais ou reservatórios que exibem uma ampla faixa de tamanhos de partículas (HAUSS, 2007).

Alguns nanocarreadores já se encontram disponíveis no mercado, como é o caso da microemulsão pré-concentrada de ciclosporina (Sandimmun-Neoral), a qual demonstrou diminuir a variabilidade farmacocinética do fármaco quando comparada com a formulação convencional. Outros exemplos para uso injetável incluem nanoemulsões de etomidato (Etomidat-Lipuro) e diazepam (Diazepam-Lipuro), micelas mistas contendo diazepam (Valium-MM) e lipossomas de anfotericina B (Ambisome). Embora este número ainda seja limitado, é esperado um aumento no número de nanocarreadores coloidais disponíveis no mercado nos próximos anos, em função dos requisitos necessários para a segurança dos medicamentos e também do aumento

do número de moléculas lipossolúveis que apresentam potente atividade farmacológica (MADER e MEHNERT, 2005).

A seguir são descritas mais informações sobre nanopartículas lipídicas sólidas, carreadores lipídicos nanoestruturados, nanoemulsões e microemulsões, uma vez que estes foram os nanocarreadores lipídicos desenvolvidos neste trabalho.

2.2.1 Nanopartículas lipídicas sólidas

As nanopartículas lipídicas sólidas (NSL) são partículas constituídas por lipídios sólidos a temperatura ambiente, apresentando tamanho médio de partícula entre 100 à 300 nm. A utilização de lipídios sólidos ao invés de líquidos para produção dos nanocarreadores tem como objetivo principal desenvolver sistemas capazes de controlar a liberação de fármacos, uma vez que a mobilidade do mesmo no carreador é consideravelmente menor do que em um lipídio líquido, como é o caso das nanoemulsões. Além disso, a estabilidade de certos fármacos também pode ser melhorada numa matriz sólida. Desta forma, as nanopartículas sólidas lipídicas foram desenvolvidas para terem características de "nanoemulsões congeladas", ou seja, além dos componentes formadores de matriz sólida serem altamente compatíveis com o meio fisiológico, o nanocarreador tem capacidade de controlar a liberação de fármacos e aumentar a sua estabilidade (MADER e MEHNERT, 2005; SAUPE e RADES, 2006). Suas principais vantagens frente a outros carreadores coloidais incluem a excelente estabilidade física, capacidade de proteção de fármacos instáveis frente à degradação, capacidade de controle da liberação, excelente tolerabilidade, possibilidade de vetorização, além de não apresentar problemas relacionados à produção em grande escala e à esterilização. Além disso, dependendo da técnica de preparação empregada, a utilização de solventes orgânicos não é necessária e este tipo de sistema possui uma ampla faixa de aplicações (dérmica, peroral, intravenosa) (WANG *et al.,* 2002; WISSING, *et al.,* 2004; MANJUNATH *et al.,* 2005; SAUPE e RADES, 2006).

Os principais componentes da formulação são o fármaco, lipídios sólidos, emulsificantes e água, mas outros componentes também podem estar presentes dependendo do tipo de aplicação do nanocarreador. O termo "lipídio" é geralmente usado para uma ampla gama de compostos como triglicerídeos altamente purificados (ex. triestearato de glicerila), misturas de glicerídeos (ex.monoesterato de

glicerila), ácidos graxos (ex. ácido esteárico), esteróides (ex. colesterol) e ceras (ex. palmitato de cetila). A escolha do emulsificante depende da via de administração a qual se destina a formulação e conseqüentemente o uso é mais limitado para administração parenteral. Uma grande variedade de surfactantes iônicos e não-iônicos com diferentes pesos moleculares tem sido utilizada para estabilizar a dispersão de lipídios. Entre os mais utilizados estão diferentes tipos de poloxamers, polissorbatos, lecitinas e sais biliares, sendo que em muitos casos, uma combinação de emulsificantes é mais eficiente para prevenir a aglomeração das partículas (MADER e MEHNERT, 2005; SAUPE e RADES, 2006).

Várias técnicas têm sido descritas na literatura para a preparação de nanopartículas lipídicas sólidas, incluindo à homogeneização a alta pressão (MEHNERT e MÄDER, 2001; WISSING, *et al*., 2004), emulsificação/evaporação do solvente (SIEKMANN e WESTESEN, 1996; TROTTA, *et al*., 2003), difusão do solvente a quente (ou injeção do solvente) (HU, 2002; SCHUBERT e MÜLLER-GOYMANN, 2003), dispersão por ultrasom (MADER e MEHNERT, 2005), inversão de fases (HEURTAULT *et al*., 2002) e dupla emulsão (GARCÍA-FUENTES *et al*., 2002).

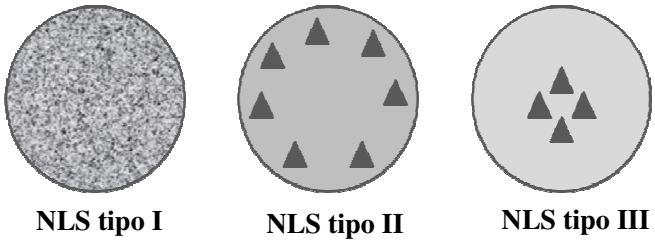

Figura 4. Modelos de incorporação de fármacos propostos para NLSs (adaptado de SOUTO e MULLER, 2007).

A elevada estabilidade física das NLSs, o uso de lipídios biocompatíveis e biodegradáveis, o tamanho em escala nanométrica e a proteção do fármaco encapsulado são características que tornam esses sistemas promissores para sua administração. Diferentes modelos de como os princípios ativos podem ser incorporados nas NLSs têm sido

descritos na literatura. Três modelos foram propostos, conforme pode ser observado na figura 4: modelo de matriz homogênea (tipo I), modelo de incorporação de fármaco na superfície (tipo II) e modelo de incorporação de fármaco no centro (tipo III) (SOUTO e MULLER, 2007).

No entanto, a capacidade de incorporação de fármacos é limitada. Tais partículas são constituídas por uma rede cristalina, em que as moléculas dos lipídeos encontram-se altamente organizadas. Desta forma, a incorporação de fármaco ocorre, em geral, apenas no espaço situado entre as cadeias dos lipídeos e em função do espaço limitado na formação nas cadeias de cristais de lipídios sólidos, a expulsão de fármacos pode ocorrer durante o processo de recristalização (FREITAS e MÜLLER, 1999). Tem sido proposto que a incorporação de fármacos pode ser aumentada pela incorporação de óleo na matriz lipídica sólida, o que deu origem aos carreadores lipídicos nanoestruturados descritos abaixo.

2.2.2 Carreadores lipídicos nanoestruturados

Os carreadores lipídicos nanoestruturados (CLN) têm sido propostos como nanopartículas lipídicas de segunda geração, pois possibilitariam uma maior incorporação de fármacos, mantendo o controle da liberação dos mesmos. Além das características físico-químicas do próprio fármaco, a composição das partículas lipídicas influencia na sua capacidade de incorporação. A incorporação de lipídios líquidos a matrizes sólidas tem sido estudada com o objetivo de formar estruturas menos densas e com mais imperfeições, as quais favoreceriam à encapsulação. Além disso, como a solubilidade dos fármacos é, em geral, maior em óleos, este sistema combinaria a alta encapsulação do fármaco, proporcionada pelo lipídio líquido, com a liberação controlada proporcionada pelo lipídio sólido (WISSING *et al*., 2004; SCHAFER-KORTING e MEHNERT, 2005).

As técnicas de preparação de CLNs são as mesmas utilizadas para as NLSs, diferindo apenas na substituição de uma fração do lipídio sólido por um líquido.

Várias estruturas foram propostas para as CLNs (Figura 5). Tipo I, o qual é constituído por uma estrutura cristalina apresentando imperfeições (este modelo é obtido quando é acrescentada uma pequena quantidade de lipídio líquido a matriz sólida); o tipo II, constituído por uma matriz amorfa (este modelo é produzido quando lipídios que não

recristalizam são utilizados, ex. isopropilmiristato) e o tipo III, descrita como um modelo múltiplo. Neste tipo de CLN pequenos nanocompartimentos de óleo são criados dentro da matriz sólida e isso pode ser obtido quando proporção de lipídio líquido exceda a sua solubilidade no lipídio sólido (Figura 5) (SOUTO e MULLER, 2007).

Figura 5. Estruturas propostas para as CLNs (adaptado de SOUTO e MULLER, 2007).

No entanto, alguns estudos têm demonstrado a existência de outros tipos de estruturas. As características físico-químicas dos dois lipídios, como sua solubilidade, podem afetar a formação da estrutura da partícula, assim como a técnica de preparação empregada, especialmente no que diz respeito à etapa de recristalização. Além disso, o aumento da proporção de lipídio líquido com intuito para exceder a sua solubilidade no lipídio sólido pode levar a uma separação de fases. Desta forma, nanocarreadores heterogêneos podem ser formados, nos quais cada lipídio está localizado em um compartimento dentro do nanocarreador (JORES *et al*., 2003 ; JORES *et al*., 2004; SCHAFER-KORTING e MEHNERT, 2005).

2.2.3 Nanoemulsões

As nanoemulsões (NE) podem ser definidas como sistemas heterogêneos composto de dois líquidos imiscíveis, sendo que um líquido se encontra disperso sob a forma de gotículas no outro, e o sistema é estabilizado por tensoativos adequados. A sua formação geralmente requer uma fonte de energia e a dispersão é termodinamicamente instável. Elas podem ser do tipo óleo em água (o/a) ou água em óleo (a/o), sendo que as gotículas em geral apresentam

diâmetro inferior a um micrômetro (geralmente entre 100 e 500 nm) (CONSTANTINIDES *et al.,* 2008; WANG *et al.,* 2009).

Os métodos de preparo das NE são similares aos das nanopartículas lipídicas sólidas citadas anteriormente, porém ao invés do uso de um lipídio sólido, utiliza-se um lipídio líquido na formulação. Os componentes das NEs, assim como das outras formulações descritas anteriormente são bem tolerados pelo organismo humano e a digestão das gotas de óleo contendo o fármaco lipossolúvel ocorre rapidamente no trato gastro-intestinal. Após serem absorvidas para circulação sistêmica as emulsões são reconhecidas como gorduras naturais do corpo e por isso, são rapidamente hidrolisadas pelas lipases. O sistema fagocítico é ativado somente quando algum lipídio é reconhecido como um corpo estranho (CHAKRABORTY *et al.,* 2009).

Dentre os sistemas de liberação lipídicos disponíveis no mercado, as nanoemulsões óleo em água são os sistemas que foram mais desenvolvidos. Alguns trabalhos têm demonstrado algumas vantagens desses sistemas no que se refere à redução de efeitos colaterais e aumento da biodisponibilidade (OLIVEIRA *et al.*, 2004). Além disso, outras vantagens das nanoemulsões incluem a possibilidade de produção em grande escala e o aumento da estabilidade física (ausência dos fenômenos cremação, floculação, coalescência e sedimentação) quando comparado a emulsões ou macroemulsões grosseiras (MEHNERT e MÄDER, 2001; CONSTANTINIDES *et al.*, 2008).

2.2.4 Microemulsões

Microemulsões (MEs) são definidas como sistemas opticamente isotrópicos, transparentes ou translúcidos e termodinamicamente estáveis, de dois líquidos imiscíveis, usualmente água e óleo, estabilizados por um filme de tensoativos. Apresentam grande potencial como sistemas de liberação de fármacos em função de sua alta capacidade de solubilizar compostos hidrofóbicos em meio aquoso ou vice-versa. As MEs foram primeiramente descritas por HOAR e SHULMAN (1943), após evidenciarem a formação espontânea de sistemas transparentes quando óleo e água eram misturados com quantidades relativamente grandes de tensoativo iônico e um álcool graxo de cadeia média. Este tipo de sistema possui uma tensão interfacial muito baixa, em torno de 0 mN/m apesar da grande área interfacial óleo-água. No entanto, é muito difícil alcançar a área interfacial necessária para a formação de um sistema microemulsionado

com a utilização de um único surfactante, por isso a utilização de um co-surfactante se faz necessária (NAZAR *et al.*, 2009).

A composição das microemulsões é determinada por um equilíbrio entre os componentes da formulação, sendo que normalmente são utilizados lipídios líquidos, tensoativos e água. Dependendo das quantidades utilizadas de cada componente, as microemulsões podem apresentar diferentes estruturas: água em óleo (a/o), óleo em água (o/a) ou estruturas bicontínuas, as quais podem exibir diferentes comportamentos para a liberação de fármacos (NAZAR *et al.*, 2009). As condições que governam as interações entre os componentes para a formação das ME são várias, no entanto, aquelas que são essenciais incluem a obtenção de uma tensão interfacial água/óleo muito baixa, a formação de um filme interfacial de tensoativo altamente fluido, a penetração e a associação das moléculas da fase oleosa com o filme interfacial de tensoativo. Além disso, a temperatura também exerce um efeito na formação da ME, visto que o balanço hidrofílico-lipofílico dos tensoativos pode ser modificado com a alteração da temperatura, desestabilizando a interface (KREILGAARD, 2002).

Estudos indicam que as microemulsões óleo-em-água possuem a habilidade de aumentar a biodisponibilidade de fármacos que apresentam problemas de absorção por via oral. Este fenômeno pode estar relacionado à melhor captura dos nanocarreadores pelo TGI e à diminuição da degradação e/ou metabolismo dos mesmos. Um exemplo de microemulsão disponível no mercado é a Sandimmun-Neoral, a qual demonstrou diminuir a flutuação plasmática da ciclosporina quando comparada com a formulação convencional. No entanto, embora haja inúmeras vantagens na utilização deste tipo de sistema de liberação, como a estabilidade termodinâmica, simplicidade da técnica de preparação, transparência e baixa viscosidade, as MEs, normalmente apresentam um alto teor de surfactantes na sua formulação. Para administração por via oral, é necessário utilizar componentes biocompatíveis e biotoleráveis, e devido à toxicidade, apenas um limitado número de surfactantes e co-surfactantes pode ser usado para a preparação destes sistemas (GUPTA *et al.,* 2005).

2.3 Administração de nanocarreadores lipídicos por via oral

Nas últimas décadas, interesse tem sido demonstrado na utilização de nanocarredores lipídicos como uma estratégia para aumentar a biodisponibilidade de fármacos hidrofóbicos pela via oral.

Esta estratégia tem sido fundamentada na observação em que uma dieta rica em gorduras pode levar o aumento da absorção de muitos fármacos lipofílicos. Neste caso, os mecanismos envolvidos no aumento da biodisponibilidade incluem: (*i*) a solubilização dos fármacos em espécies coloidais geradas pela digestão dos lipídios, como micelas, vesículas e micelas mistas, no fluido intestinal, (*ii*) a interferência dos lipídios no processos metabólicos e de transporte através dos enterócitos e (*iii*) captura seletiva de fármaco hidrofóbicos (log P > 5,0) pelo sistema linfático que faz com que ele não passe pelo metabolismo de primeira passagem no fígado, atingindo diretamente a circulação sistêmica (CHAKRABORTY *et al*., 2009)

O conhecimento dos processos de absorção de lipídios para a circulação sistêmica é de grande significância para a interpretação das propriedades biofarmacêuticas de sistemas de liberação lipídicos. Certamente, a solubilização do fármaco no TGI e sua biodisponibilidade dependem do processo de digestão pelo qual passam os componentes das formulações (PORTER *et al.,* 2008). Em geral, a digestão dos nanocarreadores lipídicos inicia com a quebra dos lipídios, ocasionada pela hidrólise dos triglicerídeos (TG) pela enzima lipase. Cada molécula de TG é digerida para gerar duas moléculas de ácidos graxos (AGs) e uma molécula de monoglicerídeos (MGs). Os produtos lipolíticos são então emulsificados por sais biliares e fosfolipídios, ocorrendo, inicialmente, a formação vesículas multilamelares. Com o aumento da incorporação de sais biliares, essas vesículas são transformadas em unilamelares, que acabam se convertendo espontaneamente em micelas ou em micelas mistas (FATOUROUS *et al*., 2007b). As espécies coloidais produzidas, como resultado da digestão dos lipídios, são então absorvidas por difusão passiva, difusão facilitada ou transporte ativo através da membrana do enterócito (PORTER *et al*., 2007; CHAKRABORTY *et al*., 2009; ROGER *et al.,* 2009).

Assim, o aumento da biodisponibilidade de fármacos hidrofóbicos quando incorporados em nanocarreadores lipídicos parece estar relacionado com vantagem que este tipo de nanocarredor possui em manter o fármaco dissolvido ao longo do TGI em um elevado grau de dispersão, a qual aumenta a área contato, resultando em uma absorção mais reprodutível e uniforme. Além disso, devido ao tamanho de partícula reduzido, uma grande área superficial é produzida, fazendo com que a enzima lipase pancreática hidrolise os lipídios mais rapidamente, acelerando a taxa de liberação do fármaco e/ou a formação

de micelas mistas contendo o mesmo, tornando-o assim mais prontamente disponível para absorção (CHAKRABORTY *et al*., 2009).

2.4 Sistemas de liberação contendo QU

Estudos tecnológicos usando a quercetina têm objetivado principalmente à melhoria da solubilização aquosa deste composto e, conseqüentemente, da sua biodisponibilidade. Muitos destes estudos envolvem a complexação da quercetina com ciclodextrinas. PRALHAD e RAJENDRAKUMAR (2004) realizaram a complexação da quercetina com 2-hidroxipropil-β-ciclodextrina (HPβ-CD) e β-ciclodextrina (β-CD) e demonstraram, através da complexação, que a solubilidade aquosa da quercetina foi aumentada significantemente (de cerca de 10 vezes). A complexação da QU com α e β-ciclodextrinas também foi realizada por CALABRÓ e colaboradores (2004). Neste estudo um aumento na solubilidade do composto também foi observado, além de incremento na atividade antioxidante do mesmo. KALE e colaboradores (2006) avaliaram o efeito da formação de complexos de inclusão de QU com sulfobutil eter-7β-ciclodextrina (SBE7βCD-QU) sobre a inibição da proliferação celular de linhagens de células humanas de eritroleucemia e de câncer de cervix *in vitro* e sobre a inibição do crescimento do tumor em modelo de melanoma murino subcutâneo, após a inoculação de células B16F10 em camundongos. Os autores demonstraram que o complexo SBE7βCD-QU foi mais potente ao inibir a proliferação celular *in vitro* e a redução da microvascularização de melanoma, evidenciando melhora na eficácia terapêutica após complexação.

JULIAN e colaboradores (2007) também realizaram a inclusão de QU em três tipos de ciclodextrinas, sendo estas a β-ciclodextrina (β-CD), hidroxipropil-β-ciclodextrina (HP-β-CD) ou sulfobutil eter-β-ciclodextrina (SBE-β-CD), e verificaram que a constante de ligação e solubilidade da quercetina determinada nas três CDS seguiu a seguinte ordem: SBE-β-CD> HP-β-CD>β-CD, sugerindo que o aumento na ligação e solubilidade está relacionado ao aumento na substituição e hidrofilicidade das ciclodextrinas (CDs). Estudos de determinação da atividade antioxidante pela capacidade de captura dos radicais livres $DPPH^{\bullet}$ e galvinoxil, demonstraram que todos os complexos apresentam uma maior capacidade de seqüestrar radicais livres do que a quercetina em água, indicando desta forma, que os complexos mantêm a atividade antioxidante da quercetina. Outro estudo de complexação da QU com

ciclodextrinas foi realizado por BORGUETTI e colaboradores (2009). Neste trabalho foi avaliada a influência das condições de preparação, tais como temperatura, tempo de agitação e excesso de QU, na complexação do fármaco com β-ciclodextrina. A maior solubilidade de QU foi alcançada quando a temperatura foi mantida a 37^{o}C, com agitação por 24 horas, utilizando 6mM de quercetina. No entanto, o aumento da solubilidade aquosa da QU foi limitado a 4,6 vezes, uma vez que o complexo sólido apresentou baixa concentração de QU (0,14% p/p) e, portanto, baixa eficiência de complexação.

PRIPEM e colaboradores (2008) compararam o efeito da administração oral da quercetina (300mg/kg/dia) com a administração oral e nasal da QU lipossomal (20mg/kg/dia) sobre as atividades cognitivas e ansiolíticas em ratos machos Wistar por meio dos testes de labirinto em cruz elevado e labirinto aquático de Morris. Os lipossomas eram constituídos de uma mistura de fosfatididilcolina de ovo, colesterol e quercetina (2:1:1; p/p), dispersados em uma solução aquosa contendo 50% de polietilenoglicol. O tamanho de partícula dos lipossomas foi de aproximadamente 200 nm, apresentando superfície carregada negativamente e a eficiência de encapsulação de 60 a 80%. Tanto a quercetina convencional quanto a lipossomal demonstrou melhoria das atividades cognitivas e ansiolíticas. Entretanto, a administração nasal da forma lipossomal provocou efeito mais rápido em uma menor dose, indicando que a via nasal foi mais efetiva em liberar QU no sistema nervoso central.

YUAN e colaboradores (2006) desenvolveram lipossomas peguilados contendo quercetina e avaliaram seu perfil de distribuição e eficácia antitumoral *in vitro* e *in vivo*. Os lipossomas foram preparados por meio da hidratação e sonicação de um filme lipídico constituído de uma mistura de lecitina, colesterol, PEG 4000 e QU (13:4:1:6, p/p) em uma solução de glicose 5%. Esta formulação resultou na formação de lipossomas pequenos unilamelares com tamanho aproximado de 130 nm. O tempo de meia vida da quercetina lipossomal foi de 2 horas após administração IV na dose de 50mg/Kg. Nos ensaios *in vivo,* a atividade antitumoral da QU lipossomal foi avaliada em modelo murino de câncer de pulmão de Lewis LL/2, adenocarcinoma de cólon CT26 e hepatoma H22, sendo que o volume do tumor e o tempo de sobrevida foram as variáveis estudadas. Além disso, o mecanismo de ação antitumoral da QU foi investigado pela detecção da densidade de microveias e expressão da proteína de choque térmico 70 (HSP 70) nos tecidos tumorais. Os resultados indicaram que a QU lipossomal inibiu o

crescimento do tumor *in vivo* de forma dose dependente. Na análise dos mecanismos envolvidos na atividade antitumoral, foi verificado efeito inibitório da expressão da proteína HSP 70. As análises imunohistoquímicas demonstraram que QU lipossomal inibiu a angiogênese e induziu a apoptose das células tumorais.

TONG-UM e colaboradores (2010) avaliaram o efeito de lipossomas de quercetina administrados por via intranasal em modelo de doença de Alzeimer em ratos Wistar. Foram realizados ensaios para avaliar as alterações cognitivas, através da avaliação da memória espacial no labirinto aquático de Morris, e bioquímicas, pela análise da atividade da acetilcolinesterase, superóxido dismutase, glutationa peroxidase e dos níveis de malondialdeído. Os lipossomas foram constituídos de fosfatidilcolina de ovo e colesterol e preparados pela técnica de formação de filme lipídico e extrusão. Os resultados demonstraram que somente os animais tratados com lipossomas contendo quercetina não perderam o desempenho cognitivo e mantiveram níveis normais dos marcadores de estresse oxidativo e da atividade de acetilcolinesterase.

SONG e colaboradores (2008) prepararam nanopartículas de PLGA contendo simultaneamente sulfato de vincristina (VCR) e quercetina por meio da técnica de emulsificação/evaporação do solvente. Os fatores de formulação estudados durante o processo de desenvolvimento dos nanocarreadores foram o peso molecular do PLGA, a relação ácido lático/ácido glicólico do polímero, a concentração do polímero e do estabilizante PVA, o teor inicial de quercetina, a proporção de acetona e diclorometano na preparação, o pH da fase aquosa e a relação fase orgânica/aquosa da formulação. As nanopartículas otimizadas apresentaram forma esférica, tamanho na ordem de 140 nm e índice de polidispersão de 0,09. A eficiência de encapsulação, estimada após análise por CLAE, foi de aproximadamente 32 e 92% para QU e VCR, respectivamente. Nanopartículas de PLGA contendo quercetina também foram preparadas por GHOSH e colaboradores (2009) e seu potencial para combater os danos hepáticos e neuronais causados pelo estresse oxidativo induzido pela contaminação da água potável por arsênio foi avaliado em ratos. As partículas foram preparadas pela técnica de emulsificação/evaporação do solvente, seguido de uma homogeneização a alta pressão. A eficiência de encapsulação da quercetina neste sistema foi de aproximadamente 98,5% e o tamanho dos nanocarreadores foi de 270 nm. Nos ensaios *in vivo*, 500 µl das nanopartículas de QU ou de uma

suspensão contendo QU na dose de 8,98 μmol/kg, foram administradas por via oral aos animais, 90 minutos antes da injeção de arsênio. Os resultados indicaram que somente as nanopartículas contendo QU preveniram a redução dos níveis de antioxidantes induzida por arsênio tanto no fígado quanto no cérebro.

A preparação das nanopartículas poliméricas contendo quercetina também foi realizada por WU e colaboradores (2008). As nanopartículas foram preparadas pela técnica de nanoprepitação a partir do Eudragit E (EU) e álcool polivinílico (PVA). Neste estudo, foi observado que utilizando a proporção de QU:EU:PVA de 1:10:10 (p/p), as partículas apresentaram tamanho de aproximadamente 85 nm, índice de polidispersão menor que 0,3, eficiência de encapsulação de 99%, sendo que praticamente 100% de QU foi liberada em 20 minutos. Estudos *in vitro* demonstraram que a atividade antioxidante das nanopartículas foi maior do que a da QU livre nos ensaios de capacidade sequestrante de radicais DPPH, formação de superóxido, seqüestro de ânion superóxido e peroxidação lipídica.

Nanocápsulas lipídicas contendo quercetina foram desenvolvidas por BARRAS e colaboradores (2009) com intuito de aumentar a sua solubilidade e/ou estabilidade. As nanocápulas foram preparadas utilizando a técnica de inversão de fases, utilizando os seguintes componentes: triglicerídeos do ácido cáprico-caprílico (Labrafac), estearato de polietilenoglicol (Solutol), lecitina de soja, NaCl e água. As nanocápsulas contendo quercetina apresentaram tamanho de partícula de cerca de algumas dezenas de nanômetros, variando conforme a proporção de Labrafac e Solutol. A encapsulação da quercetina aumentou sua solubilidade aquosa em torno de 100 vezes e as dispersões coloidais se mostraram estáveis por dez semanas, em termos de eficiência de encapsulação, sem a oxidação da quercetina.

LI e colaboradores (2006) prepararam e caracterizaram nanopartículas lipídicas sólidas contendo quercetina (QU-NLS) e avaliaram o potencial deste sistema para administração oral da QU. As nanopartículas foram obtidas pela técnica de emulsificação e solidificação a baixa temperatura, usando ácido esteárico para compor a matriz lipídica e tendo lecitina e Tween 80/polietilenoglicol 400 como estabilizantes das fases oleosa e aquosa, respectivamente. As nanopartículas formadas apresentaram tamanho de cerca de 200 nm, formato esférico e eficiência de encapsulação de cerca de 48%. A absorção oral da quercetina foi avaliada em camundongos após a administração de uma suspensão deste fármaco em CMC-Na

(carboximetilcelulose sódica) e das QU-NLS na dose de 50mg/kg. Os estudos indicaram que as NLSs produziram uma melhoria significativa na absorção da quercetina, quando comparado com a forma livre. LI e colaboradores (2009), igualmente avaliaram a absorção gastrointestinal de QU após encapsulação em NLSs em modelo de perfusão *in sito* em ratos. Neste trabalho, as nanopartículas foram constituídas de monoestearato de glicerila (GMS), mas foram igualmente preparadas pela técnica de emulsificação e solidificação à baixa temperatura. Os nanocarreadores apresentaram diâmetro médio de cerca de 150 nm, formato esférico, potencial zeta negativo e eficiência de encapsulação de QU de 90%. Nos ensaios de liberação, 99% de QU livre foram liberados em 6 horas e somente 50% de QU foram liberados a partir das NLS neste mesmo período, indicando um controle da liberação do composto a partir dos nanocarreadores. Os estudos indicaram que a absorção da QU nanoencapsulada foi de apenas 6,2%, após 2 horas no estômago. No intestino, o mecanismo de absorção foi a difusão passiva, ocorrendo principalmente no íleo e cólon. Estudos farmacocinéticos indicaram que a concentração máxima de quercetina foi de 5,90 e 12,22 μg/mL, após administração da QU livre e de QU-NLS, respectivamente, na dose de 50mg/Kg. Os valores de $ASC_{(0\rightarrow 48h)}$ foram de 56,73±9,23 (μg/mL).h e 324,18±41,35 (μg/mL).h para QU livre e encapsulada nas nanopartículas, respectivamente.

Nanoemulsões para uso tópico contendo quercetina e 3-*O*-metilquercetina foram desenvolvidas por FASOLO e colaboradores (2009). Formulações constituídas de octildodecanol, lecitina de ovo e água (NE) foram obtidas pelo método de emulsificação espontânea. Nanoemulsões apresentando carga de superfície modificada pela adição de brometo de cetiltrimetilamônio foram igualmente preparadas e denominadas CNE. O procedimento levou a formação de nanocarreadores com tamanhos de partículas de aproximadamente 200-300 nm e eficiência de encapsulação de praticamente 100%. Estudos de permeação foram realizados em células de difusão do tipo Franz utilizando-se pele de orelha de porco como modelo de membrana. Perfis de permeação lentos foram verificados para ambos os flavonóides, entretanto um maior fluxo de permeação dos mesmos foi observado quando a formulação CNE foi testada, demonstrando o efeito da carga positiva da superfície das partículas sobre a permeação cutânea.

Microemulsões (ME) foram desenvolvidas por GAO e colaboradores (2009) com intuito de aumentar a solubilidade e absorção oral de quercetina. Vários componentes foram testados durante o estudo

de formulação da microemulsão, sendo que a ME que apresentou melhores resultados foi obtida utilizando oleato de etila (7%), Tween 80 (48%) e etanol (45%) como fase oleosa, surfactante e co-surfactante, respectivamente. O diâmetro de partícula da ME foi de 38,9 nm e a solubilidade da quercetina na ME foi de 4,138 mg/mL. Os estudos de absorção em intestinos de ratos *in situ* evidenciaram a ocorrência de diferenças significativas nos parâmetros de absorção, tais como *K*a ($p<0,01$), $t_{1/2}$ ($p<0,01$) e porcentagem de captura ($p<0,05$), entre a forma microemulsionada e a forma micelar contendo quercetina. A absorção da quercetina no intestino dos ratos foi melhor e mais rápida quando a mesma foi administrada na forma microemulsionada e a melhor permeabilidade ocorreu no cólon, seguida pelo íleo e duodeno.

Capítulo 2

Desenvolvimento dos nanocarreadores lipídicos e avaliação da capacidade de incorporação de quercetina

A quercetina é um polifenol pertencente à classe dos flavonóides que tem demonstrado inúmeras atividades farmacológicas incluindo antitumoral, antiinflamatória, antioxidante, entre outras (FRESCO *et al.,* 2006). Entretanto, a biodisponibilidade oral desta substância é muito baixa, em decorrência da sua baixa solubilidade aquosa e de seu elevado metabolismo colônico e hepático (WALLE *et al.,* 2005; SOOBRATTEE *et al*., 2005; COMALADA *et. al*., 2005). Neste sentido, a encapsulação da quercetina em carreadores lipídicos pode ser considerada uma estratégia promissora para a melhoria da sua biodisponibilidade oral. Tais sistemas podem ser obtidos a partir de lipídios sólidos, líquidos ou misturas deles em diferentes proporções. Diferenciam-se ainda como sistemas matriciais ou reservatórios de diferentes tamanhos, ainda que na faixa nanométrica (< 1 μm), estando suas características estruturais e físico-químicas diretamente ligadas à composição da formulação e à técnica de preparação (WANG *et al.*, 2002; WISSING *et al.,* 2004; MANJUNATH *et al.,* 2005).

Neste trabalho, um estudo de formulação foi realizado com o objetivo de obter nanocarreadores lipídicos com elevada capacidade de incorporação da quercetina, usando a técnica de difusão do solvente a quente, para a obtenção dos mesmos. A triestearina e o óleo de rícino foram empregados como lipídio sólido e líquido, respectivamente, e foram utilizados isoladamente ou associados em diferentes proporções. Como surfactantes foram utilizados o Polomaxer 188 (Lutrol F68-Basf) ou o estearato de polietilenoglicol 660 (Solutol HS15-Basf) e como co-surfactante a fosfatidilcolina de soja higrogenada (Lipoid S75-3N). A influência do tipo e concentração do lipídio e surfactante empregados na preparação sobre as propriedades físico-químicas das partículas e sobre a capacidade de incorporar a quercetina, bem como a capacidade de controlar a sua liberação, foi avaliada. Para isto um método de cromatografia líquida de alta eficiência foi desenvolvido e validado. Os resultados deste trabalho são apresentados na forma de um artigo científico a qual foi aceito para publicação no *Latin American Journal of Pharmacy.*

Publicação 1. *Formulation study of quercetin-loaded lipid-based nanocarriers obtained by hot solvent diffusion method*

Formulation study of quercetin-loaded lipid-based nanocarriers obtained by hot solvent diffusion method

C. L. Dora[1], L. F. C. Silva[1], M. P. Tagliari[2], M. A. S. Silva[2], and E. Lemos-Senna[1*].

[1] Laboratório de Farmacotécnica, [2] Laboratório de Controle de Qualidade, Departamento de Ciências Farmacêuticas, Centro de Ciências da Saúde, Universidade Federal de Santa Catarina. Campus Trindade, 88040-900, Florianópolis, SC, Brazil.

*Author to whom correspondence should be addressed: lemos@ccs.ufsc.br

ABSTRACT

Lipid-based nanocarriers were prepared by hot solvent diffusion technique. Tristearin (TS) and/or castor oil (CO) were employed as oily phase, and poloxamer 188 or PEG 660-stearate and lecithin were employed as surfactant and cosurfactant, respectively. The influence of the formulation variables on surface charge and size of the nanocarriers and their ability to load and control the release of quercetin were investigated. Solid lipid nanoparticles (SLN), nanostructured lipid carriers (NLC), nanoemulsions (NE), and microemulsions (ME) were obtained depending on the formulation composition. QU entrapment efficacy was higher than 99% for all formulations. However, drug content was greatly affected by the formulation composition. ME exhibited the highest capacity to load QU, reaching a concentration around 1,300 times higher than its aqueous solubility. QU release profiles exhibited biphasic kinetics for all formulations. However, the release rate of QU was affected by the properties of the nanocarrier.

Keywords: Quercetin, lipid-based nanocarriers, *in vitro* drug release.

INTRODUCTION

Quercetin (QU) (Fig. 1) is a naturally occurring flavonoid, ubiquitous in fruits, vegetables, and herbs, including oranges, onions, apples, red wine, and tea. Several studies have demonstrated the health-promoting benefits of quercetin. This drug exhibits antihistamine and anti-inflammatory properties, thus useful in reducing allergy symptoms and inflammation associated with various forms of arthritis. QU also acts as an antioxidant by scavenging particles in the body known as free radicals. These particles can damage cell membranes and interact with genetic material, contributing to the development of a number of conditions including heart disease and cancer[1-3].

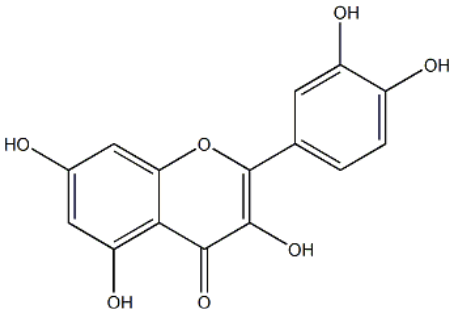

Figure 1. Molecular structure of quercetin.

In spite of its beneficial pharmaceutical properties, the bioavailability of QU is low following oral administration. Several studies have shown that this drug is extensively metabolized, undergoing pre-systemic modification in the gastrointestinal tract and first-pass metabolism in the liver, which results in a significant alteration of the species found in the systemic circulation[3]. Additionally, the low water solubility of QU restrains its absorption in the gastrointestinal tract[2]. In this context, the development of quercetin-loaded nanocarriers can be considered an interesting approach to improve the bioavailability of QU and to take advantage of its therapeutic properties in the clinical setting.

Colloidal drug carriers might differ in materials, composition, drug loading, and application range, but the characteristic they share is their submicron particle size. Such systems are characterized by their ability to protect drugs from degradation, to allow the control of drug release, to reduce undesirable side effects, and to increase the

bioavailability of poorly water-soluble drugs. Several polymeric materials have been employed in the preparation of colloidal suspensions of nanoparticles. However, over the last two decades considerable attention has been given to the development of lipid-based colloidal carriers for the administration of poorly water-soluble drugs[4,5]. Their main advantages over polymer-based drug delivery systems are their excellent physical stability, excellent tolerability, and feasibility of scaling up production[6].

Lipid-based colloidal carriers can be composed of solid or liquid lipids, or mixtures of them, in several ratios, and can be obtained by different techniques. The use of highly purified lipids, combined with the certain surfactants, can lead to the formation of matrix or reservoir drug delivery systems displaying a great range of particle sizes. Regarding their structural features, lipid-based nanocarriers resemble oil-in-water emulsions, but with a small internal phase, displaying liquid or solid consistency[7]. The smaller size of lipid-based colloidal carriers gives them the advantage of reducing the inherent limitations of slow and incomplete dissolution of hydrophobic drugs, besides presenting the drug in a dissolved or dispersed form with a large interfacial surface area for drug absorption. These formulations can also enhance drug absorption by inhibiting P-glycoprotein-mediated drug efflux and pre-absorptive metabolism by the gut enzymes, promote lymphatic transport, and increase gastrointestinal membrane permeability[4]. These proprieties can increase considerably the bioavailability of orally administered poorly water-soluble drugs.

In order to overcome the limitations inherent to the oral administration of quercetin, the development of lipid-based nanocarriers was carried out. In this paper we describe the effect of the formulation composition, i.e. type of lipid (liquid or solid) and the type and concentration of surfactant, on the formation of lipid-based nanocarriers when the hot solvent diffusion method is employed. The ability of different nanocarriers to load and to control the release of quercetin is then compared.

MATERIALS AND METHODS

Materials

Quercetin (QU) was purchased from Natural Pharma (São Paulo, Brazil). Castor oil (CO), a triglyceride in which approximately 90% of fatty acid chains are ricinoleic acid, was purchased from Natural Pharma

(São Paulo, Brazil). Hydrogenated soybean lecithin (Lipoid S75-3N) was purchased from SP Pharma (São Paulo, Brazil). According to the manufacturer, the product contains from 67 to 73 % of phosphatidyl choline. Tristearin (Dynasan 118, TS) was kindly donated by Sasol (Louisiana, USA). The fatty acid fraction was 99% pure for this triglyceride quality and hydroxyl value below 5. Polyoxypropylene-polyoxyethylene block copolymer (Poloxamer 188, Lutrol F-68 NF®) and 12-hydroxystearic acid-polyethylene glycol copolymer (PEG 660-stearate, Solutol HS-15®) were kindly donated by BASF (Trostberg, Germany). HPLC grade methanol was purchased from J.T Baker® (Phillipsburg, USA). Ethanol, acetone, phosphoric acid, and other chemicals used were analytical reagent grade.

Methods

Preparation of the lipid-based nanocarriers

The lipid nanocarriers were prepared by a hot solvent diffusion method[8]. Briefly, 10 or 20 mg of lecithin and 100 mg of tristearin (TS), castor oil (CO) or their mixture were completely dissolved into a mixture of acetone:ethanol (60:40, v/v) at 60°C to yield an organic phase containing a lecithin to lipid ratio of 1:10 or 1:5. The resulting organic solution was quickly poured into 50 mL of an aqueous solution containing 0.1; 0.5; 0.75, or 1% of the surfactant PEG-660-stearate or 1% poloxamer 188, maintained under magnetic stirring at 82°C. The resulting colloidal suspensions were then cooled to room temperature, the organic solvent was evaporated under reduced pressure, and the final volume was adjusted to 20 mL. Finally, the colloidal suspensions were filtered through an 8 μm filter paper. The formulations were made in triplicates. For the preparation of quercetin-loaded lipid nanocarriers, QU was added to the organic phase of the formulations.

Size and zeta potential measurements

The particle size and zeta potential of the lipid-based nanocarriers were determined by photon correlation spectroscopy and laser-Doppler anemometry, respectively, using a Zetasizer Nano Series (Malvern Instruments, Worcestershire, UK). The measurements were performed at 25 °C after appropriate dilution of the samples in distilled water. Each size analysis lasted 300 s and was performed with an angle detection of 173°. For measurements of zeta potential, the samples were

placed in the electrophoretic cell, where a potential of ±150mV was established. The ζ potential values were calculated as mean electrophoretic mobility values using Smoluchowski's equation.

Determination of quercetin concentration in the colloidal suspensions by HPLC

Instruments and analytical conditions

The HPLC analysis was performed using a Shimadzu LC-10A system (Kyoto, Japan) equipped with a LC-10AD pump, SPD-10AV$_{VP}$ UV detector, SCL-10A$_{VP}$ system controller, DGU-14A degasser, CTO-10AS$_{VP}$ column oven, and the sample injection was performed through a Rheodyne 7125 valve with a 20 µL loop. The detector was set at 369 nm and peak areas were integrated automatically by computer using a Shimadzu Class VP® V 6.14 software program. The experiments were carried out using a reversed-phase Zorbax ODS (Agilent Technologies, USA) C_{18} column (150 mm x 4.6 mm I.D., with a particle size of 5 µm), maintained at 40 ± 1 ºC. The mobile phase consisted of a 1% phosphoric acid:methanol mixture (45:55 v/v; pH 2.7) and was eluted isocratically at a flow rate of 1 mL min^{-1}. The HPLC method was validated according to the ICH[9] using of the following parameters: specificity, linearity, accuracy, precision, and determination of the limits of detection (LOD) and quantification (LOQ).

Determination of quercetin content, recovery and entrapment efficiency

For HPLC analysis, an aliquot of each colloidal suspension was quantitatively transferred to a 10.0 mL volumetric flask and the final volume was completed with methanol. The samples were centrifuged and an aliquot of the supernatant was transferred to a 10.0 volumetric flask and the final volume was completed with 1% phosphoric acid:methanol solution (25:75 v/v, pH 2.7). The quercetin content (total concentration) in the colloidal suspensions was calculated after determining the drug concentration in the methanolic solutions and was expressed in µg of quercetin.mL^{-1} of suspension. The quercetin recovery was calculated as being the percentage of the total drug concentration found in the suspensions in relation to the initially added amount. The entrapment efficacy (EE) was estimated as the difference between the total concentration of QU found in the colloidal

suspensions and the concentration of drug in the supernatant obtained by a suspension ultrafiltration/centrifugation procedure using Ultrafree-MC membranes (100,000 NMWL; Millipore, Billerica, USA). All samples were analyzed in triplicates.

In vitro release studies

For the experiment, 2 mL of each lipid-based colloidal suspension was placed into a dialysis bag (Spectra/Por® CE MWCO 10000, USA). The dialysis bags were placed into a dissolution apparatus containing 200 mL of PEG 400:distilled water (20:80, v/v; pH 4.0) solution. The release medium was maintained at 37°C under mechanical stirring at 75 rpm. Samples of the release medium were withdrawn after 0.5, 1, 2, 4, 6, 8, and 24 hours. The release medium was immediately replaced with fresh medium. The samples were analyzed by HPLC under the same conditions as described above. To evaluate the effect of the dialysis membrane on the drug release rate, a solution of quercetin in PEG 400 was placed into a dialysis bag and the quercetin diffusion through the membrane was assayed using the same conditions. All experiments were carried out in triplicates. The cumulative amounts of QU released (%) were plotted against time (h).

RESULTS AND DICUSSION

Macroscopic characterization and Particle size determination

In the present study, the solvent diffusion method was employed to produce the lipid nanocarriers. This method is based on the formation of a hot oil-in-water emulsion following the addition of a water-miscible organic solution containing the lipid and the lipophilic surfactant in an aqueous phase containing a hydrophilic surfactant. An interface turbulence of the emulsion droplets (Marangoni effect) is produced by the very rapid diffusion rate of the water-miscible organic solvent to aqueous phase, resulting in spontaneous droplet formation in the submicron range[10]. To achieve formulations with adequate physicochemical properties, PEG 660-stearate and poloxamer 188 were tested in different concentrations as the surfactants of the aqueous phase. All formulations were prepared using hydrogenated soy lecithin as cosurfactant. In order to obtain maximum QU encapsulation, tristearin (TS) and castor oil (CO) and their mixtures at different ratios were tested.

The macroscopic appearance of the lipid-based colloidal suspensions can be seen in Figure 2. All formulations prepared with the surfactant poloxamer 188 turned out to be macroscopically homogeneous with a milky appearance, regardless of the type of lipid material (Figure 2a). At lower concentrations and with the use of TS and CO alone or with mixtures of them, the use of PEG 600-stearate also led the production of milky colloidal suspensions (Figure 2b). However, at higher concentrations of this surfactant and when only the liquid lipid was used, the formation of an isotropic and transparent system like a microemulsion was observed (Figure 2c). In fact, when only TS, which is solid at room temperature, is employed in the preparation, solid lipid nanoparticles (SLN) displaying a matricial structure were obtained as expected[8]. In attempt to increase the capacity to load QU, blends of tristearin and castor oil were employed. These drug delivery systems have been conventionally named nanostructured lipid carriers (NLC) and this denomination was also used in this study. When only an oily lipid such as castor oil was employed, lipid-based nanocarriers structurally related to nanoemulsions (NE) or microemulsions (ME) appeared to be produced depending of the oil/surfactant/water ratio.

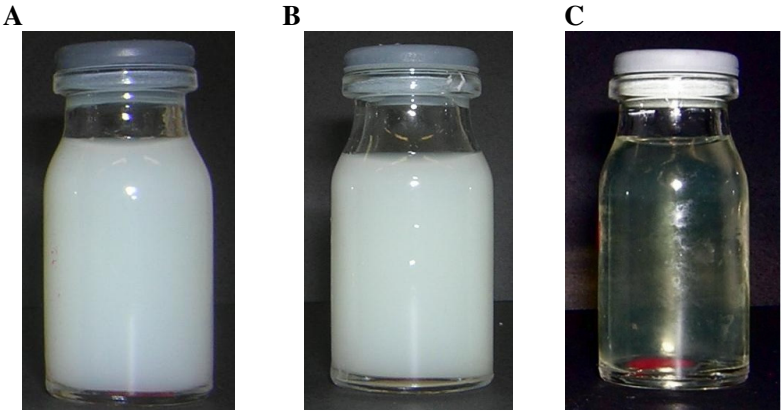

Figure 2. Macroscopic characterization of lipid-based colloidal suspensions. a) QU-NE prepared with 1% Poloxamer 188, b) QU-NE prepared with 0.1% PEG 660-stearate, and c) QU-ME prepared with 1% PEG 660-stearate.

The effect of the type and concentration of the surfactant and the lipid material on the mean particle size and particle size distribution is demonstrated in Table 1.

Table 1. Effect of formulation composition on mean diameter and polydispersity index (PDI) of lipid-based colloidal suspensions.

	Mean diameter (PDI)[a]			
	PEG 600-stearate			**Poloxamer 188**
	0.1%	**0.5%**	**1%**	**1%**
	Mean diameter (PDI)	**Mean diameter (PDI)**	**Mean diameter (PDI)**	**Mean diameter (PDI)**
QU-SLN TS:CO (100:0)	255 (0.28)	298 (0.49)	**	279 (0.24)
QU-NLC TS:CO (75:25)	204 (0.17)	373 (0.41)	**	262 (0.27)
QU-NLC TS:CO (50:50)	160 (0.09)	222 (0.22)	**	184 (0.08)
QU-NLC TS:CO (25:75)	182 (0.24)	192 (0.19)	**	168 (0.10)
QU-NE TS:CO (0:100)	130 (0.14)	157 (0.25)	**	156 (0.09)
QU-ME TS:CO (0:100)	- -	- -	22 (0.12)	-

** Samples with more than one peak.

It can be seen that the type and concentration of the surfactant, and the solid/liquid ratio affected the mean size of the particles. The increase in CO in the lipid mixture from 0 to 100% led to the reduction of the mean particle size from 298 to 130 nm. Monodispersed colloidal dispersions (PDI < 0.25) were obtained when Poloxamer 188 1% (w/v) was used as the surfactant of the aqueous phase of the formulation.

At a lower concentration (0.1%, w/v), PEG 660-stearate also produced monodispersed systems. However, the increase in PEG 660-stearate concentration to 0.5% (w/v) produced an increase in the PDI for

all TS:CO ratios tested. The use of higher concentrations of this surfactant (0.75% and 1%, w/v) led the formation of more polydisperse colloidal suspensions with more than one peak of particle size, probably corresponding to the appearance of micelles or other surfactant structures concomitantly with SLN and NLC (data not shown). On the other hand, when only CO and PEG 660-stearate 1% (w/v) were employed as lipid and surfactant, respectively, a monodispersed colloidal dispersion displaying 22 nm of mean particle size was obtained, supporting the premise that a microemulsion system was produced under these conditions.

Determination of quercetin loading

Validation of the HPLC method

A validation of the HPLC method was performed to guarantee that the analytical method generates reliable and interpretable information regarding the samples. The chromatographic conditions were adjusted relatively to the physicochemical characteristics of the drug. In the HPLC analysis, the acidification of the mobile phase and the sample solutions with phosphoric acid avoids the ionization of the phenolic groups in the flavonoidic structure, allowing the quercetin peak to be symmetrical, without tail formation[11]. After several trials, the best peak performance was achieved when the volume ratio of 1% phosphoric acid:methanol was 45:55 (v/v), with a flow rate of 1 mL min^{-1} and a column temperature of 40 ºC. In these chromatographic conditions, the quercetin retention time was around 5.7 min. Under these conditions, no interference by formulation excipients was verified, indicating that the method was specific in determining quercetin, as can be visualized in Figure 3.

The calibration graph for QU was linear over the range of 0.25 to 10 $\mu g.mL^{-1}$ with a correlation coefficient of 0.9996. The regression equation of the media calibration graph (n = 3) was y= 95880.15x – 5543.04. The variance analysis (ANOVA) confirmed the linearity of the method ($F_{caln} > F_{critical}$; P = 0.05). The LOD and LOQ calculated for HPLC were 0.036 $\mu g\ mL^{-1}$ and 0.109 $\mu g\ mL^{-1}$ respectively, indicating that the method was sufficiently sensitive to determine the quercetin content in the colloidal suspensions.

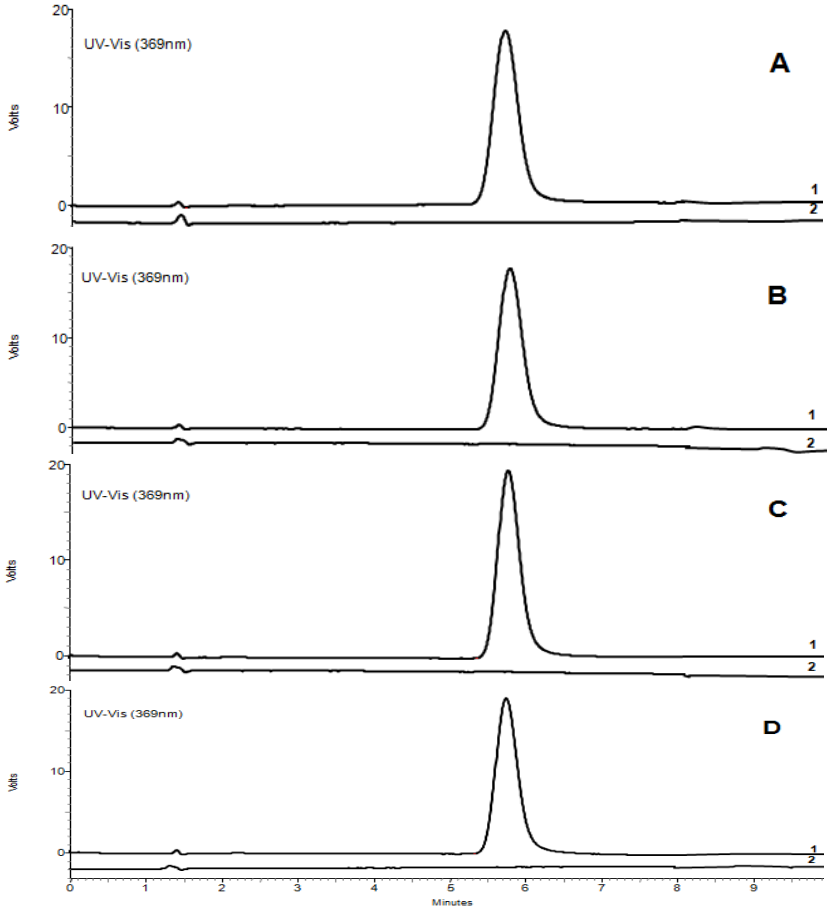

Figure 3. Typical chromatograms obtained after analysis of (1) QU-loaded lipid nanocarriers and (2) unloaded lipid nanocarriers. (A) QU-SLN and (B) QU-ME prepared using PEG 660-stearate, and (C) QU-SLN and (D) QU-NE prepared using Poloxamer 188 as surfactant.

The accuracy of the method was evaluated by determining the percentage of difference between the experimental mean concentration and the theoretical concentration of the quercetin in spiked unloaded lipid colloidal suspensions at three levels, (lower, medium, and upper concentration), corresponding to the final concentrations of 2.8, 4 and 5.2 $\mu g.mL^{-1}$. In this experiment, no significant differences were

observed between the quercetin concentrations in the colloidal suspensions analyzed ($P < 0.05$). The recovery values ranged from 97.0 to 103 % meeting the acceptance criterion for this study. The repeatability and intermediated precision were evaluated by assaying six samples of different lipid nanocarrier suspensions containing 4.0 $\mu g.mL^{-1}$ of QU. The intra-day and inter-day RSD values were lower than 3%, indicating an acceptable variability of the QU content for all analyzed lipid nanocarrier suspensions ($P < 0.05$).

Determination of QU content, encapsulation efficiency and recovery

To evaluate the effect of type and concentration of lipid and surfactant on quercetin loading, different formulations were prepared using an initial quercetin amount of 5 mg and a lecithin/lipid ratio of 1:10. The analysis of the entrapment efficacy is used to evaluate the amount of drug that is associated with the particles, since perhaps part of the drug may be dissolved in the dispersant phase. However, the quercetin concentration obtained after the supernatant analyses were under the limit of quantification of the HPLC method (< 0.109 µg/mL), indicating that most of the drug is associated with the carrier and that the entrapment efficiency is higher than 99%, regardless of the composition of the colloidal suspensions. Therefore, the ability of the different colloidal suspensions to carry QU was evaluated using drug content and recovery results (Table 2).

As seen in Table 2, the mean quercetin content and recovery varied from 17.82 to 236.48 µg.mL-1 and from 7.14 to 94.59%, respectively. The results also express the effect of the type and surfactant concentration on drug loading. When SLN were obtained, the increase in the concentration of PEG 660-stearate from 0.1% to 0.5% produced an increase in quercetin content by almost threefold. Lin and Kim (2002) observed a similar effect of the surfactant concentration on the loading of retinoic acid in SLN, and they have suggested that the drug may be associated with the particles by embedding in the surfactant layer rather than being incorporated in the innermost solid lipid[12]. Further increase in the PEG 660-stearate concentration was tested and similar values of QU content were obtained. In all cases, the QU concentration in the SLN prepared with PEG 660-stearate was higher than when prepared with Poloxamer 188 1%, in which only 7.14% of the drug added to the formulation was recovered in the colloidal suspension.

Table 2. Effect of the formulation composition on the quercetin-loading capacity of lipid-based colloidal suspensions. (n= 3).

	Quercetin content (μg.mL^{-1}) (R, %)*				
	PEG 660-stearate				Poloxamer 188
	0.1%	0.5%	0.75%	1%	1%
QU-SLN TS:CO (100:0)	73.7±0.5 (29.5±4.6)	216.7±1.5 (86.7±4.6)	203.4±7.5 (81.4±5.7)	188.1±5.6 (75.3±6.9)	17.8±0.4 (7.1±2.6)
QU-NLC TS:CO (75:25)	80.5±3.3 (32.2±6.6)	200.6±7.7 (80.2±2.4)	215.6±0.5 (86.2±4.2)	209.3±1.3 (83.7±4.7)	18.4±0.3 (7.4±3.9)
QU-NLC TS:CO (50:50)	82.8±1.1 (33.1±5.3)	215.5±4.1 (86.2±0.8)	220.2±12.0 (88.1±2.5)	219.2±7.0 (87.7±3.7)	21.3±3.0 (8.5±2.8)
QU-NLC TS:CO (25:75)	83.9±2.2 (33.6±5.2)	214.9±1.8 (85.9±6.1)	181.9±0.7 (72.7±4.4)	212.6±6.0 (85.0±6.9)	24.5±1.1 (9.8±2.7)
QU-NE TS:CO (0:100)	88.0±0.9 (35.2±2.9)	236.5±11.9 (94.6±5.8)	201.1±6.3 (80.4±4.3)	-	36.1±5.8 (14.4±3.5)
QU-ME TS:CO (0:100)		-	-	217.3±18.4 (86.9±5.3)	-

**In parenthesis: drug recovery (%)*

The effect of blending a liquid lipid (CO) and solid lipid (TS) on QU loading was also evaluated. When PEG 660-stearate 0.1% and Poloxamer 188 1% were used, the increase in the CO concentration in the blend caused an increase in QU loading, reaching a maximum value when only the liquid lipid was employed (QU-NE). This effect can be explained, in part, by the modification of the inner structure of TS nanoparticles by the addition of castor oil, which allowed the incorporation of higher amounts of the drug. On the other hand, the

higher solubilization capacity of the molten lipid can also explain the higher QU payload in the NLC[13,14]. This effect was not observed when higher concentrations of PEG 660-stearate were employed. Considering the standard deviation values obtained, mainly for QU-NE prepared with PEG 660-stearate 0.5% and for QU-ME, we can argue that almost all of the drug was incorporate into these lipid nanocarrier suspensions.

In an attempt to increase the QU loading in the different lipid-based colloidal suspensions, the lecithin to lipid ratio of the formulations was altered. No changes in mean particle size were observed with the change in the lecithin to lipid ratio from 1:10 to 1:5 (data not shown).

As seen in Table 3, the increase in lecithin amount caused an increase in the particle payload in most cases. SAXS and particle size measurements have indicated that an enrichment of lecithin on the surface of the particles occurs when increasing amounts of this surfactant are employed in the preparation of SLN[15]. Therefore, the increase observed in quercetin payload is more likely related to the drug solubilization in the surfactant layer than to its incorporation into the inner solid lipid matrix.

As described below, the use of a higher concentration of PEG 660-stearate led the formation of a lipid nanostructured drug delivery system like a microemulsion. It is widely known that microemulsions display a great capacity to solubilize lipophilic drugs in the oil phase. Furthermore, these systems display a higher physical stability when compared to emulsions and a potential to enhance drug absorption and bioavailability.

Table 3. Effect of lecithin-to-lipid ratio on quercetin-loading capacity of lipid-based colloidal suspensions.

Lecithin: Lipid ratio	Quercetin content (μg.mL^{-1}) (R, %)*					
	PEG 660-stearate (0.1%, w/v)			Poloxamer 188 (1%, w/v)		
	SLN TS:CO (100:0)	NLC TS:CO (50:50)	NE TS:CO (0:100)	SLN TS:CO (100:0)	NLC TS:CO (100:0)	NE TS:CO (100:0)
1:10	73.7±0.5 (29.5±4.6)	82.8±1.1 (33.1±5.5)	88.0±0.9 (35.2±3.0)	17.8±0.4 (7.1±2.6)	21.3±3.0 (8.5±2.8)	36.1±5.8 (14.4±3.5)
1:5	70.2±10.5 (28.1±3.8)	101.8±12.1 (40.7±4.8)	110.5±9.8 (44.2±2.5)	45.8±10.6 (18.3±3.5)	66.1±6.6 (26.4±2.9)	71.9±6.5 (28.8±1.8)

**In parenthesis: drug recovery (%)*

Thus, we were interested in investigating what effect the initial amount of QU has on microemulsion payload capacity (Table 4). The drug content in the colloidal suspensions was significantly increased in association with the increment in the amount of QU initially added to the organic phase, but was accompanied by a decrease in drug recovery. When 10 mg of QU were added, an increase of around 1,300 times in QU concentration was observed when compared to its water solubility (0.33 µg/mL) without the appearance of drug precipitates in the formulation, and so it was considered the optimal initial amount of drug to be used.

Table 4. Effect of the initial amount of quercetin added to the formulations on microemulsion payload.

Initial amount of quercetin	Drug content ($\mu g.mL^{-1}$)	Recovery (%)
5 mg	217.3±18.4	86.9±5.3
10 mg	432.6±19.2	86.5±6.8
15 mg	583.6±8.1	77.8±7.4
20 mg	699.2±53.3	69.9±4.7

Zeta potential measurements

Negatively charged lipid nanocarriers were obtained for all formulations, as would be expected since lecithin molecules are negatively charged. When SLN, NLC, and NE were obtained, the zeta potential values varied from -29.8 to -41.7 mV. Greater values were observed when Poloxamer 188 was used, perhaps due to the reduced ability of this surfactant to hide the surface charge of the particles (Figure 4). When the microemulsion was obtained, the zeta potential was significantly reduced to values close to neutral (-2 mV) (Figure 5), probably due to the complete hiding of the negative charges by the polyethylene glycol chains of the PEG 660-stearate. It is currently accepted that zeta potentials higher than |30| mV are required for full electrostatic stabilization. However, this rule does not strictly apply to systems which contain steric stabilizers. In our case, the low zeta potential values did not represent a low stability of the system. The use of highest concentration of PEG 660-stearate to obtain microemulsions decreases the zeta potential due to the shift in the shear plane of the particle, a steric stabilization was produced by this surfactant[16].

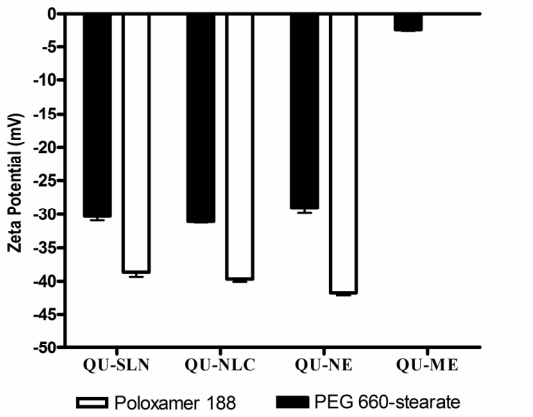

Figure 4. Zeta potential results. QU-SLN (TS:CO 100:0), QU-NLC (TS:CO 50:50), and QU-NE (TS:CO 0:100), were prepared with the lecithin to lipid ratio of 1:5 and 0.1% PEG 660-stearate or 1% Poloxamer 188. QU-ME (TS:CO 0:100), was prepared with the lecithin to lipid ratio of 1:10 and 1% PEG 660-stearate.

In vitro quercetin release

Figure 5 shows the *in vitro* release kinetics of quercetin from the different lipid-based nanocarriers in a 20:80 (v/v) PEG 400:distilled water (pH 4.0) mixture at 37 °C. These experiments were carried out in sink conditions, since the maximum concentration of quercetin that could be reached in the release medium corresponded to 0.54% of its saturation concentration (278 μg/mL). Quercetin release profiles were characterized by biphasic kinetics, consisting of a faster release in the first 8 hours, followed by a sustained release of the drug over 24 hours in most cases. Hu *et al.* (2005) demonstrated that the drug release rate was faster with the increase in oil content concentration used to prepared nanoparticles[17]. In our study, this effect was not observed. When Poloxamer 188 1% was used as surfactant, no difference in the drug release rate between the formulations was observed, reaching values of around 45% after 8 h of assay (Figure 5A). For these lipid-based formulations, the release of QU occurred at the same rate regardless of the type of nanocarrier, but differed from the release profile obtained for free drug, indicating that the particle was able to control the release of the drug.

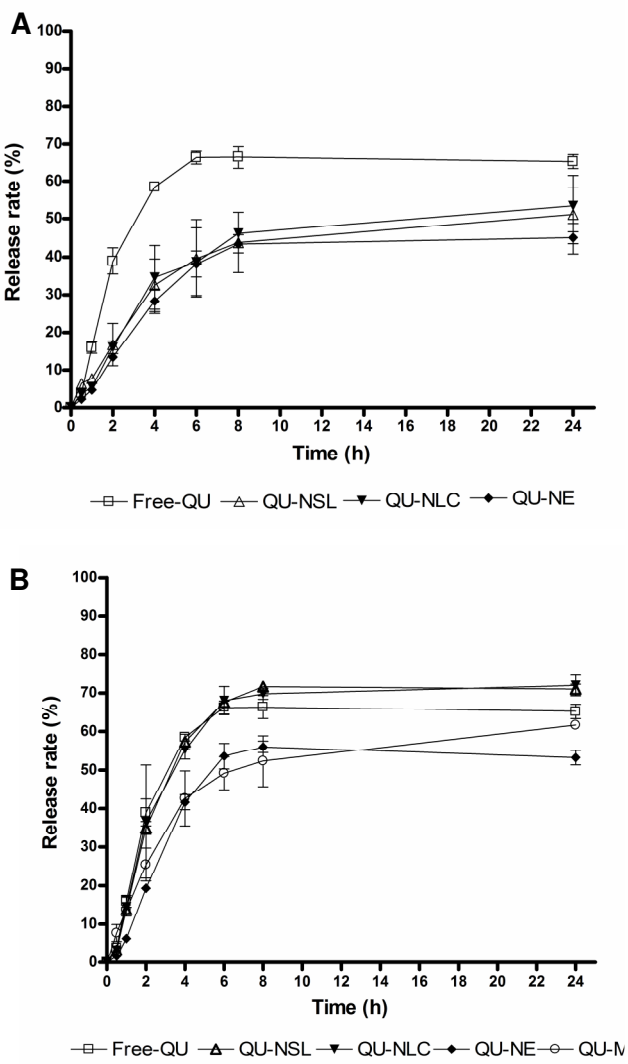

Figure 5. Cumulative percentage of QU released from lipid-based nanocarriers prepared with (A) Poloxamer 188 1% and (B) PEG 660-stearate 0.1% (SLN, NLC, and NE) and 1% (ME). QU-SLN (TS:CO 100:0), QU-NLC (TS:CO 50:50), and QU-NE (TS:CO 0:100), were prepared using a 1:5 lecithin to lipid ratio and QU-ME (TS:CO 0:100) was prepared using a 1:10 lecithin to lipid ratio.

On the other hand, when PEG 660-stearate 0.1% was employed, the release of QU from SLN (TS:CO 100:0) and NLC (TS:CO 50:50) was faster than from NE (TS:CO 0:100). In this case, 71%, 69%, and 55% were released from SLN, NLC, and NE, respectively, after 8 h of assay (Figure 5B). The release profiles obtained from SLN and NLC were very close to those obtained when free QU was assayed (66% in 8 h). These results corroborate the premise that a fraction of QU is located on the surface or closer to the surface than to the inner core of the particles as previously described in this paper.

The mixture of the surfactants lecithin and PEG 660-stearate probably self-assembled into mono or multilayers, forming a nanoparticle shell displaying high capacity to solubilize quercetin. In contrast, the release of QU from NE (Figure 5B) could be controlled to some extent, occurring probably by the diffusion of the dissolved drug in the oil towards the medium. A similar kinetic profile was obtained when drug release from microemulsion was assayed. However, for a complete comprehension of these phenomena, structural studies of the particles still need to be performed.

Conclusions

In the present study, we demonstrated that SLN, NLC, NE, and ME can be obtained by the hot solvent diffusion method, varying only in formulation composition. These lipid-nanocarriers differed not only in their physicochemical properties but also in their abilities to carry and to control the release of the quercetin. A noteworthy result was that microemulsion was able to solubilize quercetin in large scale, and it seemed to be a promising approach to increase the oral bioavailability of this drug. Studies still need to be performed to comprehensively elucidate the formation of microemulsions from PEG 660-stearate and its effects on QU absorption after oral administration.

Acknowledgements

This study was supported by FAPESC/CNPq/MCT. Cristiana Lima Dora received a grant from CAPES.

References

[1] Fresco P., F. Borges, C. Diniz & M.P.M. Marques (2006) *Med Res Rev*. 1-20.

[2] Ratnam D.V., D.D. Ankola, V. Bhardwaj, D.K. Sahana & M.N.V.R. Kumar (2006) *J Control Release.* **113**:189–207.
[3] Soobrattee M.A., V.S Neergheen, A. Luximon-Ramma, O.I. Aruoma & T. Bahorun (2005) *Mut Res*. **579**:200-213.
[4] Hauss D.J.(2007) *Adv Drug Deliv Rev*. **59** (7):667-76.
[5] Pouton C.W. & C.J. Porter (2008) *Adv Drug Deliv Rev*. **60** (6):625-37.
[6] Wissing S.A., O. Kayser & R.H Muller (2004) *Adv Drug Deliv Rev*. **56**:1257-1272.
[7] Chakraborty S., D. Shukla, B. Mishra & S. Singh (2009) *Eur J Pharm Biopharm*. **73**(1):1-15.
[8] Manjunath K., J.S. Reddy & V. Venkateswarlu (2005) *Methods Find. Exp. Clin. Pharmacology*. **27**:127-144.
[9] ICH (2005) Harmonised tripartite guideline: validation of analytical procedures: text and methodology Q2 (R1).
[10] Hu F.Q., H. Yuan, H.H. Zhang & M. Fang (2002) *Int. J. Pharm*. **239**, 121–128.
[11] Momic T., J. Savic, U. Cernigoj, P. Trebse & V. Vasic (2007) *Collection of Czechoslovak Chemical Communications*. **72**(11):1447-1460.
[12] Lim S.J. & C.K. Kim (2002) *Int J Pharm*. **243**:135-46.
[13] Westesen K., H. Bunjes & M.H.J Koch (1997) *Journal Control Release*. **48**: 223-236.
[14] Garcia-Fuentes M., M.J. Alonso & D. Torres (2005) *J colloid interface sci*. **285**:590-598.
[15] Schubert M.A., M. Harms & C.C Müller-Goymann (2006) *Eur J Pharm Sci*. **27**:226-36.
[16] Heurtault B., P. Saulnier, B. Pech, J.E. Proust & J.P Benoit (2003) *Biomaterials*. **24**:4283-4300.
[17] Hu F.Q., S.P. Jiang, Y.Z. Du, H. Yuan, Y.Q Ye & S. Zeng (2005) *Colloids and Surf B Biointerfaces*. **45**:167–173.

Capítulo 3

Caracterização estrutural e físico-química dos nanocarreadores lipídicos

No capítulo 2 desta tese foi demonstrado que diferentes tipos de nanocarreadores lipídicos podem ser obtidos pela técnica de difusão do solvente a quente, alterando unicamente a composição da formulação. Estes sistemas exibiram diferentes capacidades em incorporar a quercetina. A triestearina foi empregada para obter nanopartículas lipídicas sólidas (NLS) e o óleo de rícino para preparação de nanoemulsões (NE) e microemulsões (ME). Além disso, carreadores lipídicos nanoestruturados (CLN) foram obtidos quando a mistura dos dois lipídios foi utilizada em diferentes proporções. Para todas as formulações, estearato de PEG 660 e poloxamer 188 foram usados como surfactante hidrofílico e lecitina de soja hidrogenada como surfactante lipofílico. Os resultados demonstraram que o teor de quercetina aumentou com o aumento da concentração de óleo de rícino na formulação. No entanto, a maneira pela qual as propriedades estruturais das partículas afetaram essa maior capacidade de incorporação da QU ainda precisa ser analisada.

Desta forma, neste capítulo foram investigadas as características físico-químicas e estruturais dos nanocarreadores lipídicos desenvolvidos anteriormente que apresentaram melhores resultados.

Na primeira parte deste capítulo foi realizado um estudo com o intuito de compreender melhor a formação da ME desenvolvida anteriormente. Para isso, emulsões nanométricas óleo em água (o/a) foram obtidas empregando óleo de rícino na fase oleosa e estearato de polietilenoglicol 660 (estearato de PEG 660) e fosfatidilcolina de soja hidrogenada como surfactante e co-surfactante, respectivamente. O efeito da concentração do estearato de PEG 660 foi avaliado no que diz respeito ao tamanho e estrutura das partículas das emulsões nanométricas formadas. Várias técnicas de caracterização foram empregadas, tais como, espalhamento de luz dinâmico, microscopia eletrônica de transmissão, crio-microscopia eletrônica de transmissão e espalhamento de raios-x a baixos ângulos. Além disso, a capacidade destes sistemas de solubilizar a quercetina foi avaliada. Para isto um método de espectroscopia ultra-violeta foi desenvolvido e validado. Os resultados deste trabalho são apresentados na forma de um artigo científico a ser submetido ao *Journal of Colloidal and Interface Science.*

Na segunda parte deste capítulo, outro estudo foi realizado com objetivo de investigar as características físico-químicas e estruturais dos

outros tipos de nanocarreadores desenvolvidos anteriormente (NLS, CLN e NE). Os componentes utilizados foram os mesmos descritos no capítulo 2 e os nanocarreadores também foram preparados pela técnica de difusão do solvente a quente. A caracterização apropriada desses nanocarreadores é uma etapa essencial no processo de desenvolvimento de uma nova forma farmacêutica e se torna difícil em função do tamanho reduzido das partículas. Para que a interpretação dos dados obtidos fosse feita de forma correta foi necessário correlacionar resultados de diferentes métodos de análise, incluindo espalhamento de luz dinâmico (DLS), calorimetria exploratória diferencial (DSC), difração de raios-x (WAXS) e espalhamento de raios-x a baixos ângulos (SAXS). Além disso, análises morfológicas foram realizadas por microscopia de força atômica (AFM), microscopia eletrônica de transmissão (TEM) e crio-microscopia de transmissão (cryo-TEM). Estes resultados são apresentados em forma de um artigo científico a ser submetido na revista *Langmuir.*

Publicação 2. *Poly (ethylene glycol) hydroxystearate-based nanosized emulsions:Effect of surfactant concentration on their formation and ability to solubilize quercetin*

Poly (ethylene glycol) hydroxystearate-based nanosized emulsions: Effect of surfactant concentration on their formation and ability to solubilize quercetin

Cristiana L. Dora[1], Luis F. C. Silva[1], Jean-Luc Putaux[2], Yoshiharu Nishiyama[2], Isabelle Pignot-Paintrand[2], Elenara Lemos-Senna[1*] and Redouane Borsali[2,*]

[1] Laboratório de Farmacotécnica, Departamento de Ciências Farmacêuticas, Centro de Ciências da Saúde, Universidade Federal de Santa Catarina, Campus Universitário Trindade, Bloco K, sala 107, 88040-900, Florianópolis, SC, Brazil.
[2] Centre de Recherches sur les Macromolécules Végétales (CERMAV-CNRS), BP 53, F-38041 Grenoble Cedex 9, France - *affiliated with Université Joseph Fourier and member of the Institut de Chimie Moléculaire de Grenoble*

Corresponding authors:
lemos@ccs.ufsc.br Tel:+55 48 37215067, fax: +55 48 37219350
borsali@cermav.cnrs.fr Tel:+33 04 76 03 76 40, fax:+33 04 76 54 76 29

Abstract

Quercetin is a natural compound that has shown several biological activities. However, this drug displays a poor water solubility and, consequently, low biological availability. In this study, oil-in-water nanosized emulsions were obtained by using castor oil as oily phase and poly(ethylene glycol) (660)-12-hydroxystearate (PEG 660-stearate; Solutol HS15®) and soybean phosphatidylcholine as surfactants. The effect of the PEG 660-stearate concentration on the droplet size of the emulsions and on the ability of these systems to load quercetin was investigated. Dynamic light scattering (DLS), transmission electron microscopy (TEM), cryo-TEM, and small-angle X-ray scattering were used to characterize the nanosized emulsions. We have demonstrated that a critical concentration of PEG 660-stearate (2.5 wt.%, surfactant-to-oil weight ratio of about 5) was needed to obtain colloidal dispersions displaying clear and isotropic appearance. This colloidal dispersion did not show birefirenge, was constituted by a monodisperse population of 20 nm-large droplets, and exhibited excellent stability. Besides, this system was able to solubilize five times more quercetin than nanoemulsions prepared using 0.25 wt% PEG 660-stearate. SAXS results indicate an internal structure of a nanosized emulsion with a core-shell spherical structure. In addition to the fast diffusion of the organic solvent towards the aqueous phase, the heating of the system at a temperature above the PEG 660-stearate´s phase inversion temperature (PIT) was essential to promote nanoemulsification and to obtain clear and isotropic colloidal dispersions.

Key words: nanoemulsion, quercetin, PEG 660-stearate, dynamic light scattering, TEM, cryo-TEM, SAXS

1. Introduction

The development of new dosage forms from lipophilic drugs represents a challenge for formulators, since these drugs exhibit slow dissolution and/or release rate in the biological fluids, which is the rate-limiting step for their absorption and systemic availability [Gupta *et al.,* 2005]. One of the approaches to deal with the poor water solubility of drugs consists in their incorporation in lipid-based nanocarriers. These drug delivery systems comprise solid or liquid lipids, or mixtures of both, at various ratios, displaying a wide range of particle sizes. Their many advantages over polymer-based drug delivery systems are their excellent stability and tolerability, as well as feasibility of scaling up the production. Besides their targeting property, such systems are characterized by their ability to protect drug from degradation, to improve drug bioavailability, and to control drug release [Li *et al*., 2009a].

Quercetin (QU) is a naturally occurring polyphenol that displays anti-inflammatory, antibacterial, antioxidant, antiangiogenic and antitumor activities [Stavric, 1994]. However, QU exhibits a very low bioavailability following oral administration, which was found to be less than 17% in rats and 1% in humans. This low bioavailability has been partly attributed to its poor water solubility, which restrains its absorption in the gastrointestinal tract [Ratman *et al.*, 2006; Fresco *et al.,* 2006]. Several approaches have been developed in order to increase the oral bioavailability of QU, including the synthesis of a water-soluble derivatives [Mulholland, 2001], the complexation with cyclodextrins [Pralhad *et al.,* 2004], and the incorporation in solid lipid nanoparticles or liposomes [Priprem *et al*., 2008; Li *et al*., 2009b]. However, most of them have failed to increase QU bioavailability or they exhibited low stability towards sterilization and storage.

In a previous study, we have demonstrated that lipid-based nanocarriers (*i.e.*, solid lipid nanoparticles, nanostructured lipid carriers, nanoemulsions) could be obtained using the hot solvent diffusion method, by only changing the composition of the formulations. This method is based on the formation of a hot submicronic emulsion after the fast diffusion of a water-miscible organic solvent towards a previously heated aqueous phase [Hu *et al.,* 2002]. These lipid-based nanocarriers displayed different abilities to load QU, depending on the

type of lipid (solid or liquid) and the type and concentration of the used surfactant. In particular, oil-in-water nanosized emulsions were obtained by using castor oil as oily phase and poly(ethylene glycol) (660)-12-hydroxystearate (PEG 660-stearate; Solutol HS15®) and soybean phosphatidylcholine as surfactants. While the formation of milky colloidal dispersions was verified at lower PEG 660-stearate concentrations, optically transparent aqueous dispersions displaying reduced droplet sizes (about 20 nm) were produced by using 2.5 wt% PEG 660 stearate. Besides, this colloidal system exhibited a higher ability to incorporate QU, increasing its water solubility by about 1,300 times, supporting the premise of microemulsion formation.

Since these systems have shown to be promising nanocarriers to deliver QU, in this study, we have investigated the effect of the PEG 660-stearate concentration on the droplet size distribution of the nanosized emulsions, as well as the particle structure when using the hot solvent diffusion method. Complementary techniques such as polarized light microscopy, dynamic light scattering (DLS), zeta potentiometry, small-angle x-ray scattering (SAXS), transmission electron microscopy (TEM) and cryo-TEM were used to characterize the colloidal dispersions.

2. Materials and Methods

2.1. Materials

Quercetin and castor oil (CO) were purchased from Natural Pharma (São Paulo, Brazil). Hydrogenated soybean phosphatidylcholine (SbPC; Lipoid S75-3N) was purchased from Via Pharma (São Paulo, Brazil). Poly(ethylene glycol) (660)-12-hydroxystearate (PEG 660-stearate; Solutol HS15®) was kindly donated by BASF (Trostberg, Germany). Methanol, ethanol, acetone, and other chemicals used were analytical reagent grade.

2.2. Preparation of the colloidal dispersions

To summarize the colloidal preparation, 10 mg of SbPC and 100 mg of CO were completely dissolved into 5 mL of a mixture of

acetone:ethanol (60:40, v/v) at 60°C. The resulting organic solution was quickly poured into 50 mL of an aqueous solution containing a PEG 660-stearate solution at different concentrations, kept under magnetic stirring at 82°C. The resulting colloidal dispersions were then cooled down to room temperature. The organic solvent was evaporated under reduced pressure, and the final volume was adjusted to 20 mL to obtain final PEG-660 stearate concentrations varying from 0.25 to 5.0 wt%. Finally, the colloidal dispersions were filtered through an 8 μm filter paper. For the preparation of QU-loaded colloidal dispersions, 10 or 20 mg of the drug was added to the organic phase of the formulation.

2.3. Determination of quercetin content in the colloidal suspensions

The QU content was determined by UV spectroscopy using a Perkin-Elmer Lambda 10 UV/VIS spectrophotometer at 375 nm, after complete dissolution of the colloidal suspensions in methanol. The UV method was previously validated according to the ICH (2005). The calibration graph for QU was linear over the range of 1 to 20 $\mu g.mL^{-1}$ with a correlation coefficient of 0.999. The calculated LOD (limit of detection) and LOQ (limit of quantification) were 0.46 $\mu g.mL^{-1}$ and 1.39 $\mu g.mL^{-1}$, respectively, indicating that the method was sufficiently sensitive to determine the QU content in the colloidal suspensions. The specificity of the assay was confirmed by the individual analysis of the unloaded colloidal suspensions. The precision of the method was evaluated and all relative standard deviation (R.S.D) were below 3%, indicating an acceptable intra-day and inter-day variability of the QU content for the colloidal dispersions.

2.4. Particle size analysis

The size distribution, mean particle size and polydispersity index (PDI) of the colloidal suspensions were determined by Dynamic light scattering (DLS) using a Zetasizer Nanoseries (Marvern Instruments, UK) and an ALV 5000 (ALV-Langen, Germany). The samples were diluted in ultrapure Milli-Q® water. Each size analysis was measured during 300 sec and the temperature was set to 25°C. The analysis was performed using a single 173° scattering angle when the Zetasizer equipment was used. In the case of DLS measurements

performed with ALV-5000, the scattered light was measured at different angles ranging from 50° to 140°. The hydrodynamic radius was determined using Stokes-Einstein's equation, $R=(\kappa_B T/6\pi\eta D)$ where κ_B is Boltzmann's constant (J/K), T is the temperature (in K), D is the diffusion coefficient and η is the viscosity of the medium – water in this case (η=0.89 cP at 25°C).

2.5. Zeta potential measurement

Zeta potential (ZP) was determined by laser-Doppler anemometry using a Zetasizer Nanoseries (Marvern Instruments, UK). The samples were diluted in ultrapure Milli-Q® water and placed in the electrophoretic cell where an alternating voltage of ±150mV was applied. The ζ potential values were calculated as mean electrophoretic mobility values using Smoluchowski's equation.

2.6. Polarized light optical microscopy

A Zeiss Axioplan 2 optical microscope equipped with a CCD camera was used to evaluate the microscopic appearance of the nanosized emulsions. A drop of sample was placed between a cover slip and a glass slide and examined under polarized light.

2.7. Transmission electron microscopy

Drops of the dispersions (diluted 1000x in ultrapure Milli Q® water) were deposited on a carbon-coated copper grids and stained with 2% uranyl acetate. According to the procedure described elsewhere [Durrieu *et al.,* 2004], specimens for cryo-TEM were prepared by quench-freezing thin liquid films of the dispersions into liquefied ethane (-171°C). They were mounted in a Gatan 626 cryoholder cooled with liquid nitrogen and transferred to the microscope. The specimens were observed at low temperature (-180°C), using a Philips CM200 'Cryo' microscope operating at 80 kV. A low-dose procedure was used to reduce radiation damage in the areas of interest before actual image recording on Kodak SO163 films.

2.8. Small-angle X-ray scattering (SAXS)

SAXS measurements were performed at the SAXS2 beamline of the Laboratório Nacional de Luz Síncrotron (LNLS, Campinas, Brazil) and at the D2AM beamline of the European Synchrotron Radiation Facility (Grenoble, France). At SAXS2, horizontally focused beam obtained through an asymmetrically cut and bent Si (111) monochromator (λ = 1.488 Å), and a vertical linear gas filled position sensitive detector placed at 1.5 m away from the sample position were used. A scattering vector ranging from 0.1 - 2.26 nm^{-1} was covered. At D2AM, a 8 keV (1.53 Å) beam focused with vertical and horizontal bending mirrors, and a 2D CCD detector placed at 1.7 m away from the sample position were used, covering a *q*-range from 0.1 to 1 nm^{-1}. The measurements of sample 6 were carried out without dilution at SAXS2 and with a series of dilutions at D2AM. Samples were put in borosilicate glass capillaries with 1.5 mm outer diameter. A capillary filled with water was also x-rayed to correct for background scattering. Since the results did not show any anisotropic behavior, the scattered intensity data was radially averaged after correction of detector distortion.

3. Results

3.1. Dynamic light scattering

In order to investigate the effect of PEG 660-stearate concentration on the size distribution of the QU-loaded nanosized emulsions, different colloidal dispersions were prepared at different concentration of this surfactant ranging from 0.25 to 5.00 wt%, but keeping unchanged the concentration of the other constituents of the formulation (see Table 1).

No difference in size and PDI were observed for unloaded and QU-loaded dispersions. The resulting mean droplet sizes and polydispersity indices for the nanosized emulsions are given in Table 2. The dynamic light scattering correlation functions and the corresponding hydrodynamic radii (*R*h) of the colloidal dispersions obtained using a single 90° scattering angle are shown in Figure 1.

Table 1. Composition of the nanosized emulsions prepared by the hot solvent diffusion method

Sample	Castor oil (wt. %)	SbPC (wt.%)	PEG 660-stearate (wt. %)	Oil to PEG 660-stearate weigth ratio	Water wt.%	QU content ($\mu g.mL^{-1}$)[a]	QU content ($\mu g.mL^{-1}$)[b]
1	0.5	0.05	0.25	0.5	99.20	88.0	82.1
2	0.5	0.05	1.25	2.5	98.20	236.5	347.2
3	0.5	0.05	1.75	3.5	97.70	453.5	781.2
4	0.5	0.05	2.00	4.0	97.45	494.4	877.4
5	0.5	0.05	2.25	4.5	92.25	433.1	910.8
6	0.5	0.05	2.50	5.0	96.95	469.2	757.1
7	0.5	0.05	3.00	6.0	96.45	454.7	1081.3
8	0.5	0.05	3.75	7.5	95.70	468.6	1006.0
9	0.5	0.05	4.50	9.0	94.95	428.3	888.9
10	0.5	0.05	5.00	10.0	94.45	465.0	918.2

[a] *QU content after initial addition of 10mg or* [b] *20mg of quercetin in the organic phase.*

Table 2. Mean droplet diameter and polydispersity index (PDI) obtained for QU-loaded nanosized emulsions.

Sample	Mean size ALV 5000 (nm)[a] (PDI)	Mean size Zetasizer (nm)[b] (PDI)
1	142.6 (0.102)	127.4 (0.08)
2	153.6 (0.124)	136.2 (0.13)
3	***	***
4	***	***
5	***	***
6	19.5 (0.162)	20.1 (0.189)
7	17.7 (0.088)	17.4 (0.064)
8	16.2 (0.063)	15.9 (0.056)
9	15.3 (0.066)	15.3 (0.058)
10	15.5 (0.064)	15.3 (0.047)

[a] *scattering angle was 90°,* [b] *scattering angle was 173°*

**** samples displaying more than one peak of particle size*

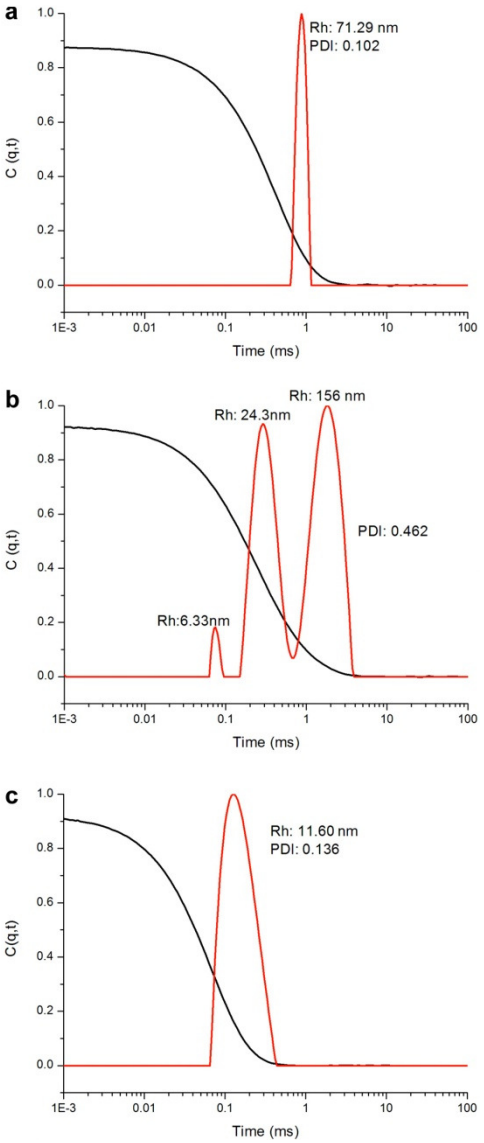

Figure 1. Correlation function and hydrodynamic radius (*R*h) obtained at 90^{o} scattering angle for samples containing (a) 0.25 wt.%, (b) 2.00 wt.%, and (c) 2.50 wt.% PEG 660-stearate.

For 0.25 and 1.25 wt% PEG 660-stearate concentration (surfactant-to-oil weight ratio ≤ 2.5), monodisperse colloidal dispersions displaying droplet sizes higher than 120 nm were obtained (Figure 1a) (samples 1 and 2, see Table 1). Using PEG 660-stearate concentrations from 1.75 wt.% to 2.25% wt% (surfactant-to-oil weight ratio varying from 3.5 to 4.5; samples 3, 4, and 5), the presence of more than one distribution of particle sizes is observed, evidencing the formation of polydisperse colloidal dispersions (see Figure 1b) and the mean particle size could not be determined in the Zetasizer or ALV 5000 instruments.

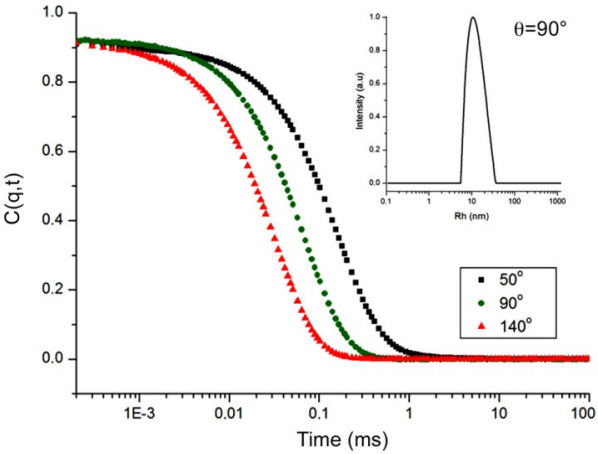

Figure 2. Correlation function and hydrodynamic radius (Rh) obtained at different scattering angles and *R*h obtained at 90°, for sample containing 2.50 wt.% PEG 660-stearate (sample 6).

At these intermediary surfactant concentrations, the colloidal suspensions appeared to be composed of oil droplets stabilized by the hydrophilic surfactant and by surfactant micelles, indicating the coexistence of different nanostructures in the samples. When the PEG 660-stearate concentration is increased to 2.5 wt% (surfactant-to-oil weight ratio of 5.0; sample 6), a single size distribution at about 10 nm is observed (see Figure 1c), which we believe corresponds to be the

mean size for a monodisperse dispersion of PEG 660-stearate swollen micelles. The particle size and size distribution of this sample were also evaluated by DLS analysis at different scattering angles. Figure 2 shows the correlation functions obtained at the scattering angles θ = 50°, 90°, and 140°, and the *R*h obtained at 90°.

The monodisperse characteristic of this sample was confirmed, since all polydispersity indices were below 0.3 for the different measured scattering angle (see Table 3). Further increasing of the PEG 660-stearate concentration above 2.5 wt% merely provoked a decrease in the hydrodynamic radius of the droplets, with however maintaining their monodispersity (samples 7 to 10). This result can be attributed to the shift of the mean droplet size of the particle size distribution due to the appearance of PEG-stearate micelles (about 10 nm in diameter) in the colloidal dispersions (Table 2).

Table 3. Hydrodynamic radius (*R*h) and polydispersity index (PDI) of the colloidal dispersion containing 2.5 wt.% of PEG 660-stearate (sample 6) determined by DLS at different scattering angles.

Scattering angle (°)	*R*h (nm)	PDI
140	9.69	0.127
130	9.64	0.134
120	9.65	0.134
110	9.66	0.137
100	9.63	0.185
90	9.75	0.162
80	9.76	0.172
70	9.80	0.190
60	9.89	0.208
50	10.01	0.241

3.2. Zeta potential

Figure 3 shows the zeta potential values of the colloidal dispersions obtained with different concentrations of PEG 660-stearate. Zeta potential values ranged from -2 to -29 mV, depending on surfactant concentration, and the result was not affected by the incorporation of

QU into the formulations, indicating that the drug is preferentially dissolved in the oily phase.

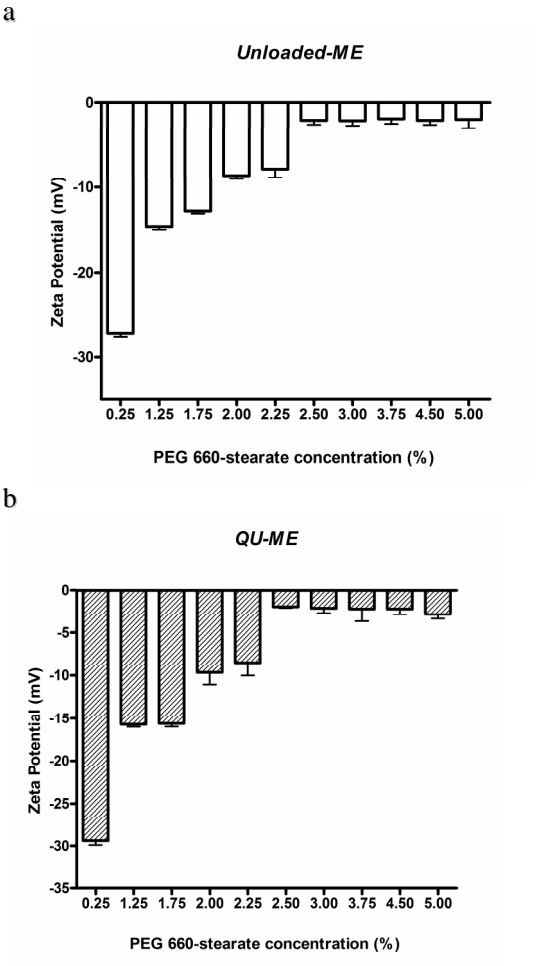

Figure 3. Potential zeta values for (a) unloaded and (b) QU-loaded colloidal dispersions.

At low surfactant concentrations, droplets exhibiting negatively charged surface were obtained due to the presence of phosphatidylcholine at the oil/water interface. A further increase in PEG 660-stearate in the formulations resulted in the decrease in zeta potential, reaching values close to zero. Sample 6 was checked for stability after 3-months of storage at room temperature and at 4°C and no variation in particle size was observed (data not shown). Such results, indicated that stabilization was obtained by the steric effect produced by the presence of polyethylenoglycol chains of PEG 660-stearate at droplet surface.

3.4. Determination of quercetin content

The colloidal suspension content was calculated after the determination of the drug concentration in the methanol solutions by UV. As seen in Table 1, the QU content in the colloidal dispersions was affected by the concentration of PEG 660-stearate. When 10 mg of QU was added, for the samples prepared with 0.25 and 1.25 wt% PEG 660-stearate (sample 1 and 2), the mean quercetin content was 88.0 and 236.7 $\mu g.mL^{-1}$, corresponding to drug recovery of 17.6 and 47.3%, respectively, taking into account the amount of drug initially added to the formulations. However, for surfactant concentrations higher than 1.75 wt%, QU content was increased to values varying from 430 to 490 $\mu g.mL^{-1}$, which correspond to the solubilization of almost all drug added to the formulations. Similar results were obtained when QU initial addition was 20 mg, In view of these results, it seems that quercetin is located in the different formed nanosized structures (i.e., micelles or swollen micelles), which in turn, depends on the surfactant concentration of the formulations. Taken into account that the QU solubility in an aqueous 2.5 wt% PEG 660-stearate solution was about 310 $\mu g.mL^{-1}$, we can state that the increasing of the QU solubility exhibited by the formulation prepared using this surfactant concentration (formulation 6) is related to the solubilization of the drug in the inner oily phase of the nanosized emulsion, rather than by the surfactant micelles.

3.5. Cross-polarized light microscopy

The colloidal dispersion containing 2.5 wt% PEG 660-stearate (sample 6) was a clear yellow liquid that appeared dark under cross-polarized light microscopy (no birefringence) and was therefore classified as isotropic dispersion of spherical droplets, supporting the assumption of a formation of a microemulsion system.

3.6. Transmission electron microscopy

TEM and cryo-TEM images of samples 1 (0.25 wt.% of PEG 660-stearate) and 6 (2.5 wt% PEG 660-stearate) are shown in Figure 4. Sample 1 contains polydisperse spheroidal particles (Figure 4a). The dark outline seen on the bigger particles is due to the fact that the film of dry uranyl acetate is rather thick and only the top part of the spherical particle protrudes out of the stain. The size distributions in negatively stained (Figure 4a) and ice-embedded (Figure 4b) preparations are visually similar suggesting that the particles did not significantly deform during drying.

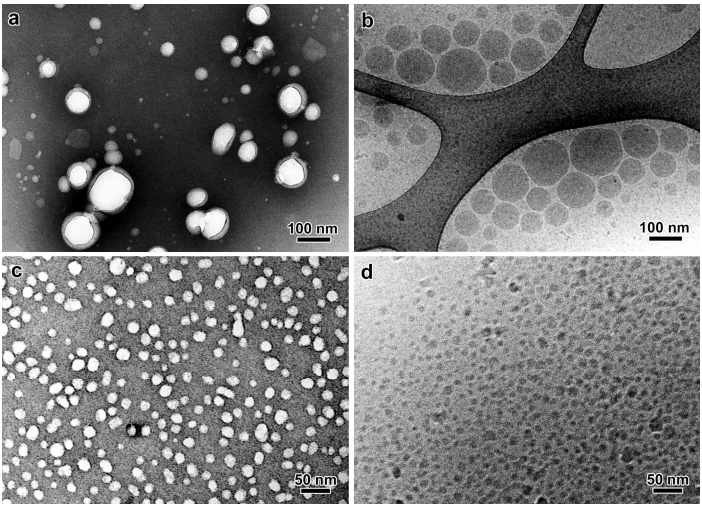

Figure 4. TEM (a; c) and Cryo-TEM (b; d) images for colloidal dispersions: (a; b) 0.25 wt.% PEG 660-stearate (sample 1) and (c;d) 2.5 wt.% PEG 660-stearate (sample 6).

Some limited particle deformation can be seen in the cryo-TEM image due to the confining effect inside the thin film of vitreous ice. Increasing the PEG 660-stearate concentration to 2.5 wt% yielded smaller particles (10-20 nm). The negatively stained particles shown in Figure 3c are slightly larger than those observed in vitreous ice (Figure 4d), suggesting that the particles may have flattened to some extent during drying. The mean size in both samples is in good agreement with light scattering measurements. In addition, the cryo-TEM observations corroborate the results deduced from the polarized light micrographs: the sample 6 is an isotropic dispersion of spherical particles.

3.7. Small-angle X-ray scattering

The scattering intensities of all investigated samples showed a broad peak at around 0.5 nm^{-1}, which did not change by varying the concentration (Figure 5). This result indicates an internal structure of the nanosized emulsion, which is not a uniform sphere. Thus, a core-shell spherical structure model with the core having electron density closer to the solvent was used to fit the intensity data. Using the radius of the whole sphere r1 and the radius of the core r2 as well as an electron density difference of the core α, the scattering amplitude of a core-shell sphere can be described using the following expression:

$$F(q) = j1(qr1)/qr1 - \alpha\, j1(qr2)/qr2) \qquad \text{(eq. 1)}$$

where j1 is the spherical Bessel function.

The curve was fitted from 0.1 to 1.0 nm-1, but the feature at higher angle could not be reproduced with this model. This is probably due to an oversimplification of the internal structure. Radius of the sphere 11.6 nm is in good agreement with hydrodynamic radius and TEM observation. The core can be tentatively attributed to castor oil which has a density of 0.961 g/cm^3.

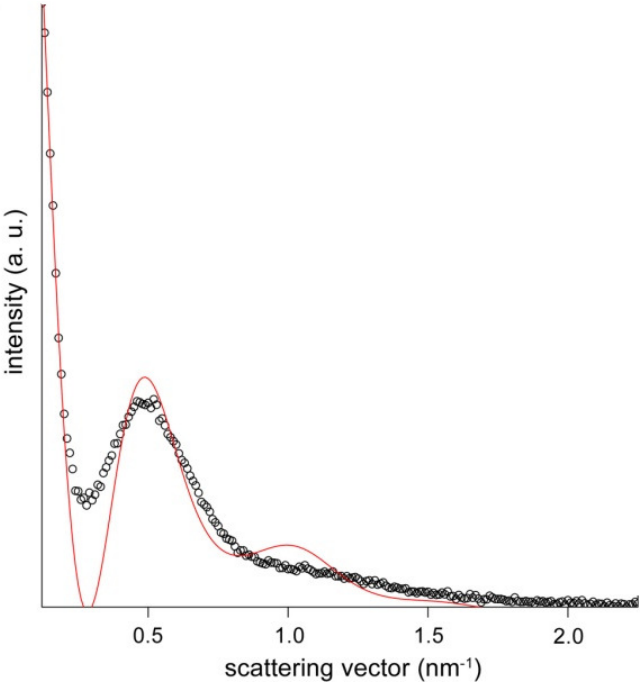

Figure 5. Small-angle X-ray scattering intensity profile of colloidal dispersions containing 2.5 wt.% PEG 660-stearate (sample 6 - black circles) with calculated scattering profile of core-shell spherical particles (solid line).

According to the fit, volume of the shell is about 140 times greater than the core, while the mass composition is only 5 times. To meet the volume ratio, the PEG part should be swollen by water to make roughly 3.5 % PEG content corresponding to a density of about 1.06 g/cm^3 [Han, 2008]. Thus the contrast fitted for core-shell model, the core being less dense than the bulk water by 43% of the contrast between the shell and the bulk water, instead of 65% from the above estimated densities, is also in a reasonable range considering the simplification of the system (Figure 6).

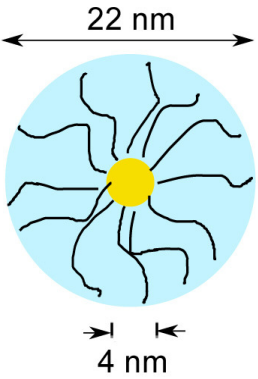

Figure 6. QU-ME schematic representation.

4. Discussion

Light scattering measurements clearly demonstrated that the mean size and size distribution of the nanosized emulsions prepared by the hot solvent diffusion method strongly depended on the PEG 660-stearate concentration. The higher the PEG 660-stearate concentration, the smaller the droplets are formed. However, the droplet size was not continuously reduced, since at intermediate surfactant concentrations (samples 3, 4, and 5), polydisperse systems constituted of different nanostructures were obtained. We observed that a critical amount of surfactant (2.5 wt%, corresponding a surfactant-to-oil weight ratio of 5) was required to obtain monodisperse colloidal dispersions displaying characteristics of microemulsion systems.

The assumption of a formation of a microemulsion system was supported by the cross-polarized light microscopy and by the cryo-TEM studies, which evidenced the formation of an isotropic dispersion of spherical droplets. The effect of the surfactant concentration on QU loading was also evaluated. The reduction of the droplet size from 140 to 20 nm allowed increasing the QU loading by 3 to 10 times, depending on the amount of QU initially added to the formulations. SAXS results indicate an internal structure of a nanosized emulsion with a core-shell spherical structure with a radius of 11.6 nm, which is in good agreement with light scattering measurements and TEM observations.

The two commonly reported processes used to produce emulsions with droplet sizes in the submicrometer-range are divided into high-energy methods, which involve the use of devices as high-pressure homogeneizers and sonifiers, and low energy methods, which employ the physical properties of the formulation compounds, mainly those of the surfactants and co-sufactants [Fernandez *et al.,* 2004; Anton *et al*., 2008]. The hot solvent diffusion method used in this study is based in the same principles of the spontaneous emulsification, differing only by the heating of the samples during the emulsification process. In this method, an emulsion is created without energy input, after the mixture of two liquids, namely an aqueous phase containing a hydrophilic surfactant and a mixture of oil, surfactant and a water-miscible solvent. The solvent displacement from the oily to the aqueous phase occurs at very fast rate, generating turbulence at interface of the emulsion droplets (Marangoni effect). At this time, the molecules of the surfactant in the aqueous phase are adsorbed around the oil phase droplets, resulting in spontaneous droplet formation in the submicron range [Kawashima *et al*., 1998; Hu *et al*., 2002].

However, PEG 660-stearate is a polyethoxilated (PEO) non-ionic surfactant that undergoes phase inversion at around 80°C. It has been demonstrated that below the PIT (phase inversion temperature), only macroemulsions are obtained using PEG 660-stearate in the same concentration range tested in this study [Jumma and Muller, 2002]. Therefore, it is reasonable to say that apart from the surfactant concentration, the heating used to produce the colloidal dispersions was also an important factor that contributed to the formation of dispersions with reduced droplet sizes. The mechanism of formation of PEG 660-stearate stabilized nanosized emulsions using the phase inversion method was described with details elsewhere. When increasing the temperature, the PEG 660-stearate becomes gradually lipophilic and migrates within the oily phase. At the PIT, discontinuous microemulsions are formed and when temperature is further increased above the PIT, phase inversion occurs leading to the formation of a water-in-oil emulsion. Anton *et al*. [2009] describes that for nanoemulsion formation, cold water must be added to the microemulsions, making the system fully hydrophilic and recreating the emulsification conditions of the spontaneous emulsification method, since surfactants spontaneously move from the oil to the aqueous phase.

In our case, probably due to the presence of the organic solvent, it was not necessary to add cold water. The microemulsions were spontaneously formed when the organic phase was poured into aqueous phase previously heated to temperature above the PIT. When decreasing the temperature, the system became hydrophilic, leading to the formation of colloidal dispersions, macroscopically transparent, having a mean particle size of around 20 nm. Therefore, we can state that microemulsion formation occurred by a combination of the two low-energy methods previously described.

In general, microemulsification is mainly governed by factors such as (1) nature and concentration of the oil, surfactant, co-surfactant and aqueous phase, (2) oil/surfactant and surfactant/c-osurfactant ratio, (3) temperature and pH of the environment and (4) physicochemical properties of the drug such as hydrophilicity/lipophilicity, p*K*a and polarity [Date, 2008]. Due to their excellent biocompatibility, phosphatidylcholines are generally used to obtain microemulsions. However, they are too hydrophobic to spontaneously form microemulsions and it is necessary to adjust the HLB (hydrophilic-lipophilic balance) of phospholipids and to inhibit their tendency to form lamellar liquid crystalline phases [Date, 2008]. The addition of PEG 660-stearate formed a mixed monolayer with SbPC between the water and oil domains, and then the flexibility of this mixed film increased compared to that of the rigid film formed by using SbPC only, because the different molecular structures of PEG 660-stearate and SbPC prevents a close packing of the molecules at the interface [Von Corswant *et al*, 1998; Jumaa and Muller, 2002; Zhao *et al.* 2005]. Furthermore, the combination of a phospholipid and a non-ionic copolymer surfactant such as PEG 660-stearate improves the stability of the system, and this is attributed to the steric stabilization of the non-ionic surfactant [Jumaa and Muller, 2002].

Acknowledgements

The authors are grateful to CNPq for the financial support to the project. We also are grateful for the support given by the Brazilian Synchrotron Light Laboratory *(*LNLS, Campinas, Brazil*)* under proposal SAXS 17718/2008. C. L. Dora and F. C. Silva received grants from CAPES and CNPq, respectively. The authours would like to thank Dr.

C. Rochas (CERMAV) for his assistance during the SAXS experiments at ESRF.

References

[1] S. Gupta, S.P. Moulik, S. Lala, M.K. Basu, S.K Sanyal, S. Datta, Drug Deliv. 12 (2005) 267.
[2] H. Li, X. Zhao, Y. Ma, G. Zhai, L. Li, H. Lou. J Control Release. 10 (2009) 238.
[3] T.P. Formariz, M.C.C. Urban, A.A. Silva, M.P.D. Gremião, A.G. Oliveira, Braz. J. Pharm. Sci. 41 (2005) 301.
[4] P.K. Ghosh, R.J. Majithiya, L.M. Umrethia, R.S.R. Murthy, AAPS PharmSciTech 7 (2006) 77.
[5] A.A. Date and M.S. Nagarsenker, Int. J. of Pharm. 355 (2008) 19.
[6] Z.-G. Gao, H.-G. Choi, H.-J. Shin, K.-M. Park, S.-J. Lim, K.-J. Hwang, C.-K. Kim, Int. J. of Pharm. 161 (1998) 75.
[7] B. Stavric, Clinical Biochem. 27 (1994) 245.
[8] D.V. Ratman, D.D. Ankola, V. Bhardwaj, D.K. Sahana and M.N.V.R. Kumar, J. Controlled Release 113 (2006) 189.
[9] P. Fresco, F. Borges, C. Diniz, M.P. Marques, Med. Res. Rev. 26 (2006) 747.
[10] P.J. Mulholland, D.R. Ferry, D. Anderson, S.A. Hussain, A.M. Young, J.E. Cook, E. Hodgkin, L.W. Seymour, D.J. Kerr, Ann. Oncol. 12 (2001) 245.
[11] T. Pralhad and K. Rajendrakumar, J. Pharm. Biomed. Anal. 34 (2004) 333.
[12] A. Priprem, J. Watanatorn, S. Sutthiparinyanont, W. Phachonpai, S. Muchimapura, Nanomed. Nanotechnol. Biol. Med. 4 (2008) 70.
[13] H. Li, X-B Zhao, Y. Ma, G.X. Zhai, L-B Li, H-X Lou, *J.* Controlled Release 133 (2009) 238.
[14] F.Q. Hu, H. Yuan, H.H. Zhang, M. Fang, Int. J. Pharm. 239 (2002) 121.
[15] ICH (2005) Harmonised tripartite guideline: validation of analytical procedures: text and methodology Q2 (R1).
[16] V. Durrieu, A. Gandini, M.N. Balcacem, A. Blayo, G. Eiselé, J.L. Putaux, J. Appl. Polym. Sci. 94 (2004) 700.

[17] Y. Kawashima, H. Yamamoto, H.Takeuchi, T. Hino T. Niwa, Eur. J. Pharm. Biopharm., 45 (1998) 41.
[18] B. Heurtault, P. Saulnier, B. Pech, J.E. Proust and J.P. Benoit, Biomaterials 24 (2003) 4283.
[19] P. Boonme, K. Krauel, A. Graf, T. Rades and V.B. Junyaprasert, AAPS PharmSciTech. 7 (2006) 45.
[20] C. Von Corswant, P. Thoren, S. Engestrom, J. Pharm. Sci., 87(1998) 200.
[21] M. Jumma and B.W. Muller, Eur. J. Pharm. Biopharm. 54 (2002) 207.
[22] X. Zhao, D. Chen, P. Gao, P. Ding and K. Li, Chem. Pharm. Bull. 53 (2005) 1246.
[23] N. Anton, P. Gayet, J.P. Benoit and P. Saulnier, Int. J. Pharm. 344 (2007) 44.
[24] N. Anton and T.F. Vandamme, Int. J. Pharm. 377 (2009) 142.

***Publicação 3**. Structural investigations of lipid-based nanostructured drug delivery systems*

Structural investigations of lipid-based nanostructured drug delivery systems

]

Cristiana L. Dora[1], Jean-Luc Putaux[3], Isabelle Pignot-Paintrand[3], Frédéric Dubreuil[3], Valdir Soldi[2], Elenara Lemos-Senna[1,] and Redouane Borsali[3,]**

[1] Laboratório de Farmacotécnica, Departamento de Ciências Farmacêuticas, Centro de Ciências da Saúde, [2] Polimat, Departamento de Química, Universidade Federal de Santa Catarina, Campus Universitário Trindade, Bloco K, sala 107, 88040-900, Florianópolis, SC, Brazil.
[3]Centre de Recherches sur les Macromolécules Végétales (CERMAV-CNRS), BP 53, F-38041 Grenoble Cedex 9, France - *affiliated with Université Joseph Fourier and member of the Institut de Chimie Moléculaire de Grenoble*

*Corresponding authors:
lemos@ccs.ufsc.br Tel:+55 48 37215067, fax: +55 48 37219350
borsali@cermav.cnrs.fr Tel:+33 04 76 03 76 40, fax:+33 04 76 54 76 29

Abstract

The classical lipid colloidal systems that have been proposed for drug delivery are composed of liquid (nanoemulsions- NEs) or solid lipids (solid lipid nanoparticles-SLN). However, due to their composition, the nanoparticles produced only with solid lipids have a limited drug loading and controlled release capacity. Recently, colloidal dispersions made from mixtures of solid and liquid lipids (nanostructured lipid carriers -NLCs) were formulated to combine controlled release characteristics with a drug loading capacity higher than that of SLNs. In this study, we have investigated the physicochemical behavior of SLNs, NLCs and NEs produced with tristearin and/or castor oil by hot solvent diffusion method when tristearin and/or castor oil were used. PEG-660-stearate or Poloxamer 188 and soybean lecithin were used as surfactant and co-surfactant, respectively. The colloidal dispersions were characterized by dynamic light scattering (DLS), differential scanning calorimetry (DSC), small- and wide-angle X-ray scattering (SAXS and WAXS), atomic force microscopy (AFM), transmission electron microscopy (TEM), and cryo-TEM. DLS measurements demonstrate a size of 340, 220, 145 nm for SLN, NLC, and NE, respectively, indicating that the size decrease with the addition of castor oil. NE particles were spherical whereas SLNs and NLCs had more complex shapes. SLNs appeared to be lamellar crystals while NLCs exhibited a mixed structure composed of a lamellar crystalline phase (assigned to tristerarin in the □-form) in contact with a liquid oil compartment.

Key-words: Solid lipid nanoparticles, Nanostructured lipid carriers, Nanoemulsions, cryo-TEM

Introduction

In the last decade, lipid-based colloidal carriers have emerged as a way to deliver poorly water-soluble drugs, mainly when the oral route is required. They can be constituted by solid or liquid lipids, or a mixture of both in various ratios, and display a wide range of particle sizes. Advantages of lipid-based formulations include a wide application spectrum, the use of biodegradable physiological lipids recognized as safe or having a regulatory accepted status, and the possibility of scaling up to industrial production level (Bunjes and Westesen, 2001, Li *et al*, 2009, Saupe *et al*., 2006). Besides, lipid-based-colloidal carriers have demonstrated a great ability to enhance oral absorption of lipophilic drugs, the mechanisms of which enclose lipid digestion by the components of the gastrointestinal tract and selective uptake by the lymphatic system (Chakraborty *et al.,* 2009).

In previous studies, we have prepared lipid-based colloidal dispersions by using the hot solvent diffusion method with the aim to carry quercetin, a lipophilic natural drug which displays antitumor, anti-inflammatory and antioxidant activities, but a very low oral bioavailability. In particular, castor oil and tristearin were employed to obtain oil-in-water nanosized emulsions (NEs) and solid-lipid nanoparticles (SLNs), respectively. Moreover, nanostructured lipid carriers (NLCs) were obtained when both solid and liquid lipid were mixed in different ratios. For all lipid formulations assayed, poly(ethylene glycol) (660)-12-hydroxystearate (PEG 660-stearate, Solutol HS15®) or Poloxamer 188 (Lutrol F68®) were used as hydrophilic surfactants and hydrogenated soybean phosphaditylcholine as lipophilic surfactant. The results demonstrated that the quercetin loading increased with increasing castor oil load in the total lipid mixture (Dora *et al.,* 2010). However, the way in which drug loading was affected by the structural properties of the particles still needs to be determined. It has been recognized that the composition of lipid formulations influences the shape and structure of the particles, which may or may not display phase separation (Saupe *et al.,* 2006).

On another hand, since lipid materials used to prepare matrix nanocarriers usually occur in different allomorphs and since the hot solvent diffusion method used for the preparation of colloidal suspensions encloses a thermal procedure and a recrystallization step,

polymorphism is an important issue that needs to be investigated. In particular, tristearin crystallizes into four allomorphs γ, α, β´, and β and their formation depends on the preparation conditions, like the cooling and agitation rates (Hartel, 2001). Formulation composition was also shown to affect the crystal structure of the particles. For instance, while the use of unmodified soybean lecithin lead to the formation of β-tristearin during the preparation of SLNs, the use of hydrogenated fully saturated soybean lecithin results in a predominant fraction of the metastable β-form (Bunjes *et al*., 2007).

Therefore, in the present study, we have investigated the structural and physicochemical characteristics of lipid-based nanocarriers prepared from tristearin and castor oil, using a hot solvent diffusion method. Complementary analytical techniques, including dynamic light scattering (DLS), differential scanning calorimetry (DSC), wide- and small-angle X-ray scattering (WAXS and SAXS), atomic force microscopy (AFM), transmission electron microscopy (TEM) and cryo-TEM were used to provide more detailed information on the morphology, structure and properties of the colloidal lipid particles.

Materials and methods

Materials

Castor oil (CO), a triglyceride in which approximately 90% of fatty acid chains are ricinoleic acid, was purchased from Natural Pharma (São Paulo, Brazil). Hydrogenated soybean lecithin (Lipoid S75-3N) was purchased from SP Pharma (São Paulo, Brazil). According to the manufacturer, the product contains from 67 to 73 % of phosphatidyl choline. Tristearin (Dynasan 118, TS) was kindly donated by Sasol (Louisiana, USA). The fatty acid fraction was 99% pure for this triglyceride quality and hydroxyl value below 5. Polyoxypropylene-polyoxyethylene block copolymer (Lutrol F-68 NF®, called in this paper as Poloxamer 188) and 12-hydroxystearic acid-polyethylene glycol copolymer (Solutol HS-15®, called in this paper as PEG 660-stearate) were kindly donated by BASF (Trostberg, Germany) (Figure 1). Ethanol, acetone, and other chemicals used were of analytical grade.

Preparation of the lipid-based nanocarriers

The lipid-based nanocarriers were prepared by a hot solvent diffusion method (Kawashima *et al.,* 1998; Hu *et al.,* 2002). Briefly, 20 mg of lecithin and 100 mg of TS, CO or their mixture (1:1) were completely dissolved into an acetone:ethanol (60:40 v/v) mixture at 60°C. The resulting organic solution was quickly poured into 50 mL of an aqueous solution containing 0.1% (w/v) PEG 660-stearate or 1% (w/v) Poloxamer 188 maintained under magnetic stirring at 82°C. The resulting colloidal suspensions were then cooled to room temperature. The organic solvent was evaporated under reduced pressure, and the final volume was adjusted to 20 mL. Finally, the colloidal suspensions were filtered through an 8 μm filter paper. For DSC and WAXS studies, SLN and NLC colloidal suspensions were freeze-dried.

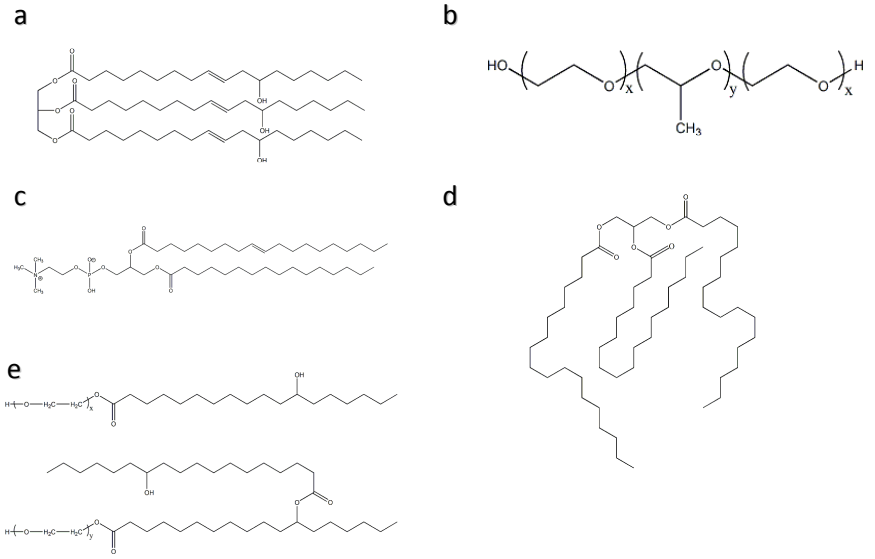

Figure 1. Molecular structure of the compounds used to prepare the lipid nanocarriers: a) castor oil; b) Poloxamer 188; c) lecithin; d) tristearin e) PEG 660-stearate.

Particle size analysis

The mean particle size and the size distribution of the colloidal suspensions were determined by DLS using an ALV 5000 (ALV, Germany). The samples were previously diluted in ultrapure Milli-Q® water. Each size analysis lasted 300 s and the temperature was set as 25°C. The analysis was performed at a scattering angle of 90°. The hydrodynamic radius was determined using the Stokes-Einstein equation $R=(\kappa_B T/6\pi\eta D)$ where κ_B is the Boltzmann constant, T is the temperature, D is the diffusion coefficient and η is the viscosity of the medium (η=0.89cP at 25°C).

Transmission electron microscopy and cryo-TEM

Drops of the suspensions (diluted 1000× in ultrapure water) were deposited on carbon-coated copper grids, stained with 2% uranyl acetate and observed at room temperature. Cryo-TEM specimens were prepared by quench-freezing thin liquid films of the suspensions into liquefied ethane (-171°C). They were mounted on a Gatan 626 cryoholder cooled with liquid nitrogen and transferred to the microscope. The specimens were observed at low temperature (-180 °C), using a Philips CM200 'Cryo' microscope operating at 80 kV. A low-dose procedure was used to reduce radiation damage in the areas of interest before actual image recording on Kodak SO163 films.

Atomic force microscopy

Drops of dilute lipid-based nanocarrier suspensions were deposited onto freshly cleaved mica. After 20 min, the samples were dried with nitrogen. AFM experiments were performed on a Molecular Imaging PicoPlus instrument. Topography images were recorded in tapping mode.

Small-angle X-ray scattering

SAXS measurement were performed on nanoparticle in suspensions at the SAXS 2 beamline of the Laboratório Nacional de Luz Síncrotron (LNLS, Campinas, Brazil), equipped with an asymmetrically cut and bent Si (111) monochromator (λ = 1.488 Å) that yields a

horizontally focused beam. A linear position sensitive gas filled X-ray detector was vertically placed at 1493.3 mm away from the sample position record the scattered intensity in the scattering vector range of 0.1 - 2.26 (nm^{-1}). The parasitic scattering was subtracted from the total scattered intensity.

Wide-angle X-ray scattering

WAXS was carried out using freeze-dried or concentrated colloidal suspensions. The powders were sealed between two Mylar foils whereas the liquids were poured into glass capillaries (0.7 mm outer diameter) that were flame-sealed. Both types of specimens were mounted on 0.2 mm collimators and X-rayed with a Ni-filtered CuKα radiation (λ=1.543 Å), using a Philips PW3830 generator operating at 30 kV and 20 mA. WAXS powder patterns were recorded on Fujifilm imaging plates, read with a Fujifilm BAS-1800II Bio-imaging Analyzer. Diffraction profiles were obtained by radially integrating the intensity over the whole spectra. The diffraction rings were calibrated using a $CaCO_3$ standard.

Differential scanning calorimetry

DSC analyses were performed using a TA Q200 instrument. About 2-20 mg of freeze-dried colloidal suspensions or the bulk materials used to prepare the lipid nanocarriers were accurately weighted into standard aluminum pans, which were tightly sealed. The samples were cooled to -20°C and then heated to 100°C at scan rate of 10°C/min. An empty pan was used as reference.

Results

Particle size

In the present study, the lipid-based nanocarriers were prepared using the solvent diffusion method. It consists in forming a hot oil-in-water emulsion following the addition of a water-miscible organic solution containing the lipid and a lipophilic surfactant in an aqueous

solution containing a hydrophilic surfactant. An interface turbulence of the emulsion droplets (Marangoni effect) is produced by the very rapid diffusion rate of the water-miscible organic solvent to aqueous phase, resulting in the spontaneous formation of submicronic droplets (Kawashima *et al*., 1998; Hu *et al.,* 2002). All formulations were prepared at 82°C to ensure that the lipid remained liquid. After cooling, the resulting colloidal dispersions were macroscopically homogeneous with a milky appearance, regardless of the type of lipid.

The mean particle size and particle size distribution of the nanocarriers determined using DLS are listed in Table 1. Colloidal dispersions displaying monodisperse populations of particles were obtained for all formulations (polydispersity index PDI < 0.2). However, the mean particle size was around 340, 200, and 140 nm for SLNs, NLCs, and NEs, respectively. The nature of the surfactant did not seem to have any effect on the particle size. These results clearly indicated that particle size depended on the composition of the lipid phase: the particle size decreased with increasing castor oil fraction.

Table 1. Mean particle size and polydispersity index (PDI) measured by DLS for the lipid-based colloidal suspensions.

	PEG 660-stearate 0.1 wt% (p/v)		Poloxamer 188 1% (p/v)	
	Mean size (nm)	PDI	Mean size (nm)	PDI
SLN TS:CO (100:0)	342 ± 3	0.186	343 ± 3	0.176
NLC TS:CO (50:50)	221 ± 10	0.110	215 ± 16	0.153
NE TS:CO (0:100)	150 ± 10	0.123	142 ± 7	0.137

Particle morphology

TEM images of NE suspensions prepared with CO as lipid component, in the presence of Polxamer 188 or PEG 660-stearate are shown in Figure 2.

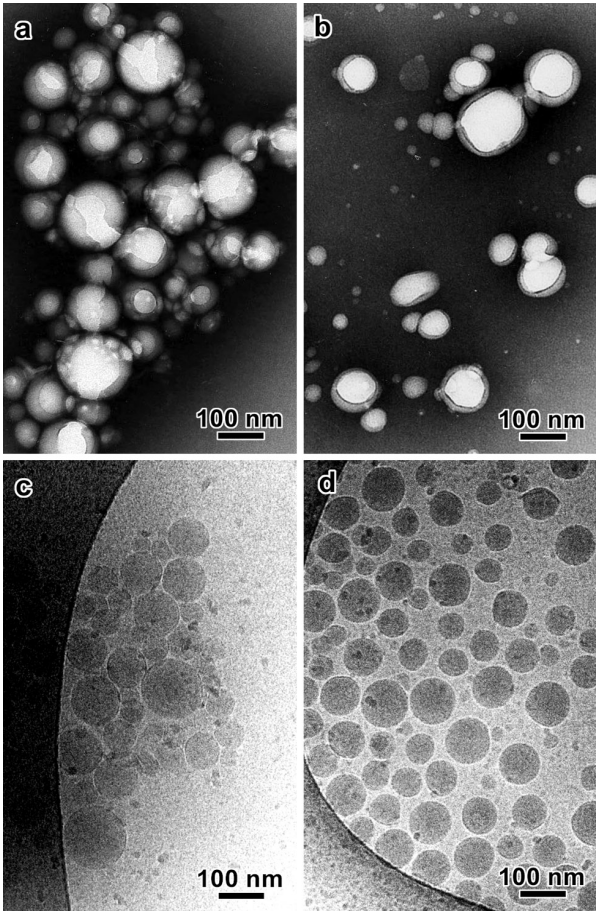

Figure 2. TEM images of NE nanocarriers prepared in the presence of Poloxamer 188 (a,c) and PEG 660-stearate (b,d) in the aqueous phase. a,b) negative staining; c,d) cryo-TEM.

Negatively stained (Figures 2a,b) and fast-frozen (Figures 2c,d) preparations both show polydisperse distributions of 20-120 nm spherical particles. The dark outline seen on the bigger particles is due to the fact that the film of dry uranyl acetate was rather thick and only the top part of the spherical particle protruded out of the stain.

For a given formulation, the size distributions of negatively stained and ice-embedded particles were quite similar, suggesting that the particles did not significantly deform during drying on the carbon film. Some limited particle deformation could be seen in the cryo-TEM images due to the confining effect inside the thin film of vitreous ice (Figures 2c and 2d).

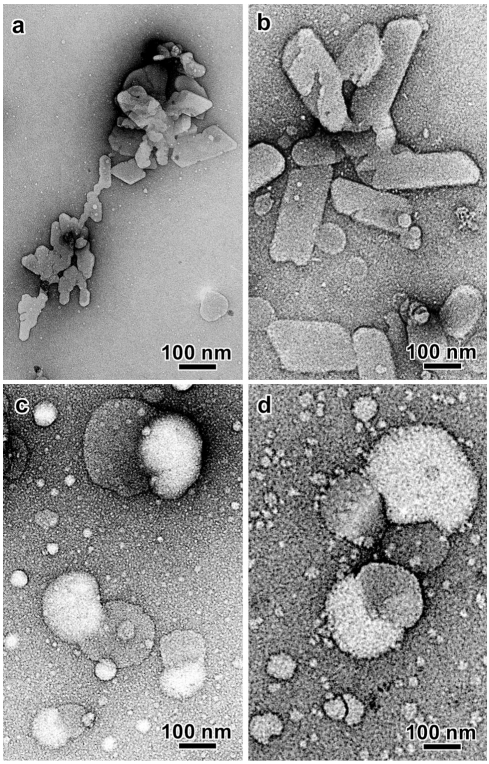

Figure 3. TEM images of negatively stained SLN (a,b) and NLC (c,d) particles prepared in the presence of Poloxamer 188 (a,c) and PEG 660-stearate (b,d) in the aqueous phase.

When only TS was used as lipid component to prepare SLNs, lamellar crystals with irregular and angular shapes were observed (Figures 3a and 3b).

The parallepipedal lamellae were larger when the SLNs were prepared in the presence of PEG 660-stearate (Figure 3b). No satisfying image of the lamellae could be recorded by cryo-TEM. The very thin crystals were systematically oriented flat within the film of embedding ice, thus generating a very poor amplitude contrast, proved to degrade extremely rapidly under electron illumination.The thickness of lamellar SLNs was estimated by AFM imaging. Figures 4a and 4b are tapping-mode images of SLNs prepared with Poloxamer 188 and PEG 660-stearate, respectively.

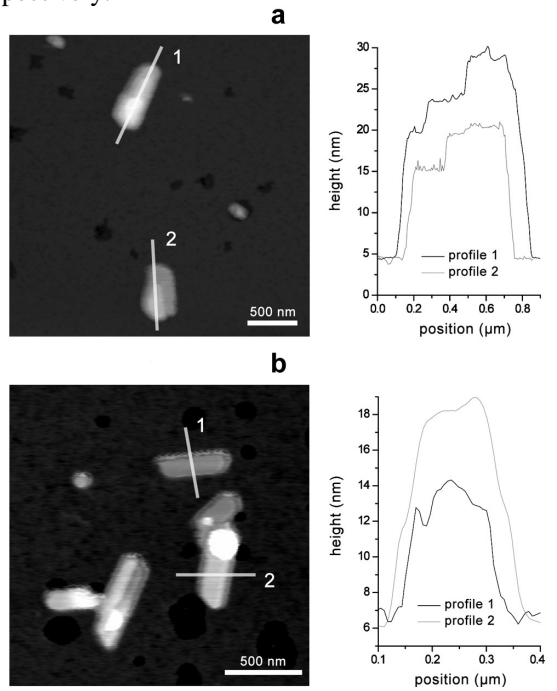

Figure 4. AFM images of SLN particles prepared with Polomaxer 188 (a) and PEG 660-stearate (b) as surfactants in the aqueous phase.

For the first sample, height profiles were taken longitudinally across objects that appear to be multilamellar. The stepped aspect of the profiles suggest that the particles are made of irregularly stacked lipid layers, with a minimum increment of about 4-5 nm. Considering the structure of β-TS this would correspond to the spacing between two lipid layers, *i.e.*, 4.5 nm (Bunjes *et al.,* 2007). In Figure 4a, particle 1 would thus consist of a first group of 4 lipid layers (about 15 nm) with two additional smaller layers on the top, each of them creating a step of about 5 nm, for a total thickness of about 25 nm. Particle 2 would consist in a first group of 3 lipid layers (about 10 nm) with an additional smaller layer on the top (5 nm) for a total thickness of about 15 nm. The stepped aspect was less clearly defined for SLNs prepared with PEG 660-stearate (Figure 4b). Height profiles were taken from two particles. Average thicknesses of about 5 and 10 nm were measured from particles 1 and 2, respectively. The 5 nm increment is in agreement with the value measured from SLNs prepared with Poloxamer 188. Particles 1 and 2 would thus be made of 2 and 3 lipid layers, respectively.

As seen in Figures 3c and 3d, negatively stained NLCs particles prepared by mixing CO with TS presented a clearly different aspect. Irregular 100-400 nm bilobular objects were mostly observed, surrounded by 10-50 nm particles. In particular, in the NLC sample prepared in the presence of PEG 660-stearate, a population of monodisperse 10 nm particle was clearly observed that likely correspond to micelles of PEG 660-stearate in excess (Figure 3d). For the larger particles in both types of NLC preparations, one lobe is rather clear while the other is darker. Hypotheses can be made to account for this peculiar contrast, assuming that each lobe corresponds to the liquid and solid lipid phases: i) both lobes have a different thickness, the thickest one protruding more out of the stain layer; ii) the stain may preferentially interact with one of the lobes (hence the darker contrast). Cryo-TEM images confirmed that the NLCs particles had a variety of shapes and sizes (Figure 5).

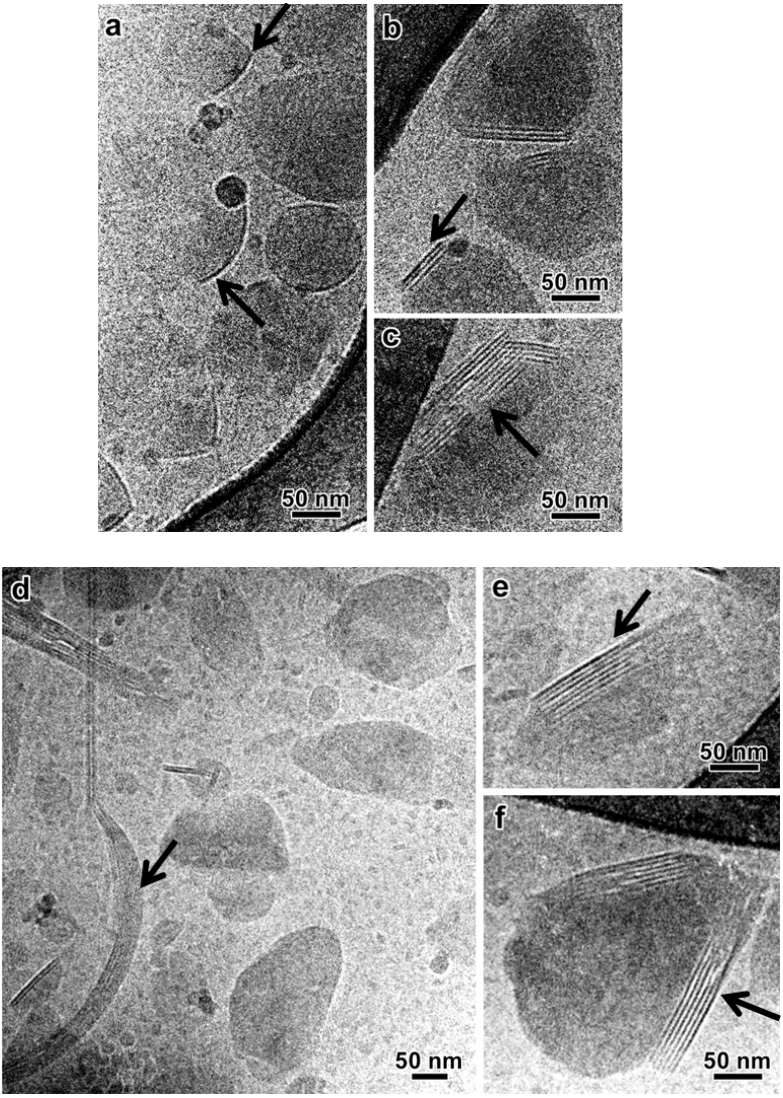

Figure 5. Cryo-TEM images of NLC suspensions prepared using Poloxamer 188 (a-c) and PEG 660 stearate (d-f) as surfactants in the aqueous phase.

Several NLCs particles prepared in the presence of Poloxamer 188 are discoidal or spheroidal but part of their periphery is outlined by a discontinuous dark fringe (Figure 5a). In these regions, the curvature is lower and sometimes, two dark fringes join and give a triangular shape to the particle. This higher rigidity and darker contrast are likely related to the presence of a single organized layer of TS. Some particles are covered by stacks of more than one layer and in that case, there is no curvature (Figures 5b and 5c). After calibration of the images and assuming that the stacks were seen oriented edge-on, we measured an interlayer distance of about 4.5 nm, in perfect agreement with the value of the lamellar spacing in β-TS and what was measured from the AFM images of SLNs particles. Similar stacks were reported by Bunjes et al. (2007) in TS dispersions stabilized with soybean lecithin.

Several types of NLCs particles prepared in the presence of PEG 660-stearate were also observed by cryo-TEM (Figures 5d to 5f). They are distributed among 10 nm micelles of excess PEG 660-stearate, in agreement with what was observed from negatively stained preparations (Figure 3d). The particles have facetted irregular shapes and, again, seem to contain two regions with different light and dark contrasts (Figure 4d). Like in the case of NLCs prepared with Poloxamer 188, some particles are irregularly covered with stacks of 2 to 6 4.5 nm-spaced dark layers that likely correspond to β-TS (Figures 5e and 5f). More rarely, particles with a more complex shape were observed. For instance, the spoon-like particle seen in Figure 5d is constituted by a straight and a curved regions, and both regions appear to be layered.

Particle structure

SAXS diffractograms of SLN and NLC and NE dispersions are shown in Figure 6.

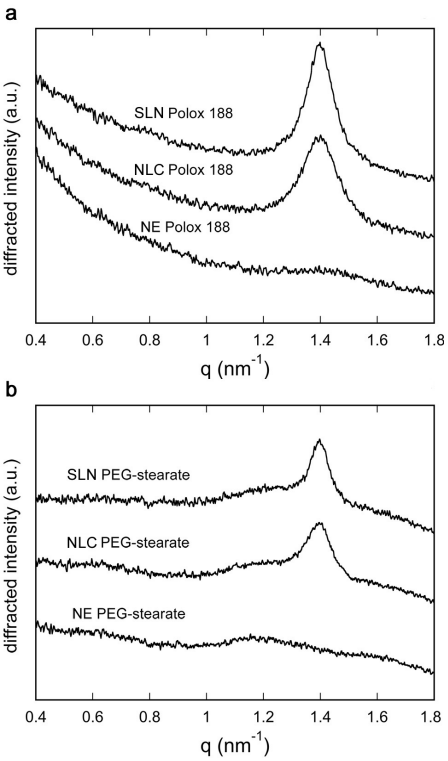

Figure 6. SAXS profiles of colloidal suspensions prepared with Poloxamer 188 (a) and PEG 660-stearate (b) as surfactants in the aqueous phase.

For SLNs and NLCs, a clear peak located at $q = 1.4$ nm^{-1} was mainly observed. This value corresponds to a spacing of 4.48 nm, in agreement with the 4.50 nm value previously reported in solid lipid nanoparticles prepared by high pressure homogenization (Bunjes *et al.,* 2007) and which correspond to the spacing between two β-TS layers. This peak was not observed for the NE suspensions that contained only CO.

WAXS profiles of the samples (concentrated suspensions or lyophilized powders) were collected in order to determine the allomorphic form of TS (Figure 7). The samples tested as concentrated

suspensions (Figure 7a) yielded diffraction patterns exhibited 5 main peaks at diffraction angles 2θ of 6, 16.5, 19, 23 and 24°, corresponding to crystal spacings of 1.47, 0.54, 0.46, 0.39 and 0.37 nm, respectively.

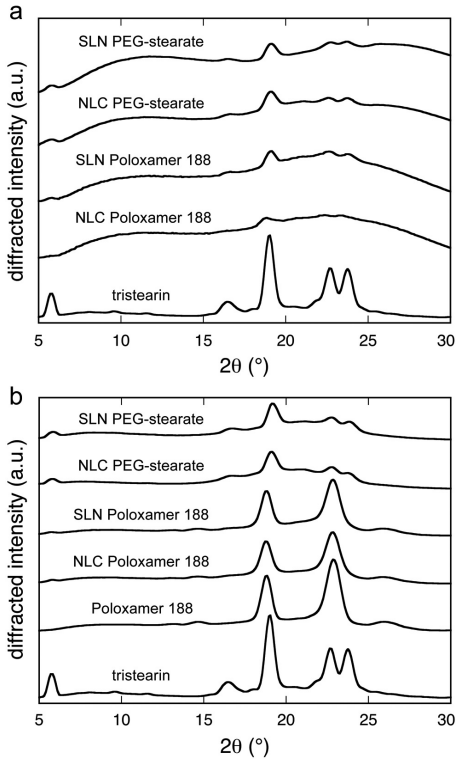

Figure 7. WAXS profiles of concentrated (a) and freeze-dried (b) lipid-based colloidal suspensions. The diffraction profile of tristearin has been added as a reference.

These peaks show that, independent of the type of surfactant used in the preparation, TS is present in the sample in its β-form (Oh *et al.,* 2002). The diffraction profiles recorded from the freeze-dried specimens prepared with PEG 660-stearate also exhibited the same peaks (Figure 7b). However, the peak distribution in the profile of the specimens prepared with Poloxamer 188 was different. The WAXS profile demonstrated 5 peaks located at about 6, 14.5, 18.5, 23 and 26° (Figure

7b). In fact, this WAXS profile corresponds to that of Poloxamer 188. Since Poloxamer 188 is in 5:1 proportion with respect to TS in the formulation, it is most probable that the peaks from the solid lipid were masked by those from the surfactant.

Thermal properties

The DSC thermograms of castor oil and lecithin are shown in Figure 8a while those of TS, Poloxamer 188, and PEG 660-stearate are shown in Figure 8b. The corresponding thermal events are summarized in Table 2. As can be visualized in this figure, lecithin, TS, poloxamer 188, and PEG-stearate exhibited endothermic events at 75.9°, 73.6°, 54.3°, and 24.3°C, respectively.

Freeze-dried SLNs and NLCs prepared using PEG 660-stearate or Poloxamer 188 show two endothermic peaks (Figure 8c). For the samples prepared with PEG 660-stearate, the peaks are located at about 70 and 18°C. For the samples prepared with Poloxamer 188, the peaks are at about 70 and 51°C. For the four samples, the peaks at 70°C were assigned to β-TS melting, although the temperature is slightly lower than that of pure TS (73.6°C) and the other peak is related to the respective surfactant.

Table 2. Parameters obtained from DSC measurements of freezed-dried lipid-based colloids prepared with TS, Poloxamer 188 and PEG 660-stearate.

	Tristearin		**Poloxamer 188**		**PEG 660-stearate**		**Lecithin**	
	T_m (^oC)	ΔH (J/g)	T_m (^oC)	ΔH (J/g)	T_m (^oC)	ΔH (J/g)	T_m (^oC)	ΔH (J/g)
Raw material	73.6	207.6	54.3	129.0	24.3	78.3	75.9	47.1
SLN *Poloxamer 188* [a]	70.9	159,5	51.4	138,4	-	-	-	-
NLC *Poloxamer 188* [b]	69.5	197.9	50.3	134.1	-	-	-	-
SLN *PEG 660-stearate* [a]	70.7	122.4	-	-	17.9	56.1	-	-
NLC *PEG 660-stearate* [b]	70.5	146.3	-	-	18.2	29.8	-	-

[a] **SLN** *Poloxamer 188;* **NLC** *Poloxamer 188*: colloidal suspensions prepared using poloxamer 188 as hydrophilic surfactant of aqueous phase

[b] **SLN** *PEG 660-stearate;* **NLC** *PEG 660-stearate*: colloidal suspensions prepared using PEG 660-stearate as hydrophilic surfactant of aqueous phase.

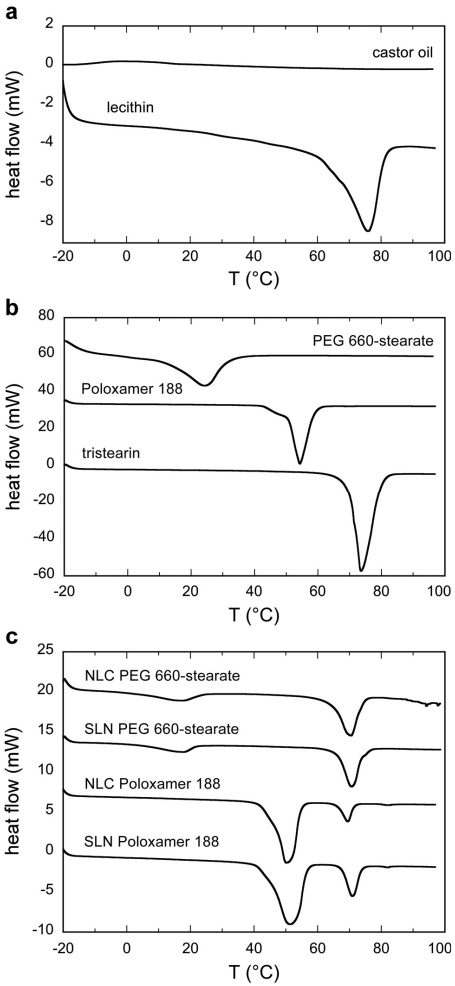

Figure 8. DSC thermograms of castor oil and lecithin (a), TS, Poloxamer 188 and PEG 660 stearate (b) and freeze-dried SLN and NLC particles prepared using both PEG 660-stearate or Poloxamer 188 (c)

This slight reduction in the TS melting temperature may result from the small particle size of the lipid nanocarriers, since lipid

nanocrystals were found to melt at a temperature 3-5°C lower than the corresponding bulk material (Heurtault *et al*., 2003). No significant difference in the melting point was observed for TS when SLNs and NLCs were analyzed, indicating that the presence of CO did not induce any change in the lipid arrangement of the solid lipid.

Discussion

In the present study, three nanoparticulate systems (SLNs, NLCs and NEs) were investigated, and differences in their ultrastructure were evaluated. The lipid components (TS and CO) displays in this study display similar structures which both consist of triglycerides containing 18-carbon fatty acid chains (Figure 1). The inclusion of a liquid lipid in the formulation of the nanoparticles led the reduction in particle size, in agreement with the results of Garcia-Fontes *et al.* (2005). However, the morphological evaluation clearly showed that platelet-shaped nanoparticles were obtained when only TS was used as lipid and, therefore, their anisometric shape should have contributed to some extent to the larger sizes obtained for SLNs. Since anisometric particles have a smaller diffusion coefficient than spherical particles and since larger spheres have a slower Brownian motion, their hydrodynamic diameter may be overestimated. In addition, as shown by TEM and cryo-TEM images, the mixture of CO and TS resulted in heterogeneous particles. In fact, ricinoleic acid, the main constituent of castor oil, is a monounsaturated, 18-carbon fatty acid, which has a hydroxyl functional group on the 12^{th} carbon (Figure 1). This functional group makes castor oil a more polar structure, which may have contributed to the segregation of the solid and liquid lipids in the nanoparticle structure. Schematic structures of the lipid nanocarriers produced are demonstrated in Figure 9.

TS crystallizes into four different crystalline forms, namely γ, α, β', and β, and their formation mainly depends on the cooling and stirring rates (Hartel, 2001). Polymorphism is one of the important physical degradation routes which affect the stability of solid dosage forms because, even though they are chemically identical, they generally have different thermal properties (melting temperature), crystal structure and solubility.

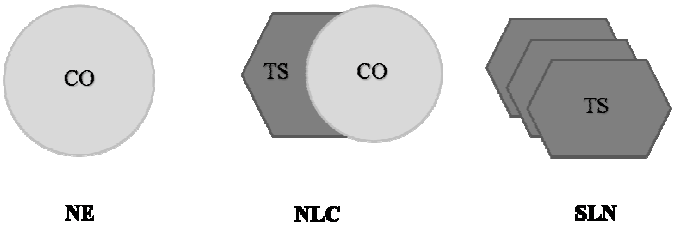

Figure 9. Schematic structures of the lipid nanocarriers developed.

The α-form has the tendency to quickly transform into the β´-form that has a tighter chain packing. The β-form is the most stable. Therefore, the transition of liquid (melt) from α to β, via β´ is the transition pathway followed by triglycerides to achieved an optimum packing of the molecules. Using cryo-TEM, Bunjes *et al.* (2007) have shown that β-TS occurred as layered platelets and α-TS as spherical multilayered particles. In our study, the morphological evaluation, as well as WAXS and DSC analyses indicated the formation of β-TS in SLNs. This result may be associated to the preparation method. By using the hot solvent diffusion method to obtain the lipid nanocarriers, hot nanosized emulsions are obtained by mixing the organic and aqueous phase at a temperature 10°C above of that of melting temperature of the solid lipid and, subsequently, they are maintained under magnetic stirring to cool down until to reach the room temperature. This procedure could have favored the formation of allomorph β since the recrystallization step is slow.

In a previous study, we have demonstrated that the increase of CO in the formulation led to an increase in the quercetin content, but SLNs and NLCs were not able to retard the drug release. Correlating this result with those of this study, we can say that the oil compartment increased the incorporation capacity of the system, due to the ability of the oily lipid into dissolve a hydrophobic drug, rather than to produce particles displaying a less organized matrix structure. In addition, the retard in the drug release did not occur because the castor oil was not in the inner core surrounded by the solid lipid.

Acknowledgements

The authors are grateful for the support given by the Brazilian Syncontron Light Laboratory (LNLS, Campinas, Brazil) under proposal SAXS 17718/2008. We thank M.B. Cardoso (LNLS) for his help in SAXS data processing. C. L. Dora benefited from a PhD grant from CAPES.

References

(1) Bunjes, H ; Westesen, K. In: *Crystallization Processes in Fats and Lipid Systems;* Garti, N. , Sato K., Eds.; Marcel Dekker: Switzerland, **2001** p 457.
(2) Li H., Zhao X., Ma Y., Zhai G., Li L., Lou H. *J. Control. Release* **2009**, 10, 238-244.
(3) Jores, K., Mehnert, W., Drechsler, M., Bunjes, H., Johann, C., Mader, K. *J. Control. Release* **2004**, 95(2), 217-227.
(4) Dora C.L., Silva, L. F. C., Tagliari, M. P., Silva, M. A. S., Lemos-Senna, E. Latin American Journal of Pharmacy. Article accepted.
(5) Bunjes, H., Westesen, K., Koch, M. *Int. J. Pharm.* **1996**, 129, 159-173.
(6) Muller, R., Radtke, M., Wissing, S. *Int. J. Pharm*. **2002**, 242, 121-128.
(7) Muller, R., Radtke, M., Wissing, S. *Adv. Drug Delivery Rev.* **2002b** 54(Supplement 1): S131-S155.
(8) Uner M. *Pharmazie.* **2006** 61(5)375-86.
(9) Saupe A., Gordon K., Rades T. *Int. J. Pharm.* **2006** 314 56–62.
(10) Kawashima Y., Yamamoto H., Takeuchi H., Hino T., Niwa T. Eur. J. Pharm. Biopharm. **1998** 45-41.
(11) Hu F.Q., Yuan H., Zhang H., Fang M. *Int. J. Pharm*. **2002** 239, 121–128.
(12) Heurtault B., Saulnier P., Pech B., Proust J., Benoit J. *Biomaterials*. **2003** 24:4283-4300.
(13) Bunjes, H., Steiniger, F., Richter W. *Langmuir.* **2007**, 23, 4005-4011.
(14) Hartel R. *Crystallization in foods.* Aspen Publishers:USA. **2001**. p15-22.

(15) Jenning, V., Thunemann, A., Gohla, S. *Int. J. Pharm.* **2000** 199 167–177.
(16) Oh J., McCurdy A., Clark S., Swanson B. Food chemistry and toxicology. 2002 67(8) 2911.

Capítulo 4

Investigação da atividade farmacológica da quercetina microemulsionada e da estabilidade da formulação

Muitos metabólitos secundários de plantas têm apresentado potente atividade terapêutica para uma série de doenças. Especialmente a quercetina, é um flavonóide, amplamente encontrado na nossa dieta, sendo suas principais fontes, cebola, chá, maças e vinho tinto (HERTOG *et al.,* 1993, CALIXTO *et al.*, 2003; CALIXTO *et al*., 2004). Muitos estudos *in vitro* demonstraram que este composto apresenta pronunciada atividade antiinflamatória e antitumoral, no entanto, a quercetina aglicona possui baixa solubilidade aquosa e é extensivamente metabolizada pelo intestino e fígado, o que faz com que este composto apresente uma baixa biodisponibilidade, limitando sua utilização por via oral (HOLLMAN *et al.,* 1995; CHO *et al*., 2003). Sistemas lipídicos de liberação de fármacos, como as microemulsões, têm sido propostos com intuito de aumentar a absorção de fármacos lipofílicos. Estes sistemas caracterizam-se por serem misturas líquidas isotrópicas, termodinamicamente estáveis de óleo, água e surfactantes com aspecto transparente/translúcido. A fase dispersa lipofílica atua como um reservatório de fármacos lipofílicos que em contato com membranas semi-permeáveis pode facilitar o transporte dos mesmos através dessas barreiras (GUPTA *et al.,* 2005, FORMARIZ *et al.,* 2007).

Assim, neste capítulo é descrita a avaliação biológica da quercetina microemulsionada em dois modelos farmacológicos *in vivo*. Primeiramente, o efeito antiinflamatório da microemulsão contendo quercetina (QU-ME) foi avaliado em um modelo experimental de asma alérgica em camundongos, após administração oral. Este trabalho é apresentado na forma de um artigo científico, o qual se encontra publicado no periódico *Pharmacological Research*. A segunda parte deste capítulo trata da avaliação do efeito antitumoral da microemulsão contendo quercetina em modelo de melanoma subcutâneo B16F10, em camundongos. Visto que, alguns estudos têm demonstrado efeito sinérgico entre polifenóis e quimioterápicos (CIPAK *et al.,* 2003), o efeito da combinação de QU livre e QU-ME com o fármaco cisplatina sobre a inibição do crescimento do tumor também foi avaliada. Os resultados deste estudo são demonstrados na forma de um artigo científico a ser submetido em periódico qualificado. Finalmente, considerando que via de administração oral foi empregada, e que resultados promissores foram obtidos no que diz respeito ao aumento da absorção oral da quercetina após microemulsificação, um estudo de estabilidade da microemulsão em meio gástrico e intestinal simulado e em meios biorrelevantes foi realizado, usando para isto a técnica de espalhamento dinâmico da luz. Neste estudo foi verificado o efeito dos componentes destes meios sobre a distribuição de tamanho de partícula

da microemulsão, correlacionando os resultados com o provável destino da formulação ao longo do trato gastrointestinal. Estes resultados também foram apresentados na forma de um artigo científico.

Publicação 4. *Anti-inflammatory effect of quercetin-loaded microemulsion in the airways allergic inflammatory model in mice*

Anti-inflammatory effect of quercetin-loaded microemulsion in the airways allergic inflammatory model in mice.

Alexandre P. Rogerio[a,1], Cristiana L. Dora[b], Edinéia L. Andrade[a], Juliana S. Chaves[a], Luis F.C. Silva[b], Elenara Lemos-Senna[b], João B. Calixto[a,*]

[a]Departamento de Farmacologia, Universidade Federal de Santa Catarina, Campus Universitário Trindade, Centro de Ciências Biológicas, Florianópolis, SC, Brazil
[b]Laboratório de Farmacotécnica, Departamento de Ciências Farmacêuticas, Centro de Ciências da Saúde, Universidade Federal de Santa Catarina, Campus Trindade, Florianópolis, Brazil.

* Corresponding author:
Departamento de Farmacologia, Universidade Federal de Santa Catarina, Campus Universitário, Trindade, Bloco D, CCB, Caixa Postal 476, Florianópolis, Santa Catarina, CEP 88049-900, Brazil. Tel.: +55 48 3721 9491/55 48 3721 9764; fax: +55 48 3337 5479.
E-mails: calixto@farmaco.ufsc.br or calixto3@terra.com.br (J.B. Calixto)

Abstract

Quercetin is a plant-derived flavonoid widely known by its anti-oxidant and anti-inflammatory properties, but its oral bioavailability is very poor and this becomes difficult to assess its therapeutic potential. Here we have compared the anti-inflammatory effect of quercetin-loaded microemulsion (QU-ME) and quercetin suspension (QU-SP) in an experimental model of airways allergic inflammation. Mice received daily oral doses of QU-ME (3 or 10 mg/kg; in an oil-in-water microemulsion content 0.02:0.2:1 of lecithin: castor oil:solutol HS15®), QU-SP [10 mg/kg, in carboxymethylcellulose (CMC) 0.5% in water] or vehicle from the 18th to the 22nd day after the first immunization with ovalbumin (OVA). Dexamethasone was used as positive control drug. Every parameter was evaluated in the 22nd day (24 h after the second OVA-challenge). We have also tried to assess by HPLC-MS a quercetin metabolite in the blood of rats treated with QU-SP or QU-ME. QU-ME was better orally absorbed when compared with QU-SP. Furthermore, oral administration of QU-SP failed to interfere with leukocyte recruitment, while QU-ME inhibited in a dose-dependent, the eosinophil recruitment to the bronchoalveolar lavage fluid (BALF). QU-ME also significantly reduced both IL-5 and IL-4 levels, but failed to interfere with CCL11, IFN-γ and LTB_4 levels. In addition, QU-ME oral treatment inhibited the nuclear transcription factor kappa B (NF-κB) activation, P-selectin expression and the mucus production in the lung. The present results show that QU-ME exhibits pronounced anti-inflammatory properties in a murine model of airways allergic inflammation and suggest that it might present therapeutic potential for the airways inflammatory diseases management.

Keywords:

Quercetin-loaded microemulsion
Airways allergic inflammation
Eosinophils
Oral bioavailability

1. Introduction

Allergic asthma is a complex inflammatory disorder characterised by airway hyperresponsiveness, eosinophilic inflammation and hypersecretion of mucus by goblet cells. This disease is frequently accompanied by high serum levels of immunoglobulin (Ig)E and associated with increasing intrapulmonary production of certain interleukins (IL), especially IL-4, IL-5 and IL-13 by allergen-specific T-helper 2 (Th2) cells [1]. Integrated signaling events between IL-4 and IL-13 is believed to regulate pulmonary eosinophilia by stimulating eosinophil-specific adhesion pathways and by modulating the local production of IL-5 and CCL11, which in turn, selectively drive eosinophil recruitment. Furthermore, IL-5 also plays a critical role in the regulation of bone marrow and blood eosinophilia [2].

Although, a great progress has been obtained in the last decades in our understanding of the cellular and molecular mechanisms underlying the allergic asthma, few effective and safe drugs are currently available for this disease management. Corticosteroids are the most established therapy for controlling most type of inflammatory reaction, eosinophilic included, exerting a strong effect on leukocyte recruitment, when administered locally or systemically [3]. Though these drugs have pronounced pharmacological activity, they exhibit severe adverse effects that preclude their long term use. Furthermore, pharmacologically active compounds capable of inhibiting eosinophil function or inflammatory cells infiltration into the lung, with less adverse effects, are still needed for the treatment of patients with atopy/allergic, parasitic disorders, hypereosinophilic syndromes, and other eosinophil-related diseases.

Most plant-derived secondary metabolites are capable of directly affecting inflammatory mediators, as well as the production/activity of second messengers, transcription factors and key pro-inflammatory molecules expression [4, 5]. Flavonoids are common secondary metabolites found in the plant kingdom. The flavonoid quercetin is largely found in the diet and its main sources are tea, onions, apples and red wine [6]. Studies carried out *in vitro* have shown that quercetin exhibits, besides other activities, pronounced anti-inflammatory property, an effect that seems to be associated with its ability to block some inflammatory mediators [7], adhesion molecules expression [8], inducible enzymes [9] and nuclear transcription factor activation [10]. In asthma models, quercetin administered by oral [11, 12] or intraperitoneal [13] routes or by aerosol [14, 15] was able to reduce the allergic airway inflammation [11, 13-15],

hyperresponsiveness [13-15] and bronchial hyperactivity [12] as well as to modulate the Th1/Th2 cytokines [11, 13] associate with reduction of the histamine contents [14-15]. Despite its potential systemic anti-inflammatory property, quercetin aglycone is well known to possess poor water solubility. Previous findings have showed that it is less absorbed than quercetin glycosides and that its absorption seems to depend on the type and position of the sugar moieties [16, 17]. In the above studies, DMSO and polietilenoglicol have been used as coadjuvants to improve the quercetin solubilization and absorption. However, these substances are not approved to be used in humans.

When quercetin aglycone (100 mg) was administrated in humans by intravenous route it bound 98% to plasma proteins and it was mainly excreted in urine as a conjugated metabolite (7.4%) as unchanged (0.65%). On the other hand, when quercetin (4g) was given orally to human it was detected neither in the plasma nor in urine, either unchanged or in a metabolized form [18].

The colloidal drug delivery system, such as microemulsions, has been proposed to improve the absorption and therapeutic index of several drugs [19]. Microemulsions are isotropic liquid mixtures of oil, water and surfactant, frequently found in combination with a co-surfactant and present translucence and thermodynamic stability. The dispersed phase generally lipophilic, act as a potential reservoir of lipophilic drugs, which in contact with semi permeable membranes, such as skin or mucous membrane can facilitate the transport of drugs through these barriers [20, 21].

In this study, we sought to compare the quercetin oral absorption in the quercetin suspension (QU-SP) and quercetin-loaded microemulsion (QU-ME). In addition, we have also assessed the oral anti-inflammatory effect of both formulations in an experimental allergic model in mice.

2. Material and methods

2.1. Materials

Quercetin (purity 98.2%), castor oil and carboxymethylcellulose (CMC) were purchase from Natural Pharma (São Paulo, Brazil). Hydrogenated soybean lecithin (Lipoid S75-3N) was purchase from Via Pharma (São Paulo, Brazil). 12-hydroxystearic acid-polyethylene glycol copolymer (Solutol HS-15®) was kindly donated by Basf (Trostberg, Germany). Dexamethasone, ovalbumin, periodic acid-Schiff stain,

ethanol, acetone, methanol were purchased from Sigma-Aldrich (Missouri, USA). The solvents employed for HPLC-MS analysis were HPLC grade (JBaker: Xalostoc, Mexico). HPLC grade water (18 mΩ) was prepared using a Milli-Q system (Millipore: Massachusetts, USA).

2.2. Animals

Experiments were conducted by using female BALB/c mice (8 weeks old and weighing 20-25 g) and male Wistar rat (12 weeks old weighing 200-250 g) kept in controlled room temperature (22 ± 2ºC) and humidity (60-80%) under a 12:12 h light-dark cycle (lights on 06:00 h). At appropriate time intervals, mice were killed by isoflurane overdose. All procedures used in the present study was approved by UFSC Ethics Committee on the Use of Animals (protocol number 110), which follows the 'Principles of Laboratory Animal Care' from NIH publication Nº 85-23.

2.3. Preparation of quercetin suspension and quercetin microemulsion

The quercetin microemulsion (QU-ME) was prepared by a hot solvent diffusion method [22]. Briefly, 10 mg of quercetin, 10 mg of lecithin and 100 mg of castor oil were completely dissolved into a mixture of acetone:ethanol (60:40, v/v) at 60ºC. The resulting organic solution was quickly poured into 50 ml of an aqueous solution containing 1% of the surfactant (Solutol HS15®), maintained under magnetic stirring at 82°C. Then, the sample was cooled to room temperature, the organic solvent was evaporated under reduced pressure, and the final volume was adjusted to 20 ml. Finally, the nanocarrier was filtered through an 8 µm filter paper.

The quercetin suspension (QU-SP) was prepared by adding quercetin in aqueous carboxymethylcellulose dispersion (0.5%) in order to obtain a final quercetin concentration equal to microemulsion.

2.4. Quercetin content determination and microemulsion recovery

The quercetin content in the microemulsion was determined by UV spectrophotometric method using a Perkin-Elmer Lambda 10 UV/VIS spectrophotometer. The sample was diluted in methanol and the absorption was measured at 375 nm. The quercetin content was estimated by using a quercetin standard solution analyzed in the same

conditions and expressed in µg of quercetin/ml of microemulsion. The quercetin recovery was calculated as being the percentage of the quercetin total concentration found in the microemulsion in relation to the amount initially added.

2.5. Particle size analysis

The mean particle diameter of the microemulsion and the polydispersity index were determined by photon correlation spectroscopy using a Zetasizer Nanoseries (Marvern Instruments: Worcestershire, UK). Each size analysis lasted 300 s and was performed at 25°C with an angle detection of 173°.

2.6. HPLC-MS analysis

HPLC analysis was performed on a LCMS-2010EV apparatus with a diode array detector (SPD M20A, Shimadzu: Kyoto, Japan) and mass spectrometer (2010EV, Shimadzu), coupled with an auto injector (SIL-20A, Shimadzu), both using the software LC-MS Solutions 3.0 (Shimadzu). A Shim-pack VP-ODS column (5µm, 150 x 2.0 mm: Shimadzu) coupled with a guard-column (5 µm, 5 x 2.0 mm: Shimadzu) were used. The mobile phase consisted of a gradient solvent system of aqueous formic acid 0.2% (A) and acetonitrile (B). The elution profile was, 0 to 4 min: 9 to 20% B (linear); 4 to 9 min: 20 to 100% B (linear); 9 to 14 min: 100 to 20% B min (linear); 14 to 18: 20 to 9% B (linear); 18 to 23: 9% B (isocratic). The flow rate was 200 µl/min. The mass spectrometer operated in the negative and positive ionization mode. ESI-MS parameters were: potential of the ESI source 1.5 kV, CDL temperature heater 250^{o}C, block heater 200^{o}C, nitrogen served as collision gas 1.5 ml/min. MS analyses were recorded in the SCAN and SIM mode (*m/z* 301, 303).

2.7. Quercetin oral absorption in rats

Animals were non-fasted by 12 h and then were orally treated by gavage with QU-ME (10 mg/kg), QU-SP (10 mg/kg) or unloaded microemulsion. After 2 or 3 hours, animals were anaesthetized intraperitoneally with ketamine (70 mg/kg) and xylazine (10 mg/kg), submitted to laparotomy and the blood samples were collected by cardiac punction. The samples were immediately centrifuged at 3700 x *g* for 15 min to separate the plasma. It is noteworthy to mention that each

animal were used once for blood collection and for each time point analyzed was used three animals.

2.8. Sample preparation for chromatographic analysis

Samples were prepared by protein precipitation, evaporation and re-dissolving steps. One milliliter of acetone and 10 µl of acetic acid were added to 100 µl of plasma. After mix in vortex for 3 min, the mixture was centrifuged for 15 min at 20 800 x *g*. The supernatant was separated and evaporated to dryness by a gentle stream of nitrogen at 40°C. The samples were reconstituted by addition of 100 µl of acetonitrile: water (1:1), of which 20 µl was injected onto HPLC-MS system.

2.9. Antigen immunisation, booster, and airway challenge

Mice were immunised on days 0 and 7 by subcutaneous injection of 4 µg of ovalbumin (OVA) plus 1.6 mg of aluminium hydroxide in 0.4 ml of saline followed by two intranasal challenges (on post-immunisation days 14 and 21) with 10 µg of OVA in 50 µl of saline, delivered into the nostrils under light ether anaesthesia with the aid of a micropipette. The control group consisted of non-immunised mice that received two intranasal instillations of OVA. All determinations were made at 24 h time point after the second OVA challenge (on post- immunization day 21) [23].

2.10. Evaluation of leukocyte influx into the bronchoalveolar space

Mice were killed by isoflurane overdose. Subsequently, a polyethylene cannula was introduced into the trachea, and phosphate-buffered saline (PBS) containing heparin (10 UI/ml) was instilled in three aliquots (0.3, 0.3 and 0.4 ml) in a total of 1 ml. The BALF was recovered and placed on ice. Total cell and differential leukocyte count were made according Rogerio et al. [23]. Following centrifugation (400 x *g*, 5 min, 4ºC), supernatants of the BALF were collected and stored at -70°C for subsequent cytokine and chemokine determination.

2.11. Treatments

To investigate the possible therapeutic anti-inflammatory effects, QU-ME (at doses 3 or 10 mg/kg) or QU-SP (10 mg/kg) or unloaded microemulsion (an o/w microemulsion content 0.02:0.2:1 of lecithin: castor oil:solutol HS15®) or aqueous solution content CMC 0.5% were given orally by gavage with a volume varying between 140-580 µl according to the animals' weight and the dose, from day 18th to 22nd day after the first immunization with OVA. The positive control consisted of a one group that received dexamethasone (1 mg/kg, subcutaneous injection). The doses and period of treatment were carried out in according to previous study [11].

2.12. Measurement of IL-4, IL-5, CCL11, IFN-γ and LTB_4 levels

The IL-4, IL-5, CLL11 and IFN-γ levels were measured by specific ELISA (RayBiotech: Georgia, USA). LTB_4 were assayed according to the manufacturer's instructions (R&D Systems: Minnesota, USA). LTB_4 in the BALF competed with a fixed amount of horseradish peroxidase (HRP)-labeled LTB_4 for sites on a chicken polyclonal antibody. During the incubations, the chicken polyclonal antibody becomes bound to the rabbit anti-chicken antibody coated onto the microplate. Following a wash to remove excess conjugate and unbound LTB_4 of BALF, a substrate solution was added to the wells to determine the bound enzyme activity. Following color development, the assay was stopped, and the absorbance was read at 450 nm. The intensity of the color was inversely proportional to the concentration of LTB_4 in the sample. Sensitivities were > 10 pg/ml.

2.13. Analysis of mucus secretion in the lung histology

The lungs were removed, immersed in 4% phosphate-buffered formalin, and embedded in paraffin. Tissues were cut into 5 µm sections, which were then stained with periodic acid-Schiff stain to evaluate mucus production. Mucus hypersecretion by goblet cells in the airway epithelium was analyzed using a five-point scoring system as previously described [24]. The scoring system was: 0, no goblet cells; 1, less than 25%; 2, 25–50%; 3, 50–75%; and 4, more than 75%. Goblet cell scoring was examined in three independent fields of lung section from each mouse.

2.14. Immunohistochemical studies

Immunohistochemical detections of NF-κB p65 subunit and P-selectin were carried out in the lung (5 μm slices), using polyclonal rabbit anti-phospho-p65 NF-κB (#3037, 1:100) from Cell Signaling Technology (Massachusetts, USA) and polyclonal goat anti-P-selectin (#6943, 1:2000), from Santa Cruz Biotechnology (California, USA) as described in previous study [23].

2.15. Statistical analysis

The data are reported as mean ± S.E.M. The statistical significance among different treatments in each individual experiment was compared by ANOVA. When significant differences were identified, individual comparisons were subsequently made with Tukey's test. Values of $p < 0.05$ were considered statistically significant.

3. Results

3.1. Microemulsion characterization

A colloidal dispersion displaying mean particle size of approximately 20 nm and polydispersed index of 0.156 was obtained by the hot solvent diffusion technique, as described in material and methods section. The drug content and drug recovery were 430 μg/ml and 86%, respectively. Regarding the quercetin solubility in water (0.33 μg/ml), the microemulsion allowed to increase the drug concentration about 1.300 times in an aqueous dispersion. We have prepared the quercetin suspension (QU-SP) with the same quercetin final concentration of QU-ME (430 μg/ml).

3.2. Oral absorption of quercetin-loaded microemulsion in rats

Plasma samples obtained from rats were pre-treated with acetone and acetic acid, followed by centrifugation to precipitate plasma proteins and give the supernatant. The HPLC-MS analysis showed that retention time (t_R) of quercetin under developed conditions was 10.25 min and the most abundant ion was *m/z* 301 (negative mode) both at 2 and 3 h (Fig. 1A). No peak of quercetin in plasma was observed in this region after the treatment with vehicle (unloaded microemulsion) or QU-SP (Supplementary Fig. 1A and B). In the same conditions, it was

possible to detect a quercetin metabolite in plasma rats treated orally with QU-ME (Fig. 1B). This compound, so far not yet identified, represents a minor polar metabolite (t_R = 11.25 min), and it was detected in the positive mode and showed molecular ion *m/z* 303.

Fig. 1

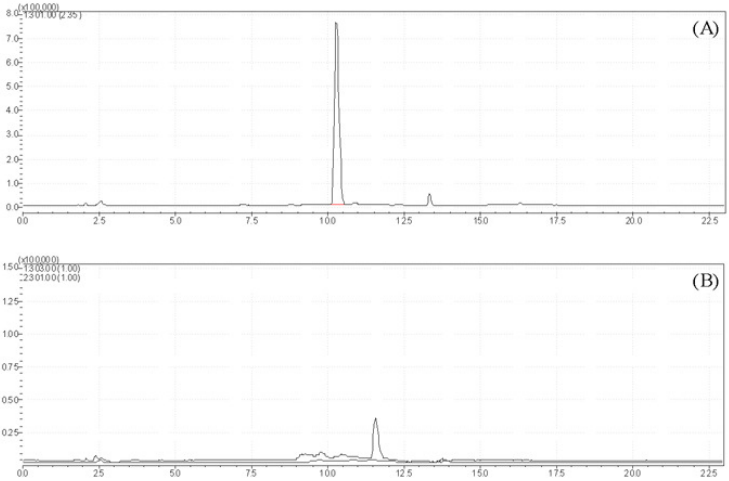

Fig. 1. HPLC-MS chromatograms (TIC x Tr): (A) quercetin standard; (B) rat sample plasma (n = 3) after oral treatment with QU-ME (10 mg/kg of quercetin). Mobile phase consisted of a gradient solvent system of aqueous formic acid 0.2% (A) and acetonitrile (B). The elution profile was, 0 to 4 min: 9 to 20% B (linear); 4 to 9 min: 20 to 100% B (linear); 9 to 14 min: 100 to 20 % B min (linear); 14 to 18: 20 to 9 % B (linear); 18 to 23: 9 % B (isocratic). The flow rate was 200 µl/min. ESI source operated in SIM mode (negative ionization: *m/z* 301, positive ionization: *m/z* 303).

3.3. Therapeutic effect of QU-ME on the leukocytes number in the BALF

The volume usually recommended by oral route administration in mice is 0.1 ml/10 g of weight. However, as the quercetin concentration achieved was 430 µg/ml the administration volume was 2.32 times higher than the recommended to reach the dose to be

administrated. However, no important alterations were observed in the mice after the administration of the highest volume.

To assess the possible therapeutic anti-inflammatory property of QU-ME and QU-SP, OVA-immunized mice were treated with QU-ME (at doses 3 or 10 mg/kg), with QU-SP (10 mg/kg) or with the respective vehicle from day 18th to 22nd day. No significant difference was observed between the OVA-immunized and -challenged groups treated with unloaded microemulsion (an oil-in–water microemulsion content 0.02:0.2:1 of lecithin: castor oil:solutol HS15®) or aqueous solution content CMC 0.5% (data not shown).

Fig. 2

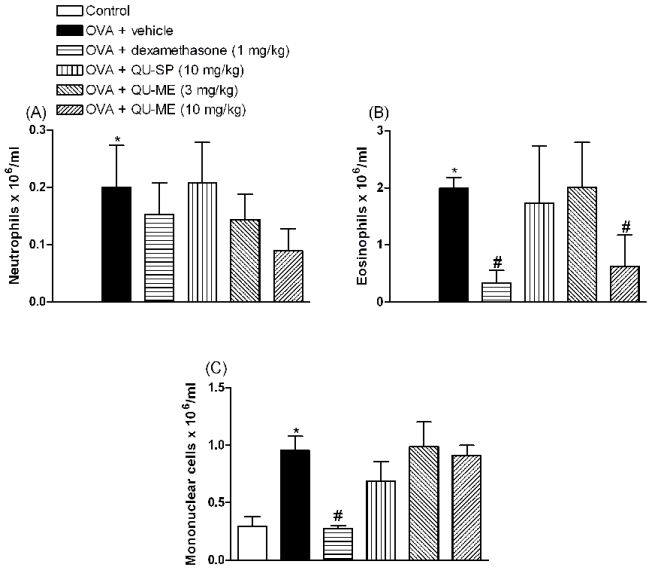

Fig. 2. The therapeutic oral treatment effect with QU-ME on the recruitment of neutrophils (A), eosinophils (B) and mononuclear cells (C) number in BALF of mice immunized and then challenged with OVA. Mice were treated orally with QU-ME (3 or 10 mg/kg), QU-SP (10 mg/kg), vehicle or dexamethasone (1 mg/kg, s.c.) from the 18th day to the 22nd day after the first immunization. Samples were collected 24h

after the second OVA- challenge. The means of at least three independent experiments and their standard errors are depicted (n = 6 per treatment). $^{*}p < 0.05$ compared with control group; $^{\#}p < 0.05$ compared with OVA + vehicle group; $^{+}p < 0.05$ compared with OVA + QU-SP group according to Tukey test.

As can be seen in Fig. 2A-C mice that received only the vehicle (unloaded microemulsion) exhibited a significant increase in neutrophil, eosinophil and mononuclear cells numbers in the BALF when compared control animals. QU-ME given orally at 10 mg/kg, like dexamethasone (1 mg/kg), significantly decreased the eosinophil recruitment (68 ± 4% and 84 ± 3%, respectively) to the BALF, when compared with vehicle-treated group (Fig. 2B). In addition, dexamethasone also reduced the mononuclear cells numbers. No significant differences were observed in the groups treated orally with QU-ME at dose of 3 mg/kg, as well as in the animals treated with QU-SP (Fig. 2). Moreover, no alteration in the neutrophil numbers was observed in the treated groups with QU-SP, QU-ME and dexamethasone, when compared to vehicle. QU-ME at dose 10 mg/kg reduced significantly the eosinophil recruitment (62 ± 9%) to the BALF when compared with QU-SP.

Since that QU-SP did not show any anti-inflammatory effect, as evidenced by the lack of reduction in the number of neutrophils, eosinophils and mononuclear cells when compared with OVA + vehicle group, all subsequent experiments were carried out only with QU-ME.

3.4. Effects of QU-ME on the IL-4, IL-5, IFN-γ, CCL11 and LTB_4 levels in the BALF

As only QU-ME (10 mg/kg) exhibited significant oral anti-inflammatory activity, we selected this dose to evaluate the cytokines (IL-4, IL-5 and IFN-γ), the chemokine (CCL11) and the lipid (LTB_4) levels in the BALF. In OVA-immunized and -challenged mice treated with vehicle (unloaded microemulsion), the IL-4, IL-5, CLL11 and LTB_4 levels were significantly elevated when assessed 24 h after the last OVA-challenge and compared with control group. The therapeutic treatment with QU-ME significantly prevented the IL-5 and IL-4 levels (62 ± 2% and 71 ± 8%, respectively), when compared with vehicle-treated animals (Fig. 3A and B). However, no statistically significant differences were observed in CCL11 and LTB_4 levels (Fig. 3 C and D,

respectively). Dexamethasone, used as the positive control, significantly reduced the IL-5 (68 ± 3%), IL-4 (69 ± 6%), CCL11 (63 ± 15%) and LTB_4 (61 ± 12%) levels (Fig. 3A-D). No alteration of IFN-γ levels was observed among the experimental groups (data not shown).

Fig. 3

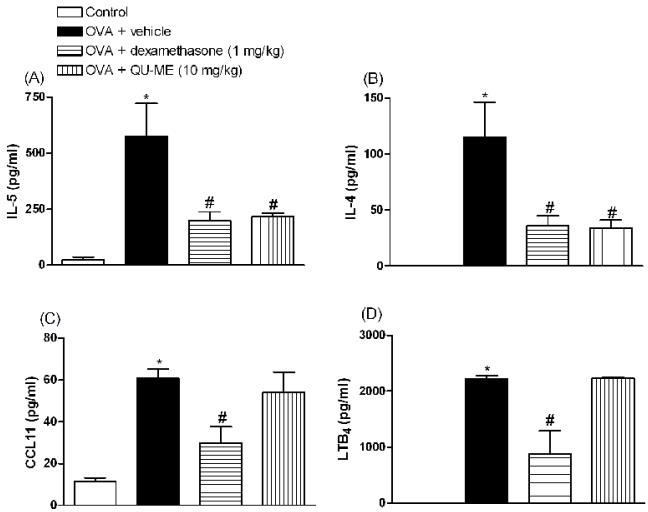

Fig. 3. The therapeutic oral treatment effect with QU-ME on IL-5 (A), IL-4 (B), CCL11 (C) and LTB_4 (D) levels in the BALF. Mice were treated orally with QU-ME (10 mg/kg), vehicle or dexamethasone (1 mg/kg, s.c.) from the 18th day to the 22nd day after the first immunization. Samples were collected 24h after the second OVA challenge. The means of at least three independent experiments and their standard errors are depicted (n = 6 per treatment). *$p < 0.05$ compared with control group; $^{\#}p < 0.05$ compared with OVA + vehicle group according to Tukey test.

3.5. Effects of QU-ME on the mucus secretion in the lung

In order to investigate the effects of QU-ME on mucus secretion, the lung tissues were stained with periodic acid-Schiff. A

hyperproduction of mucus by globet cells was observed in the bronchi of OVA-immunized and -challenged mice treated with vehicle (Fig. 4B and E) when compared with control group (Fig. 4A). Therapeutic treatment with QU-ME (Fig. 4D and E) or with dexamethasone (Fig. 4C and E), significantly decreased the degree of mucus secretion (62 ± 21% and 50 ± 12%, respectively) when compared with OVA-immunized and -challenge mice treated with vehicle.

Fig. 4

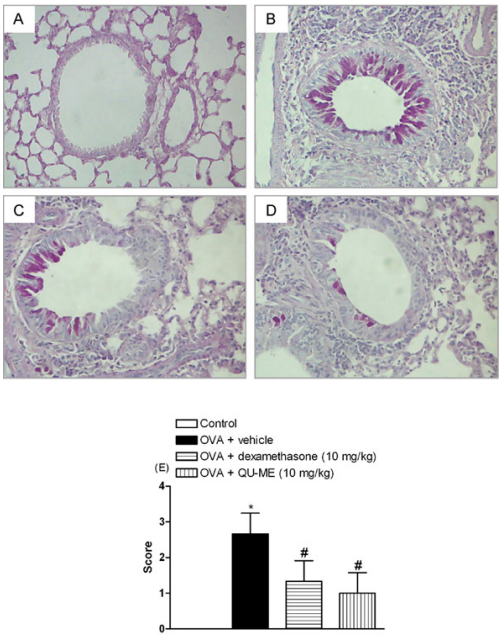

Fig. 4. The therapeutic oral treatment effect with QU-ME (10 mg/kg) on the airway mucus. Representative lung tissue sections from control mice (A), immunised and OVA-challenged mice given vehicle (B), dexamethasone (C) or QU-ME (D) were stained with periodic acid Schiff (magnification: x 200). Mucus production (indicated by arrows) in the lung tissues was scored (E). The means of at least two independent experiments and their standard errors are depicted (n = 4 per treatment). $^{*}p < 0.05$ compared with control group; $^{\#}p < 0.05$ compared with OVA + vehicle group according to Tukey test.

3.6. Effect of QU-ME on the NF-κB activation and P-selectin expression in the lung

The effects of QU-ME treatment on P-selectin expression and the phosphorylation state of p65 NF-κB were evaluated by immunohistochemistry technique. Under homeostatic conditions, there was not significant activation of p65 NF-κB was found in the lung cells (Fig. 5A).

Fig. 5

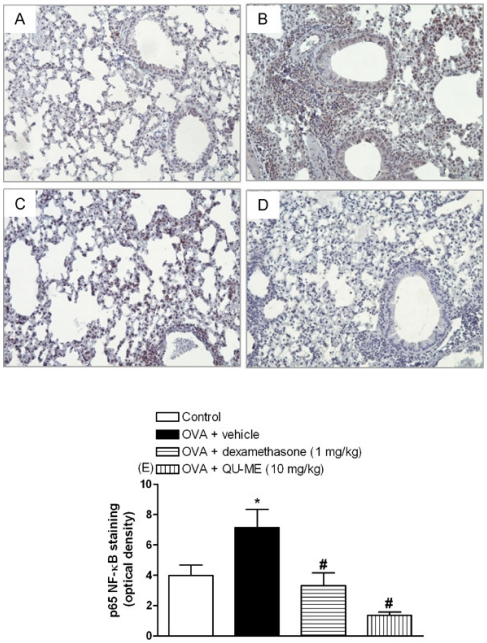

Fig. 5. The therapeutic oral treatment effect with QU-ME (10 mg/kg) on the activation of p65 NF-κB. Representative images of phospho-p65 NF-κB imunohistochemistry staining (indicated by arrows) of control (A), OVA + vehicle (B), OVA + dexamethasone (C), and OVA + QU-ME (D) groups (magnification: x 200). The mean intensity of phospho-p65 NF-κB staining was determined from image analysis and represented as arbitrary units (E). The means of at least two independent

experiments and their standard errors are depicted (n = 4 per treatment). *$p < 0.05$ compared with control group; $^{\#}p < 0.05$ compared with OVA + vehicle group according to Tukey test. However, a constitutive staining for P-selectin was observed (Fig. 6A). In the lung tissue of OVA-immunized and -challenged mice treated with vehicle it was detected the phosphorylated p65 subunit of NF-κB (Fig. 5B) in the nucleus of endothelial and inflammatory cells around the bronchiolar epithelium. In addition, P-selectin staining was also significantly increased in these cells (Fig. 6 B). Of note, QU-ME given orally to mice, significantly reduced the p65 NF-κB activation (57 ± 19%, Fig. 5 D and E), and also the P-selectin expression (87 ± 5%) (Fig. 6 D and E) in the lung, when compared to the vehicle-treated animals. Likewise, dexamethasone, almost completely inhibited the activation of p65 NF-κB (99 ± 2%) (Fig. 5 C and E), but it failed to prevent the P-selectin expression in the lung (Fig. 6 C and E).

Fig. 6

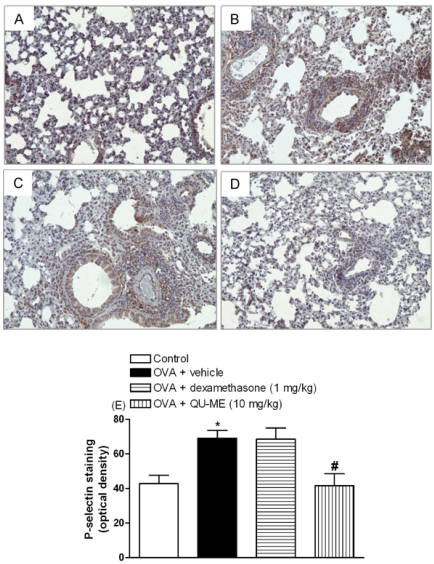

Fig. 6. The therapeutic oral treatment effect with QU-ME (10 mg/kg) in the P-selectin expression. Representative images of P-selectin imunohistochemistry staining (indicated by arrows) of control (A), OVA

+ vehicle (B), OVA + dexamethasone (C), and OVA + QU-ME (D) groups (magnification: x 200). The mean intensity of P-selectin staining was determined from image analysis and represented as arbitrary units (E). The means of at least two independent experiments and their standard errors are depicted (n = 4 per treatment). *$p < 0.05$ compared with control group; $^{\#}p < 0.05$ compared with OVA + vehicle group according to Tukey test.

4. Discussion

The main findings that emerge for the present study was the demonstration that, in contrast to QU-SP, QU-ME like the steroidal anti-inflammatory drug dexatamethasone, exhibits pronounced oral anti-inflammatory property when evaluated in OVA-induced allergic airway inflammation. Also relevant, the HPLC-MS analysis carried out in plasma of rats treated orally with QU-ME, differently of QU-SP, revealed the presence of a substance detected as ion $[M + H]^+$ *m/z* 303, that probably represents an active metabolite of quercetin. Together, these data strongly support the notion that QU-ME represents an effective delivery system that improves the oral bioavailability of this flavonoid.

Due to the low oral absorption of quercetin because of its low solubility in water, several techniques have also been previously used in order to increase its solubility, including the complexation with cyclodextrins and liposomes. One of the major drawbacks of such technologies is the stability problem during sterilization and storage [25, 26]. Hence, the development of a safe, stable and efficient delivery method for quercetin could present an interesting approach to investigate its potential therapeutic property.

Microemulsions and related systems represent pharmaceutically versatile formulations for various applications. They have the unique ability to solubilize nonpolar compounds in polar media and vice-versa, and for that reasons present good potential in pharmacy and medicine. Oil-in-water microemulsions are known to improve the bioavaliability of a poorly absorbed drug. This phenomenon may be related to the better uptake of the nanocarriers through to the gastrointestinal tract and also due to the decrease of degradation and/or metabolization of drugs. However, in spite of numerous advantages in comparison with other colloidal vehicles, such as thermodynamic stability, simple technology of preparation, transparency and low viscosity, microemulsions often require a high surfactant contents. For *in vivo* applications, the delivery

vehicle must be prepared from biocompatible and biotolerable components and due to its toxicity, only a limited number of surfactants and co-surfactants can be used to prepare pharmaceutical microemulsions [27, 19].

Taken the above mentioned fact, here we have evaluated a possible increase of the quercetin oral bioavailability and its anti-inflammatory activity in experimental airways allergic inflammation, by using the quercetin-loaded microemulsion prepared only with components approved for use by oral route. In this study, the maximal dose of QU-ME administrated orally to mice was 10 mg/kg. Concerning the transposition of this dose to humans, the use of the principle of extrapolation scaling for size differences is not consistent due to problems associated with drug transport and metabolism and also regarding the dose-response relationship. Thus, it was suggested is a specific methodology for drugs dose transposition from animal to human, formulated by FDA [28]. Considering the FDA approach, the human equivalent dose (HED) of QU-ME would be about 0.81 mg/kg. Moreover, earlier studies have showed that high doses of quercetin (1200 mg/day) are safe and well tolerable [29, 30]. Thus, the HED of QU-ME seems to be within of the tolerable limits.

By using HPLC-MS system it was possible to detect the ion $[M + H]^+$ *m/z* 303 only in the plasma of rat treated with QU-ME. Such ion might represent several fragments of quercetin metabolites which can be quercetin diglucoronide, quercetin monoglucoronide, quercetin sulfate monoglucoronide or monoglucuronide/gluthathionyl methyl quercetin [31]. It is not clear in the present stage of our study which quercetin metabolite is responsible for the anti-inflammatory action of this flavonoid.

Eosinophilia is a hallmark of allergic and parasite diseases. The initial exposure to allergen or parasite antigen leads to activation of T helper 2 (Th2) cells which orchestrate the immune response in these diseases through cytokine secretions such as interleukin IL-4 and IL-5 [32, 33]. Additionally, the trafficking of eosinophils into inflammatory sites involves the chemokine interactions (e.g. eotaxin), lipids (e.g. LTB_4) and adhesion molecules (e.g. P-selectin) [34, 35].

We have evaluated in the present study the potential anti-eosinophilic of QU-ME. Confirming and extending the HPLC-MS plasma analysis of QU-ME, the results show that the oral treatment with QU-ME decreased in a dose-dependent way, the eosinophil recruitment to the BALF. In contrast, corroborating the HPLC-MS data, no significant oral anti-inflammatory effect was observed in mice treated

with QU-SP. Therefore, it become clear by using both HPLC-MS and *in vivo* studies that QU-ME when given orally (10 mg/kg) reach enough plasma concentration that rendered it a consistent oral anti-inflammatory property.

We next investigate further some possible mechanisms underlying the anti-inflammatory action of QU-ME in the allergic airway inflammatory model. Accumulated evidences indicate that IL-5 exerts a critical role in the eosinophil migration process from bone marrow to blood [36, 37]. Furthermore, it is known that IL-5 also contributes for terminal differentiation and proliferation of eosinophil precursors, as well as for activating mature eosinophils [38-41]. Concerning IL-4, this cytokine seems to be essential for the differentiation to a Th2 axis and consequently blocks the differentiation towards Th1 axis by down-regulating interferon-γ (IFN-γ) gene transcription [42]. Of note, the present study shows that QU-ME given orally to mice, like dexamethasone, significantly reduced both the IL-5 and IL-4 levels in the BALF. Interestingly, no significant differences in the level of IFN-γ, CCL11 and LTB_4 levels in the BALF in QU-ME-treated animals have been noted. These results collectively indicate that QU-ME might selectively interfere with cytokines Th2, a key mediator which exerts a critical role in airway eosinophilic inflammation in the asthma.

A new and also interesting data reported in the present study was the demonstration that QU-ME, dosed orally to mice, in contrast to dexamethasone, significantly reduced the adhesion molecule P-selectin expression in the BALF. A great number of evidence indicates the P-selectin modulates the eosinophil influx to the inflammatory tissues [35]. So, the P-selectin expression inhibition caused by QU-ME is thought to contribute for the anti-inflammatory action of QU-ME, specially its ability in decreasing the eosinophil recruitment observed in BALF.

Early studies suggest that in certain allergic diseases the expressions of some relevant genes encoding cytokines (e.g. IL-5), adhesion molecules (e.g. P-selectin) among others are critically controlled by nuclear factor κB [43-45]. Previous studies have shown the *in vitro* quercetin action in decreasing the NF-κB activation [46, 47]. The present study shows for the first time, that QU-ME administered orally to mice was able to significantly prevent the NF-κB activation in the lung of OVA-sensitized and -challenged mice. It is tempt to suggest that the inhibition of NF-κB activation following mice oral treatment

with QU-ME might be associated with its ability to prevent the IL-4, IL-5 levels and P-selectin expression in the BALF and consequently the eosinophil number.

Another reported important asthma feature is the mucus airway hypersecretion. The mucus production is caused by the increase of goblet cell numbers in the airway epithelia and by the increasing submucosal gland sizes which leads to airflow obstruction [48]. In this study we have reported that QU-ME, like dexamethasone, significant reduced the mucus production in the OVA-immunized and -challenge mice. However, further studies are still needed to elucidate the precise mechanism in which QU-ME reduces the mucus hyperproduction.

5. Conclusion

The results presented herein revealed for the first time that, the quercetin-loaded microemulsion reduced the most relevant phenotypes involved in the asthma process namely the eosinophil recruitment, IL-4 and IL-5 levels in the BALF, the P-selectin expression and mucus secretion in the lung, probably associated with its ability to blockade the NF-κB activation. As the plant-derived flavonoid quercetin is part of many foods and seems to be safe even following long term use in animals and humans [29], the its microemulsion would constitute an interesting and practical formulation to increase its oral bioavailability and, in turn, to evaluate its potential clinical interest to treat certain inflammatory and allergic diseases.

Acknowledgement

This work was supported by grants from the Conselho Nacional de Desenvolvimento Científico e Tecnológico (CNPq), Coordenação de Aperfeiçoamento de Pessoal de Nível Superior (CAPES) and Fundação de Apoio a Pesquisa do Estado de Santa Catarina (FAPESC) (Brazil). AP Rogerio hold postdoctoral fellowship from CNPq. CL Dora is a PhD student in pharmacy receiving a grant from CAPES. EL Andrade is a PhD student in pharmacology receiving a grant from CNPq. JS Chaves is postdoctoral receiving a grant from CNPq, FC Silva is a pharmacy student receiving a grant from CNPq.

References

[1] Neurath MF, Finotto S, Glimcher LH. The role of Th1/Th2 polarization in mucosal immunity. Nat Med 2002;8:567-73.

[2] Foster PS, Mould AW, Yang M, Mackenzie J, Mattes J, Hogan SP et al. Elemental signals regulating eosinophil accumulation in the lung. Immunol Rev 2001;179:173-81.

[3] Barnes PJ. Corticosteroids: the drugs to beat. Eur J Pharmacol 2006;533:2-14.

[4] Calixto JB, Campos MM, Otuki MF, Santos AR. Anti-inflammatory compounds of plant origin. Part II. Modulation of pro-inflammatory cytokines, chemokines and adhesion molecules. Planta Med 2004;70:93-103.

[5] Calixto JB, Otuki MF, Santos AR. Anti-inflammatory compounds of plant origin. Part I. Action on arachidonic acid pathway, nitric oxide and nuclear factor kappa B (NF-kappaB). Planta Med 2003;69:973-83.

[6] Hertog MG, Feskens EJ, Hollman PC, Katan MB, Kromhout D. Dietary antioxidant flavonoids and risk of coronary heart disease: the Zutphen Elderly Study. Lancet 1993;342:1007-11.

[7] Cho SY, Park SJ, Kwon MJ, Jeong TS, Bok SH, Choi WY et al. Quercetin suppresses proinflammatory cytokines production through MAP kinases and NF-kappaB pathway in lipopolysaccharide-stimulated macrophage. Mol Cell Biochem 2003;243:153-60.

[8] Ying B, Yang T, Song X, Hu X, Fan H, Lu X et al. Quercetin inhibits IL-1 beta-induced ICAM-1 expression in pulmonary epithelial cell line A549 through the MAPK pathways. Mol Biol Rep 2009;36:1825-32.

[9] García-Mediavilla V, Crespo I, Collado PS, Esteller A, Sánchez-Campos S, Tuñón MJ et al. The anti-inflammatory flavones quercetin and kaempferol cause inhibition of inducible nitric oxide synthase, cyclooxygenase-2 and reactive C-protein, and down-regulation of the nuclear factor kappaB pathway in Chang Liver cells. Eur J Pharmacol 2007;557:221-9.

[10] Reiterer G, Toborek M, Hennig B. Quercetin protects against linoleic acid-induced porcine endothelial cell dysfunction. J Nutr 2004;134:771-5.

[11] Rogerio AP, Kanashiro A, Fontanari C, da Silva EV, Lucisano-Valim YM, Soares EG et al. Anti-inflammatory activity of quercetin

and isoquercetrin in experimental murine allergic asthma. Inflamm Res 2007;56:402-8.

[12] Dorsch W, Bittinger M, Kaas A, Müller A, Kreher B, Wagner H. Antiasthmatic effects of *Galphimia glauca*, gallic acid, and related compounds prevent allergen- and platelet-activating factor-induced bronchial obstruction as well as bronchial hyperreactivity in guinea pigs. Int Arch Allergy Appl Immunol 1992;97:1-7.

[13] Park HJ, Lee CM, Jung ID, Lee JS, Jeong YI, Chang JH et al. Quercetin regulates Th1/Th2 balance in a murine model of asthma. Int Immunopharmacol 2009;9:261-7.

[14] Jung CH, Lee JY, Cho CH, Kim CJ. Anti-asthmatic action of quercetin and rutin in conscious guinea-pigs challenged with aerosolized ovalbumin. Arch Pharm Res 2007;30:1599-607.

[15] Moon H, Choi HH, Lee JY, Moon HJ, Sim SS, Kim CJ. Quercetin inhalation inhibits the asthmatic responses by exposure to aerosolized-ovalbumin in conscious guinea-pigs. Arch Pharm Res 2008;31:771-8.

[16] Hollman PC, de Vries JH, van Leeuwen SD, Mengelers MJ, Katan MB. Absorption of dietary quercetin glycosides and quercetin in healthy ileostomy volunteers. Am J Clin Nutr 1995;62:1276-82.

[17] Hollman PC, Van Trijp JM, Buysman MN, van der Gaag MS, Mengelers MJ, de Vries JH et al. Relative bioavailability of the antioxidant flavonoid quercetin from various foods in man. FEBS Lett 1997;418:152-56.

[18] Gugler R, Leschik M, Dengler HJ. Disposition of quercetin in man after single oral and intravenous doses. Eur J Clin Pharmacol 1975;9:229-34.

[19] Gupta S, Moulik SP, Lala S, Basu MK, Sanyal SK, Datta S. Designing and testing of an effective oil-in-water microemulsion drug delivery system for in vivo application. Drug Deliv 2005;12:267-73.

[20] Formariz TP, Chiavacci lA, Sarmento VHV, Santilli CV, Tabosa do Egito ES, Oliveira AG. Relationship between structural features and in vitro release of doxorubicin from biocompatible anionic microemulsion. Colloids Surf B Biointerfaces 2007;60:28-35.

[21] Vicentini FTMC, Simi TR, Del Ciampo JO, Wolga NO, Pitol DL, Iyomasa MM et al. Quercetin in w/o microemulsion: In vitro and in vivo skin penetration and efficacy against UVB-induced skin damages evaluated in vivo. Eur J Pharm Biopharm 2008; 69:948-57.

[22] Hu FQ, Jiang SP, Du YZ, Yuan H, Ye YQ, Zeng S. Preparation and characteristics of monostearin nanostructured lipid carriers. Int J Pharm 2006;314:83-9.

[23] Rogerio AP, Andrade EL, Leite DFP, Figueiredo CP, Calixto JB. Preventive and therapeutic anti-inflammatory properties of the sesquiterpene α-humulene in experimental airways allergic inflammatory model. Br J Pharmacol 2009.

[24] Kuperman DA, Huang X, Koth LL, Chang GH, Dolganov GM, Zhu Z et al. Direct effects of interleukin-13 on epithelial cells cause airway hyperreactivity and mucus overproduction in asthma. Nat Med 2002;8:885-9.

[25] Pralhad T, Rajendrakumar K. Study of freeze-dried quercetin–cyclodextrin binary systems by DSC, FT-IR, X-ray diffraction and SEM analysis. J Pharm Biomed Anal 2004;34:333-9.

[26] Yuan ZP, Chen LJ, Fan LY, Tang MH, Yang GL, Yang HS et al. Liposomal quercetin efficiently suppresses growth of solid tumors in murine models. Clin Cancer Res 2006;12:3193-9.

[27] Vicentini FT, Simi TR, Del Ciampo JO, Wolga NO, Pitol DL, Iyomasa MM et al. Quercetin in w/o microemulsion: in vitro and in vivo skin penetration and efficacy against UVB-induced skin damages evaluated in vivo. Eur J Pharm Biopharm 2008;69:948-57.

[28] Sharma V, McNeill JH. To scale or not to scale: The principles of dose extrapolation. Br J Pharmacol 2009;157:907-21.

[29] Harwood M, Danielewska-Nikiel B, Borzelleca JF, Flamm GW, Williams GM, Lines TC. A critical review of the data related to the safety of quercetin and lack of evidence of in vivo toxicity, including lack of genotoxic/carcinogenic properties. Food Chem Toxicol 2007;45:2179-205.

[30] Okamoto T. Safety of quercetin for clinical application. Int J Mol Med 2005;16:275-8.

[31] Hong YJ, Mitchell AE. Identification of glutathione-related quercetin metabolites in humans. Chem Res Toxicol 2006;19:1525-32.

[32] Zheng W, Flavell RA. The transcription factor GATA-3 is necessary and sufficient for the Th2 cytokine gene expression in CD4 T cells. Cell 1997;89:587-96.

[33] Nakayama T, Yamashita M. Initiation and maintenance of Th2 cell identity. Curr Opin Immunol 2008;20:265-71.

[34] Rothenberg ME, Hogan SP. The eosinophil. Annu Rev Immunol 2006;24:147-74.

[35] Wardlaw AJ. Eosinophil trafficking in asthma. Clin Med 2001;1:214-8.

[36] Faccioli LH, Mokwa VF, Silva CL, Rocha GM, Araujo JI, Nahori, MA et al. IL-5 drives eosinophils from bone marrow to blood and tissues in a guinea-pig model of visceral larva migrans syndrome. Mediators Inflamm 1996;5:24-31.

[37] Rogerio AP, Sá-Nunes A, Albuquerque DA, Anibal FF, Medeiros AI, Machado ER et al. *Lafoensia pacari* extract inhibits IL-5 production in toxocariasis. Parasite Immunol 2003;25:393-400.

[38] Sanderson CJ, Warren DJ, Strath M. Identification of a lymphokine that stimulates eosinophil differentiation in vitro. Its relationship to interleukin 3 and functional properties of eosinophils produced in cultures. J Exp Med 1985;162:60-74.

[39] Yamaguchi Y, Suda T, Suda J, Eguchi M, Muira Y, Harada N et al. Purified interleukin-5 (IL-5) supports the terminal differentiation and proliferation of murine eosinophilic precursors. J Exp Med 1988;167:43-56.

[40] Clutterbuck EJ, Sanderson CJ. Human eosinophil hematopoiesis studied in vitro by means of murine eosinophil differentiation factor (IL-5): production of functionally active eosinophils from normal human bone marrow. Blood 1988;71:646-51.

[41] Coeffier E, Joseph D, Vargaftig BB. Activation of guinea pig eosinophils by human recombinant IL-5. Selective priming to platelet-activating factor-acether and interference of its antagonists. J Immunol 1991;147:2595-602.

[42] Nakamura T, Kamogawa Y, Bottomly K, Flavell RA. Polarization of IL-4- and IFN-γ-producing $CD4^+$ T cells following activation of naive $CD4^+$ T cells. J Immunol 1997;158:1085-94.

[43] Anrather J, Csizmadia V, Brostjan C, Soares MP, Bach FH, Winkler H. Inhibition of bovine endothelial cell activation in vitro by regulated expression of a transdominant inhibitor of NF-kappa B. J Clin Invest 1997;99:763-72.

[44] Atreya I, Atreya R, Neurath MF. NF-kappaB in inflammatory bowel disease. J Intern Med 2008;263:591-6.

[45] Yang L, Cohn L, Zhang DH, Homer R, Ray A, Ray P. Essential role of nuclear factor kappaB in the induction of eosinophilia in allergic airway inflammation. J Exp Med 1998;188:1739-50.

[46] Sato M, Miyazaki T, Kambe F, Maeda K, Seo H. Quercetin, a bioflavonoid, inhibits the induction of interleukin 8 and monocyte chemoattractant protein-1 expression by tumor necrosis factor-alpha in cultured human synovial cells. J Rheumatol 1997;24:1680-4.
[47] Hämäläinen M, Nieminen R, Vuorela P, Heinonen M, Moilanen E. Anti-inflammatory effects of flavonoids: genistein, kaempferol, quercetin, and daidzein inhibit STAT-1 and NF-kappaB activations, whereas flavone, isorhamnetin, naringenin, and pelargonidin inhibit only NF-kappaB activation along with their inhibitory effect on iNOS expression and NO production in activated macrophages. Mediators Inflamm 2007;2007:45673.
[48] Evans CM, Kim K, Tuvim MJ, Dickey BF. Mucus hypersecretion in asthma: causes and effects. Curr Opin Pulm Med 2009;15:4-11.

Publicação 5. *Quercetin-loaded microemulsion: in vivo activity in B16-F10 melanoma*

Quercetin-loaded microemulsion: *in vivo* activity in B16-F10 melanoma

C. L. Dora[1], L. F. C Silva[1], L. Mazzarino[1], J. M. Siqueira[2], D. Fernandes[2], L. K. Pacheco[2], J. Assreuy[2] and E. Lemos-Senna[1]

[1]Departamento de Ciências Farmacêuticas, Centro de Ciências da Saúde, Laboratório de Farmacotécnica, [2]Departamento de Farmacologia, Centro de Ciências Biológicas, Universidade Federal de Santa Catarina, Campus Trindade, Florianópolis, Brazil, 88040-970

Correspondence to: Elenara Lemos-Senna (Telephone: 55 48 37215067; Fax: 55 48 37219350; E-mail: lemos@ccs.ufsc.br)

Abstract

Quercetin is a natural compound that has shown several biological activities, including potential anticancer activity. However, the utilization of this drug has been limited by its poor water solubility, and its low bioavailability (FRESCO *et al.*, 2006). Therefore, the development of quercetin-loaded nanocarrier system may be considered a promising to exploit its therapeutic properties in clinic, including in the cancer treatment. In this study, a microemulsion containing quercetin was developed and the antitumor activity of this drug delivery system, as well their association with cisplatin, were evaluated on subcutaneous melanoma in mice inoculated with B16-F10 cells. Besides, the renal and hepatic toxicity were also evaluated in the end of the study. Quercetin, as free drug or as drug-loaded microemulsion, was administrated at a dose of 5 mg/kg twice a week for 17 days. Cisplatin was administrated at dose of 5 mg/Kg once a week. No differences in tumor growth were observed with treatment with free quercetin, however, quercetin-loaded microemulsion significantly reduced tumor volume ($P < 0.001$ vs. control). The association of both drugs (Quercetin and cisplatin) did not showed synergic effect. Besides, no renal or hepatic toxicities were observed after administration of QU-ME. These results suggesting that the quercetin incorporation in the colloidal dispersion enhance the drug bioavailability and therefore the pharmacological effect was observed.

Keywords: Quercetin, Microemulsions, Drug Delivery Systems, Melanoma, B16-F10 Cells, Antitumor Activity.

1. Introduction

Melanoma is the leading cause of death from cutaneous malignancies. Malignant transformation could be associated with general enzymatic changes leading towards increased proteolytic and fibrinolytic activity in tumor cells (GHOSH and MAITY, 2007). The incidence rate is increasing faster than any other tumor, and the World Health Organization (WHO) estimates 132,000 new cases of cutaneous melanoma per year (GIBLIN and THOMAS, 2007). Sun exposure, patient phenotype, family history and previous history of melanoma are the major risk factors related to melanoma (BRAUD *et al*., 2003).

Quercetin (QU) (Fig. 1) is a naturally occurring polyphenol found in the plant kingdom. It is a component of most edible fruits and vegetables, with the highest concentrations being found in onions, apples, and red wine. This compound displays many biological activities, such as anti-inflammatory, antibacterial, antioxidant, antiangiogenic and antitumor (REDDY *et al*., 2003). Several studies have demonstrated not only the benefits of the use of the quercetin in cancer prevention and treatment, but also a synergistic effect have been observed when it is administered in combined treatment with drugs currently used in the chemotherapy (SCAMBIA *et al*., 1994; CIPAK *et al*., 2003). However, the majority of the studies have been carried out in cell culture, which not translates the *in vivo* real potential benefits, since quercetin is extensively metabolized in the large intestine and further, by the first-pass metabolism in the liver (KAWAII *et al.,* 1999; CASAGRANDE e DARBON, 2001; RODRIGUEZ *et al.,* 2002; MERTENS-TALCOTT e PERCIVAL, 2005; RUSAK *et al*., 2005; KUBO *et al.,* 2007). The oral bioavailability of quercetin was demonstrated to be less than 17% in rats and only 1% in men (LI *et al*., 2009).

In the last decade, the development of lipid nanocarriers have emerged as a useful strategy to improve the bioavailability of orally administered drugs. Some studies have demonstrated the potential of nanostructured drug delivery systems to render hydrophobic agents like quercetin dispersible in aqueous media, thus circumventing the drawback of its poor water solubility, while maintaining its antitumor activity against a number of cancer cell lines (YUAN *et al*., 2006; MOHANRAJ and CHEN, 2006). The mechanisms of enhancement of

drug bioavailability enclose the solubilization of drugs in the colloidal species, which has the advantage of presenting the drug in a dissolved form with a large interfacial surface area for absorption. Also, the fine droplets offer large surface area for pancreatic lipase to hydrolyze the lipids and thereby enhance the rate of drug release and/or generation of mixed micelles containing the drug (CHAKRABORTY *et al.,* 2009).

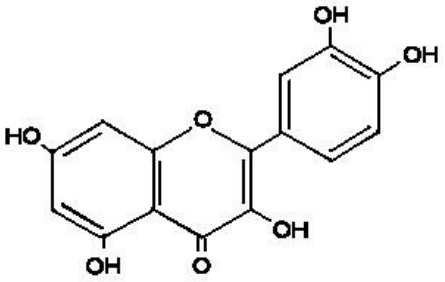

Figure 1. Molecular structure of quercetin.

In particular, liposomes and solid lipid nanoparticles have been assayed with the aim to improve the oral bioavailability of hydrophobic drugs. However, while the use of liposomes is often associated to stability problems in the presence of the components of the gastrointestinal tract, the solid lipid nanoparticles, in most cases, have demonstrated a limited ability to incorporate drugs in the lipid matrix constituted of well-organized lipid molecules (YUAN *et al*., 2006; LI *et al*., 2006). On the other hand, the use of microemulsions has been described as a satisfactory approach to enhance oral bioavailability of hydrophobic drugs (NORNOO *et al*, 2009). Microemulsions are optically transparent, low viscous, and thermodynamically stable dispersions of oil and water stabilized by an interfacial film of a surfactant, usually in combination with a cosurfactant, which displays a high ability to solubilize lipophilic drugs. The increase of the oral bioavailability of drugs provided by microemulsion systems has also been related to the better uptake of the nanocarrier through

gastrointestinal tract and decrease of degradation and/or metabolization of drugs (BOONME *et al*., 2006).

Previous formulation studies were carried out in our research group with the aim to obtain lipid-based nanocarriers with a high quercetin-payload. In these studies, we have demonstrated that when castor oil, PEG 660-stearate, hydrogenated soy lecithin, and water are used in a specific ratio, colloidal carriers displaying microemulsion properties were obtained by using the hot solvent diffusion method. These systems were able to increase the concentration of quercetin in an aqueous dispersion by around 1,300 times, regarding its water solubility (DORA *et al.*, 2010). Pharmacology studies carried out in a murine airways allegic inflammation model demonstrated that orally administered QU-loaded microemulsion was able to reduce significantly the most relevant phenotypes implicated in the asthma process, namely the eosinophil recruitment, IL-4 and IL-5 levels in the bronchoalveolar lavage fluid, P-selectin expression and mucus secretion, probably due its ability to blockade the NF-κB activation. The reduction of the eosinophil recruitment was not verified after the oral administration of a quercetin suspension at the same dose. Besides, after HPLC-MS analysis of the rat plasma, the quercetin metabolite was only detected after administration of the QU-microemulsion, suggesting that the increasing of the quercetin absorption occurred when the drug was solubilized in the inner oily core of the microemulsion (ROGÉRIO *et al.,* 2010).

In this study, we evaluated if the orally administered quercetin-loaded microemulsion is able to inhibit the B16F10 melanoma growth, after subcutaneous injection of B16F10 melanoma cells in mice. As scientific evidence also has been showed that quercetin may have a synergic effect with some chemotherapeutic agents in cell culture (SCAMBIA *et al*., 1994; CIPAK *et al*., 2003), we also verify the effect of the co-administration of cisplatin and quercetin on the inhibition of the tumor growing.

2. Materials and Methods

2.1 Materials

Quercetin, castor oil (CO) and carboxymethylcellulose were purchase from Natural Pharma (São Paulo, Brazil). Hydrogenated soybean lecithin (Lipoid S75-3N) and polyethyleneglycol 400 were purchase from Via Pharma (São Paulo, Brazil), and SP Pharma (São Paulo, Brazil), respectively. 12-hydroxystearic acid-polyethylene glycol copolymer (Solutol HS-15®) was kindly donated by Basf (Trostberg, Germany). All reagents and solvents were of analytical grade.

2.2 Preparation of quercetin microemulsion

The microemulsion (unloaded-ME) was prepared by a hot solvent diffusion method (HU *et al*., 2006). Briefly, 10 mg of lecithin and 100 mg CO were completely dissolved into a mixture of acetone:ethanol (60:40, v/v) at 60°C. The resulting organic solution was quickly poured into 50 mL of an aqueous solution containing 1% (w/v) of the PEG-660 stearate, maintained under magnetic stirring at 82°C. The resulting colloidal dispersion was then cooled to room temperature, the organic solvent was evaporated under reduced pressure, and the final volume was adjusted to 20 mL. Finally, the colloidal dsipersion was filtered through an 8 μm filter paper. For the preparation of quercetin-loaded microemulsion (QU-ME), 10 mg of the drug was added into the organic phase of the formulation

2.3 Determination of quercetin content in the microemulsion

The QU content was determined by a reversed-phase HPLC method after complete dissolution of the colloidal dispersion in 1% phosphoric acid:methanol solution (25:75 v/v, pH 2.7). The HPLC analysis was performed using a Shimadzu LC-10A system (Kyoto, Japan) equipped with a LC-10AD pump, SPD-10AV$_{VP}$ UV detector, SCL-10A$_{VP}$ system controller, DGU-14A degasser, CTO-10AS$_{VP}$ column oven, and the sample injection was performed through a Rheodyne 7125 valve with a 20 μL loop. The detector was set at 369 nm and peak areas were integrated automatically by computer using a Shimadzu Class VP® V 6.14 software program. The experiments were carried out using a reversed-phase Zorbax ODS (Agilent Technologies, USA) C_{18} column (150 mm x 4.6 mm I.D., with a particle size of 5 μm), maintained at 40 ± 1 ºC. The mobile phase consisted of a 1% phosphoric

acid:methanol mixture (45:55 v/v; pH 2.7) and was eluted isocratically at a flow rate of 1 mL min^{-1}. The HPLC method was validated according to the ICH. The calibration graph for QU was linear over the range of 0.25 to 10 $\mu g.mL^{-1}$ with a correlation coefficient of 0.9996. The calculated LOD and LOQ were 0.036 $\mu g\ mL^{-1}$ and 0.109 $\mu g\ mL^{-1}$ respectively, indicating that the method was sufficiently sensitive to determine the QU in the microemulsion. The specificity of the assay was confirmed by the individual analysis of the unloaded microemulsion. The precision of the method was evaluated and all relative standard deviation (R.S.D) were below 3%, indicating an acceptable intra-day and inter-day variability of the QU content for the colloidal dispersion.

2.4 Size and zeta potential measurements

The particle size and zeta potential of the unloaded and quercetin-loaded-ME were determined by photon correlation spectroscopy and laser-Doppler anemometry, respectively, using a Zetasizer Nano Series (Malvern Instruments, Worcestershire, UK). The measurements were performed at 25 °C after appropriate dilution of the samples in distilled water. Each size analysis lasted 300 s and was performed with an angle detection of 173°. For measurements of zeta potential, the samples were placed in the electrophoretic cell, where a potential of ±150mV was established. The ζ potential values were calculated as mean electrophoretic mobility values using Smoluchowski's equation.

2.5 Cell Lines

A highly metastatic B16-F10 mouse epithelial-like melanoma cell line was donated from Bio-Rio (Rio de Janeiro, Brazil). The cells were cultured in a Dulbecco's modified Eagle's medium (DMEM, Sigma-Aldrich) pH 7.4 supplemented with 10% fetal calf serum, 100 U/ml penicillin, 100 µg/ml streptomycin and 10 mM HEPES in a humidified atmosphere containing 5 % CO_2 at 37 °C. For *in vivo* experiments, cells were harvested with a trypsin:EDTA (0.05:0.03 w/v) solution, washed and inoculated into mice in phosphate-buffered saline (PBS; pH 7.4).

2.6 Evaluation of in vivo antitumor activity

Male specific pathogen-free C57BL/6 3-month-old mice were used. The animals were kept in a light controlled room (12-hour-light-dark cycle) at a room temperature of 23 ± 2 °C and 60 ± 10 % humidity. Food and water were given ad libitum. All animal studies were carried out in accordance with the procedures outlined in protocol number PP00161/CEUA, for the care and ethical use of animals in research (CEUA/UFSC, Florianópolis, SC, Brazil).

B16-F10 melanoma cells (1 x 10^6 cells suspended in 100 µl of DMEM medium) were subcutaneously inoculated into the back of male C57BL/6 mice (n = 8). Seven days after inoculation of B16-F10 cells, free quercetin, unloaded or quercetin-loaded microemulsion were administered by oral route at a dose of 5 mg/kg, twice a week, corresponding to a total of five doses, according to the experimental schedule previously tested. In order to improve the dispersion of quercetin in the vehicle, the drug was suspended in PBS pH 6.0 containing 0.5 % (w/v) of carboxymethylcellulose. The negative control received the cells and PBS while the positive control received the cells and cisplatin. This drug was administered intraperitoneally at a dose of 5 mg/kg, once a week. In this case, the same protocol of quercetin (5mg/Kg) was administrated twice a week and on day eleven a dose of 5 mg/kg of cisplatin was administrated intraperitoneally.

Tumor volumes were measured in the days of treatment throughout 17 days of experiment using a precision calipter and estimated according to the following standard formula: tumor volume (mm^3) = $width^2$ x length x 0.52, according to Lee *et al* (2003) The animal body weight was verified in the begging and the end of the experiment. Seventeen days after treatment, mice were sacrificed by cervical dislocation and tumors were excised and weighted. The statistical analysis was performed using analysis of variance followed by Bonferoni's post-hoc.

2.7 Toxicity studies

The renal and hepatic toxicity of the free drug and of the quercetin microemulsion were evaluated using blood collected by cardiac puncturing in heparinized syringes. Plasma levels of urea

nitrogen, creatinine, aspartate transaminase (AST) and alanine transaminase (ALT) were measured by using commercially available clinical assay kits (BioClin, Belo Horizonte, Brazil).

3. **Results and Discussion**

3.1 Characterization of QU-ME loaded microemulsion

Unloaded-ME and QU-ME prepared by the hot diffusion solvent method displayed a mean particle diameter of 21 and 22 nm, respectively. Zeta potential values were close to neutrality (-2 mV) for both quercetin loaded and unloaded microemulsion, probably due to the complete hiding of the lecithin negative charge by the polyethylene glycol chains of the PEG-660 stearate. The quercetin content in the microemulsion system was 470 μg/mL, which corresponds to an increase of the quercetin concentration by around 1,300 times, regarding its aqueous solubility (0.33 μg/mL).

3.2 Inhibition of tumor growth in mice inoculated with B16-F10 melanoma cells

To evaluate the effect of free quercetin and quercetin-loaded microemulsion and their association with cisplatin on tumor growth, C57BL/6 mice were inoculated subcutaneously with B16-F10 melanoma cells (1×10^6 in 100 μl/animal) and treated with the samples. The results are summarized in Figures 2 and 3, which display the ***tumor growth curves*** of ***B16F10*** melanoma in mice and the tumor weight at the end of the experiments, respectively**.**

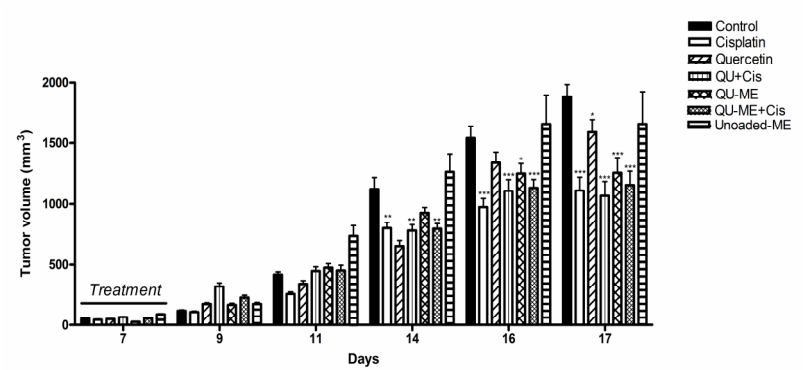

Figure 2. Tumor growth curves obtained after administration of quercetin, unloaded microemulsion and quercetin-loaded microemulsion alone and in combination with cisplatin, after inoculation of mice with $1x10^6$ B16-F10 melanoma cells. * P<0.05, ** P< 0.01 and *** P<0.001 compared with control (n=10).

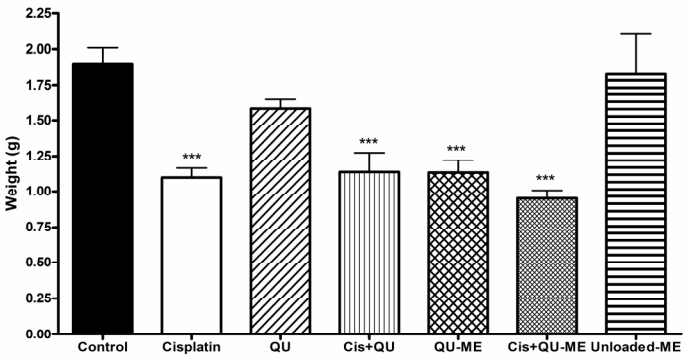

Figure 3. Effect of free quercetin, unloaded microemulsion, and quercetin-loaded microemulsion alone or in combination with cisplatin on tumor growth inhibition in mice inoculated with 1 x 10^6 B16-F10 melanoma cells. *** P<0.001 compared with control (n=10).

Figure 4 shows the subcutaneous melanoma tumors of the mice that receive the different treatments. Give twice a week, at a dose of 5 mg/kg, quercetin-loaded microemulsion significantly decreased tumor growth rate throughout the 17 days of experiment. By the end of the experiment, tumor growth was significantly inhibited by around 66% (1256.58 mm^3), after treatment with quercetin microemulsion when compared to the control group treated with cell culture medium only (1886.60 mm^3) ($P < 0.001$). Cisplatin at a dose of 1 mg/kg, once a week, decreased the tumor volume by 59 % (1111.96 mm^3). No difference was found in the reduction of tumor volume in mice administered with free quercetin (1587.63 mm^3), as well as with the administration of unloaded microemulsion (1656.40 mm^3), when compared to the control group. The combinated treatment of quercetin and cisplatin did not cause a significant reduction in the tumor growth.

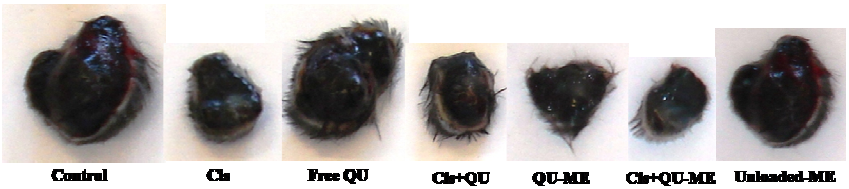

Figure 4. Subcutaneous B16F10 melanoma tumors obtained from mice that receive the different treatments.

The association of the quercetin with the colloidal system seemed to be beneficial, since a reduction in the tumor growth was observed. This effect was not evidenced with the oral administration of the quercetin suspension (free quercetin). The inhibition of tumor growth after administration of the QU-ME can be related to the increase of the drug absorption when it was solubilized in the inner oily phase of the microemulsion.

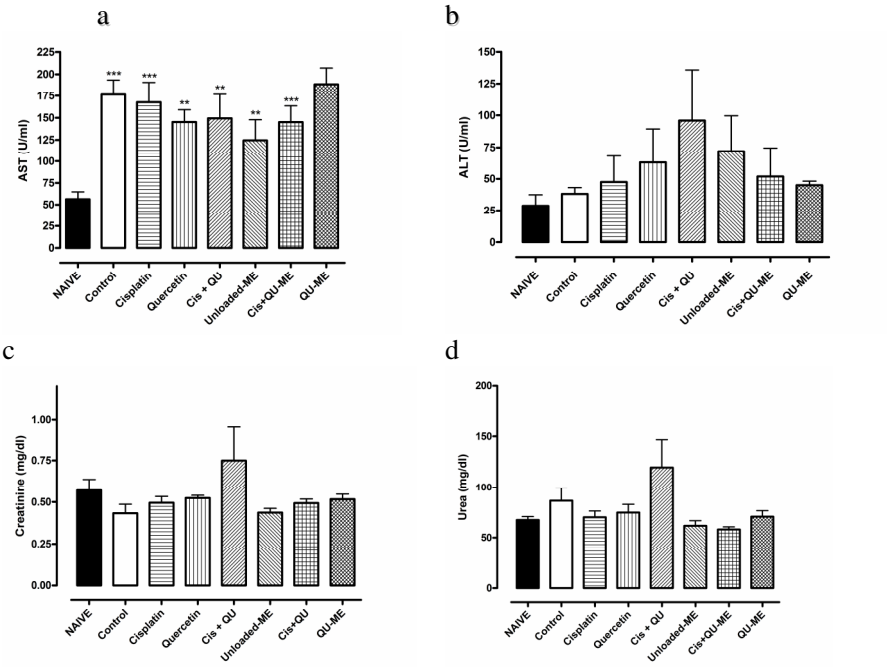

Figure 5. Evaluation of hepatic and renal toxicity after oral treatment with free quercetin and QU-ME and their association with cisplatin in mice inoculated with $1x10^6$ B16-F10 melanoma cells. (a) aspartate transaminase (AST), (b) alanine transaminase (ALT), (c) urea and (d) creatinine.

The results obtained in the evaluation of the hepatic and renal toxicity after the treatment of the animals with different samples are demonstrated in Figure 5. The results obtained from hepatic markers (Figure 4a and 4b) indicated the increasing of the levels only of the aspartate transaminase (AST) for all groups that were inoculated with the melanoma cells, including the control, being therefore related to the melanoma disease. No significant differences were observed for the renal markers urea and creatinine, when compared with the negative control (Figure 4c and 4d), indicating that the administration of the quercetin microemulsion by the oral route did not produce renal toxicity.

4. Conclusion

In this study we demonstrated that a significant inhibition of B16F10 melanoma growth occurred when a quercetin-loaded microemulsion was administrated by the oral route, compared to the negative control, without renal or hepatic toxicity. The significant reduction was not observed when a quercetin suspension was administrated at the same dose, suggesting that an improvement in the oral bioavailability of quercetin occurred when this compound was dissolved in the oily phase of a microemulsion.

Acknowledgments

The authors are grateful to FAPESC for the financial support to the project. C. L. Dora and F. C. Silva received grants from CAPES and CNPq, respectively. The authors also wish to thank the Centro de Pesquisas Oncológicas (CEPON/Santa Catarina, Brazil) for providing materials for the experiments.

References

Fresco P, Borges F, Diniz C, Marques MP. **2006**. New insights on the anticancer properties of dietary polyphenols. *Med Res Rev* 26(6):747-766.

Ghosh, S. and Maity, P. **2007.** *International Immunopharmacology*, 7, 1598–1608.

Giblin AV, Thomas JM **2007**. Incidence, mortality and survival in cutaneous melanoma. *J Plast Reconstr Aesthet Surg* 60(1):32-40.

Braud F, Khayat D, Kroon BBR, Valdagni R, Bruzzi P, N. Cascinelli. **2003**. Malignant melanoma. *Crit Rev Oncol Hematol* 47(1):35-63.

Reddy, L.; Odhav, B.; Bhoola, K. D. **2003.** Natural products for cancer prevention: a global perspective. *Pharmacology & Therapeutics* 99, 1-13.

Scambia, G., Ranelletti, F. O., Panici, P. B., Vincenzo, R., Bonanno, G., Ferrandina, G., Piantelli, M., Bussa, S., Rumi, C., Cianfriglia, M.,Mancuso, S. **1994**. Quercetin Potentiates the Effect of Adriamycin in a Multidrug-Resistant Mcf-7 Human Breast-Cancer Cell Line: P-Glycoprotein As A Possible Target. *Cancer Chemotherapy and Pharmacology,* 34 (6): 459-464.

Cipak, L.; Rauko, P.; Miadokova, E.; Cipakova, I.; Novotny, L. **2003.** Effects of flavonoids on cisplatin-induced apoptosis of HL-60 and L1210 leukemia cells. *Leukemia Research.* 27: 65-72.

Kawaii, S., Tomono, Y., Katase, E. and Ogawa, K. **1999**. Antiproliferative activity of flavonoids on several cancer cell lines. *Biosci Biotechnol Biochem*., 63: 896-899.

Casagrande, F.; Darbon, J.-M. **2001.** Effects of structurally related flavonoids on cell cycle progression of human melanoma cells: regulation of cyclin-dependent kinases CDK2 and CDK1. *Biochem Pharmacology*, 61:1205-1215.

Rodriguez, J., Yanes, J., Vicente V., Alcaraz, M., Benavente-Garcia O., Castillo, J., Lorente J., Lozano J. **2002.** Effects of several Favonoids on the growth of B16F10 and SK-MEL-1 melanoma cell lines: relationship between structure and activity. *Melanoma Research*, 12: 99-107.

Mertens-Talcott, S. U.,Percival, S. S. **2005**. Ellagic Acid and Quercetin Interact Synergistically with Resveratrol in the Induction of Apoptosis and cause Transient Cell Cycle Arrest in Human Leukemia Cells. *Cancer Letters,* 218 (2):141-151.

Rusak, G., Gutzeit, H. O.,Muller, J. L. **2005**. Structurally Related Flavonoids With Antioxidative Properties Differentially Affect Cell Cycle Progression and Apoptosis of Human Acute Leukemia Cells. *Nutrition Research,* 25 (2):143-155.

Kubo I., Nitoda T., Nihei, K-I. Effects of Quercetin on Mushroom Tyrosinase and B16-F10 Melanoma Cells. **2007.** *Molecule*, 12:1045-1056.

Li, H.; Zhao, X.;Ma, Y.; Zhai. G.; Li, L.; Lou, H. **2009.** Enhancement of gastrointestinal absorption of quercetin by solid lipid nanoparticles *Journal of Controlled Release*. 133 (3): 238–244

Yuan, Z.P., Chen, L.J., Fan, L.Y., Tang, M.H., Yang, G.L., Yang, H.S., Du, X.B., Wang, G.Q., Yao, W.X., Zhao, Q.M., Ye, B., Wang, R., Diao, P., Zhang, W., Wu, H.B., Zhao, X., Wei, Y.Q., **2006**. Liposomal quercetin efficiently suppresses growth of solid tumors in murine models. *Clin. Cancer. Res*. 12, 3193–3199.

Mohanraj V, Chen Y **2006**. Nanoparticles - a review. *Trop J Pharm Res* 5:561-573.

Chakraborty, S.; Shukla, D.; Mishra, B.; Singh S. **2009.** Lipid – An emerging platform for oral delivery of drugs with poor bioavailability. *European Journal of Pharmaceutics and Biopharmaceutics,* 73, 1–15.

Li, H. *et al.* **2006**. Studies on the preparation of quercetin solid lipid nanoparticles and oral absorption in mice. *Nanoscience*, 11(4):306-310.

Nornoo, A. O., *et al.* **2009.** Oral microemulsions of paclitaxel: In situ and pharmacokinetic studies. *European Journal of Pharmaceutics and Biopharmaceutics*, 71(2):310-317.

Boonme, P.; Krauel, K.; Graf, A.; Rades, T.; Junyapraset, V. B. **2006** *AAPS PharmSciTech*.**,** 7 (2), E1-E6.

Dora C.L., Silva, L. F. C., Tagliari, M. P., Silva, M. A. S., Lemos-Senna. **2010**. Formulation Study of quercetin-loaded lipid-based nanocarriers obtained by hot solvent diffusion method. *Latin American Journal of Pharmacy*. Article accepted.

Rogério, A. P., Dora, C. L., Andrade, E. L., Chaves, J. S.. Silva, L. F. C., Lemos-Senna, E., Calixto, J. B. **2010**. Effect of quercetin-loaded microemulsion in the eosinophilic inflammatory process in an experimental airway allergic inflammation. *Biochemical Pharmacology*, 61 (4): 288-297.

Hu, F-Q.; Yuang, H.; Zhang, H-H.; Frang, M. Preparation of solid lipid nanoparticles with clobetasol propionate by a novel solvent diffusion method in aqueous system and physicochemical characterization. **2002**. *International Journal of Pharmaceutics*, 239: 121-128.

Lee YS, Yang HO, Shin KH, Choi HS, Jung SH, Kim YM, Oh DK, Linhardt RJ, Kim YS. The flavonoid quercetin inhibits dimetylnitrosamine-induced liver damage in rats.. **2003**. *Eur J Pharmacol* 465(1-2):191-198.

Publicação 6. *Poly (ethylene glycol) hydroxystearate/lecithin/castor oil-based microemulsion: investigation of the effect of the gastrointestinal fluids on the droplet size by dynamic light scattering*

Poly (ethylene glycol) hydroxystearate/lecithin/castor oil-based microemulsion: investigation of the effect of the gastrointestinal fluids on the droplet size by dynamic light scattering

Cristiana L. Dora[1], Elenara Lemos-Senna[1,*] and Redouane Borsali[2,*]

[1] Laboratório de Farmacotécnica, Departamento de Ciências Farmacêuticas, Centro de Ciências da Saúde, Universidade Federal de Santa Catarina, Campus Universitário Trindade, Bloco K, sala 107, 88040-900, Florianópolis, SC, Brazil.
[2] Centre de Recherches sur les Macromolécules Végétales (CERMAV-CNRS), BP 53, F-38041 Grenoble Cedex 9, France - *affiliated with Université Joseph Fourier and member of the Institut de Chimie Moléculaire de Grenoble*

*Corresponding authors:
lemos@ccs.ufsc.br Tel:+55 48 37215067, fax: +55 48 37219350
redouane.borsali@cermav.cnrs.fr Tel:+33 04 76 03 76 03, fax:+33 04 76 54 72 03

Abstract

In this study, we investigated the *in vitro* gastrointestinal stability of a PEG660-stearate/SbPC/CO-based microemulsion in several simulated and biorelevant GI fluids, with or without enzymes, using dynamic light scattering as technique of analysis. Oil-in-water ME was obtained by using castor oil as oily phase, and poly(ethylene glycol) (660)-12-hydroxystearate (PEG 660-stearate; Solutol HS15®) and soybean lecithin (SbPC) as surfactant and cosurfactant, respectively. The size of ME was not altered after 6 h of incubation in simulated gastric fluids. This results was attributed to the coating produced by polyethyleneglycol chains of the PEG 660-stearate, that allowed the protection of the castor oil and SbPC from acidic degradation. After incubation in the intestinal fluids without pancreatin, the ME was also demonstrated to be stable during the 24 h of experiment. However, in the presence of this enzyme, the peak corresponding to the particle size distribution of the ME disappeared with concomitant appearance of others peaks, suggesting that in this case, the microemulsion undergone a digestion process and others structures, like vesicles, micelles and aggregates, were formed.

Key-words: Microemulsion, similar gastrointestinal fluids, biorelevant fluids

Introduction

The fact that the oral bioavailability of poor water soluble drugs may be enhanced when co-administrated with a meal rich in fat have lead to an increasing in the development of lipid-based formulations in the last decades. Specially, lipid-based colloidal systems are able to carry hydrophobic drugs in aqueous media, besides to possess the advantage of presenting the drug in a dissolved form with a large interfacial surface for absorption (PORTER *et al*., 2007; PORTER *et al*., 2008; CHAKRABORTY *et al*., 2009). Among them, microemulsions display characteristics that make them good candidates for the oral administration of poorly water soluble drugs. Microemulsions are optically transparent, low viscous and thermodynamically stable dispersions of oil and water stabilized by an interfacial film of a surfactant and cosurfactant molecules, displaying droplet sizes less than 100 nm (GAO 1998). They have been reported to improve the rate and extent of absorption of many lipophilic drugs (GHOSH *et al,* 2006). The bioavailability enhancing properties of microemulsions has primarily been attributed to the ability of the vehicles to keep the compound in solution in the GIT, maintaining a maximal free drug concentration and omitting a rate determining dissolution (PORTER and CHARMAN, 2001).

However, the processing of lipid-based nanocarriers in the human body is highly complex and the fate of these systems as well the mechanisms of drug absorption are still not clear. The solubilization of drug in the GIT and its bioavailability depend on the intraluminal processing to which the formulations compounds, especially the lipids, are subjected prior to absorption. In general, the lipids are rapidly digested by gastric and intestinal enzymes and absorbed in the form of micellar structures by enterocytes (ROGER *et al.,* 2009). In the case of colloidal carriers, the reduced size of droplets also offer a large surface for lipid hydrolyze, enhancing the rate of drug release and/or the generation of mixed micelles containing the drug (CHAKRABORTY *et al*., 2009).

Previous studies (ROGÉRIO *et al.,* 2010) carried out in our research group have demonstrated that when castor oil, PEG 660 stearate, hydrogenated soy lecithin, and water are used in a specific ratio, colloidal carriers displaying microemulsion properties are obtained by using the hot solvent diffusion method. This drug delivery system was able to increase the water solubility and oral absorption of

quercetin, a hydrophobic polyphenol which exhibits important biological effects, but a very low bioavailability when administered by the oral route. These results were evidenced after analysis of the plasma of rats by HPLC-MS, in which a metabolite of quercetin was only detected after the oral administration of the quercetin microemulsion, but not after oral administration of a suspension of this drug in carboxymethylcellulose.

Some researchers have evaluated the stability of lipid-based nanocarrier in the presence of simulated gastrointestinal fluids. The dynamic lipolysis model has been used to simulate the self-nanoemulsifying drug delivery systems digestion in the GIT. Techniques as dynamic light scattering, small-angle X-ray scattering, and cryo-transmission electron microscopy have demonstrated to be powerful tools in the attempt to elucidate the digestion process undergone by the lipid formulations in the GIT (FATOUROS *et al.,* 2007a, FATOUROUS *et al.,* 2007b). Considering that the knowledge and characterization of the structure formed in the GI fluid in the presence of powerful digestive enzymes is very important for interpretation of the biopharmaceutical properties of orally administered lipid-based nanocarriers, the aim of this study was to investigate the effect of simulated and biorelevant GI fluids would have on the particle size of the previously developed microemulsion by using dynamic light scattering.

Materials and methods

Materials

Castor oil (CO), a triglyceride in which approximately ninety percent of fatty acid chains are ricinoleic acid, was purchased from Natural Pharma (São Paulo, Brazil). Hydrogenated soybean lecithin (SbPC; Lipoid S75-3N) was purchased from SP Pharma (São Paulo, Brazil). According to manufactures´specification the product contains from 67 to 73 % of phosphatidyl choline and lysophophatidyl choline. 12-hydroxystearic acid-polyethylene glycol copolymer (PEG 660-stearate, Solutol HS-15®) were kindly donated by Basf (Trostberg, Germany). Purified water was obtained from a MilliQ System (Millipore). Sodium chloride, potassium monobasic phosphate, sodium

monobasic phosphate, pancreatin (8×USP specification), pepsin, sodium taurocholate, lecithin, sodium hydroxide were purchased from Sigma–Aldrich. The other chemicals used were analytical reagent grade.

Methods

Preparation of PEG660-stearate/SbPC/CO microemulsion

The microemulsion was prepared by the hot solvent diffusion method (HU *et al*., 2002). Briefly, 10 mg of SbPC and 100 mg of CO were completely dissolved into a mixture of acetone:ethanol (60:40, v/v) at 60°C. The resulting organic solution was quickly poured into 50 mL of an aqueous solution containing a 1% of PEG-660 stearate (p/V), kept under magnetic stirring at 82°C. The resulting colloidal dispersion was then cooled to room temperature, the organic solvent was evaporated under reduced pressure, and the final volume was adjusted to 20 mL. Finally, the colloidal dispersion was filtered through an 8 μm filter paper. The final colloidal dispersion was constituted by a PEG660-stearate/SbPC/CO/water ratio of 2.5/0.05/0.5.

Particle size analysis

The size distribution, mean particle size and polydispersity index (PDI) of the PEG660-stearate/SbPC/CO microemulsion was determined by dynamic light scattering (DLS) using an ALV 5000 (ALV, Germany). The sample was previously diluted in ultrapure Milli-Q® water. The size analysis lasted 300 s and the temperature was set as 25°C. The analysis was performed using a single 90° scattering angle. The hydrodynamic radii was determined using Stokes-Einstein's equation, $R=(\kappa_B T/6\pi\eta D)$ where κ_B is Boltzmann's constant (J/K), T is the temperature (in K), D is the diffusion coefficient and η is the viscosity of the medium (η=0.89 cP at 25°C).

Composition of the simulated gastrointestinal media

Simulated gastric fluid (SGF) and simulated intestinal fluid (SIF) were prepared according to USP XXIV (US Pharmacopeia XXIV, 2006). The media were tested without enzymes to estimate the stability

in the different pHs; 1.2 for SGF and 6.8 for SIF media. For the experiments carried out in the presence of enzymes, 0.32% (w/v) of pepsin was added to the SGF medium and 1% (w/v) pancreatin was added to the SIF.

The composition of biorelevant fluids is summarized in Table 1 and 2. The fasted state simulating gastric fluid (FaSSGF) simulates the stomach fluid in the fasted state and has a pH of 1.6. The simulating of the gastric fed state (FeSSGF) cannot be measure by DLS because one of the compounds was milk and therefore, the fluid had a turbid aspect. The fasted state simulating intestinal fluid (FaSSIF) and the fed state simulating intestinal fluid (FeSSIF) represents a simplification of the proximal small intestine composition in both fasted and fed states. FaSSIF and FeSSIF have a pH of 6.5 and 5.0, respectively. These media were also tested with the addition of the enzyme pancreatin (1% w/v).

Table 1. Composition of the fasted state simulated gastric fluid (FaSSGF).

Composition/medium	***FaSSGF***
Sodium taurocholate	80 µM
Lecithin	20 µM
Pepsine	0.1 mg/mL
NaCl	6.186 g
HCl qs	pH 1.6
Purified water qs	1000 mL

Table 2. Composition of the fasted state (FaSSIF) and fed state (FeSSIF) simulated intestinal fluids.

Composition/medium	***FaSSIF***	***FeSSIF***
Sodium taurocholate	6 mM	15mM
Lecithin	1.5 mM	3.75 mM
NaOH (pellets)	0.348 g	4.04 g
$NaH_2PO_4.H_2O$	3.954 g	-
Glacial Acetic Acid	-	8.65 g
NaCl	6.186 g	11.874 g
Purified water qs	1000 mL	1000 mL

Stability study

An aliquot of 200µl of the PEG660-stearate/SbPC/CO microemulsion was added to 1800 µl different simulated GIT media and the mixtures were incubated at 37◦C. The experiments carried out in the simulated gastric fluids, samples were collected at times 0, 15 min, 30 min, 1, 2, 3 and 6 h, while for the experiments carried out in simulated intestinal fluids with or without pancreatin, samples were collected at times 0, 1, 2, 4, 6 and 24h. Particle size and size distribution were determined by dynamic light scattering as described above.

Results

Characterization of PEG660-stearate/SbPC/CO microemulsion

Figure 1 shows the correlation function *versus* time obtained at the scattering angle θ = 90°. The autocorrelation functions are essentially represented by a single exponential decay. The hydrodynamic radii of the particles was determined using Stokes-Einstein's relation and it was 11.6 nm. The polydispersity index was inferior to 0.2, indicating that a monodisperse distribution of oil droplets was obtained.

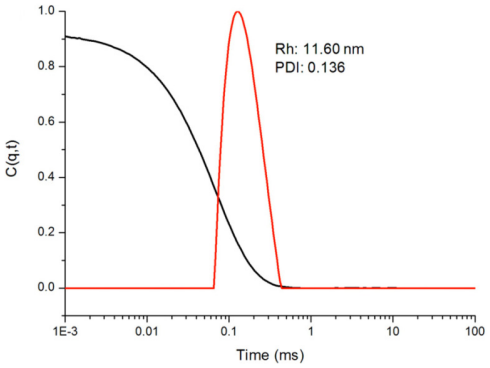

Figure 1. Correlation function and hydrodynamic radii (*R*h) obtained at 90° scattering angle for PEG660-stearate/SbPC/CO microemulsion.

Effect of the simulated gastric media on droplet size and size distribution of the microemulsion

The particle size of PEG660-stearate/SbPC/CO microemulsion after incubation in the simulating gastric media, with or without pepsin was determined by DLS . Table 3 shows the results of particle size obtained after 6 hours. Figure 2 and 3 demonstrates the hydrodynamic radii (Rh) of the PEG660-stearate/SbPC/CO microemulsion after incubation in SGF with or without pepsine and in FaSSGF, respectively. As can be observed, the particle size of the microemulsion was not affected by the gastric environment after 6h of incubation and the addition of pepsin did not reveal any changing in the distribution of the particle size.

Table 3. Hydrodynamic radii (R*H*) of PEG660-stearate/SbPC/CO microemulsion following 6 h incubation in simulated gastric fluid (SGF) and fasted stated simulated gastric fluid (FaSSGF).

Time (h)	SGF without pepsin	SGF with pepsin	FaSSGF
	R_H *(nm)*	R_H *(nm)*	R_H *(nm)*
0	9.3 ± 0.1	9.6 ± 0.2	9.3 ± 0.4
0.25	9.4 ± 0.2	9.8 ± 0.3	9.5 ± 0.4
0.5	9.6 ± 0.4	9.3 ± 0.7	9.7 ± 0.1
1	9.7 ± 0.3	9.8 ± 0.3	9.8 ± 0.1
2	9.8 ± 0.1	9.7 ± 0.1	9.9 ± 0.1
3	9.6 ± 0.5	9.6 ± 0.3	9.8 ± 0.3
6	10.1 ± 0.1	9.4 ± 0.4	9.7 ± 0.3

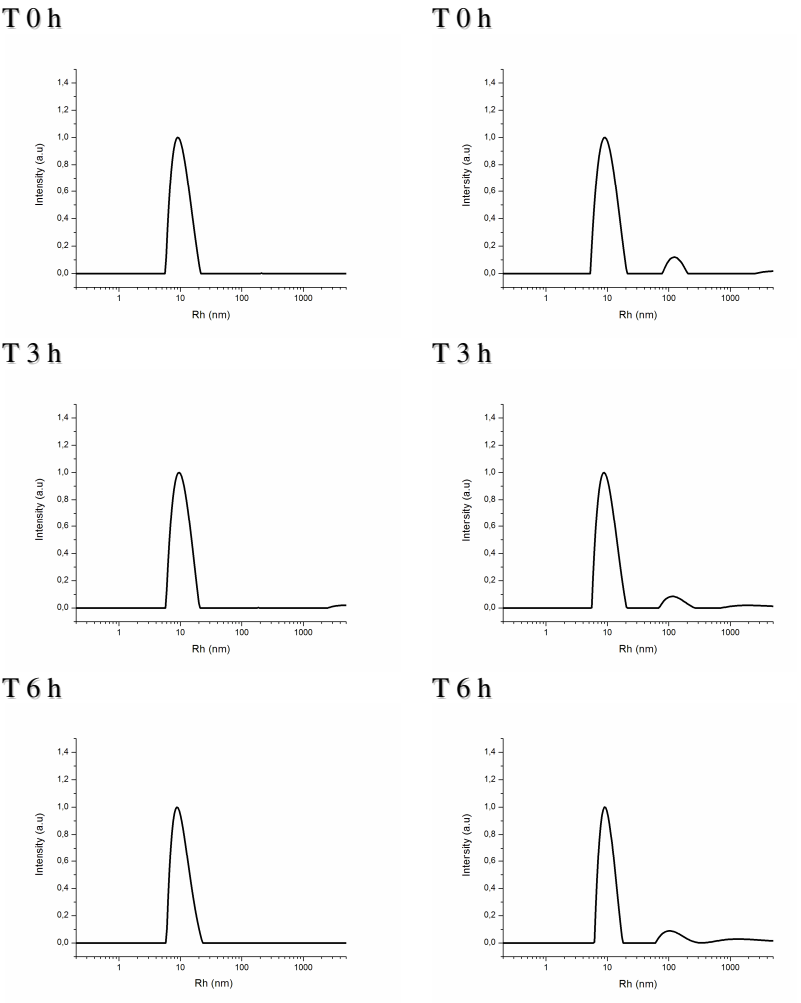

Figure 2. Particle size distribution of PEG660-stearate/SbPC/CO microemulsion after 0, 3 and 6 hours of incubation in SGF without pepsin (right side) and with pepsine (left side).

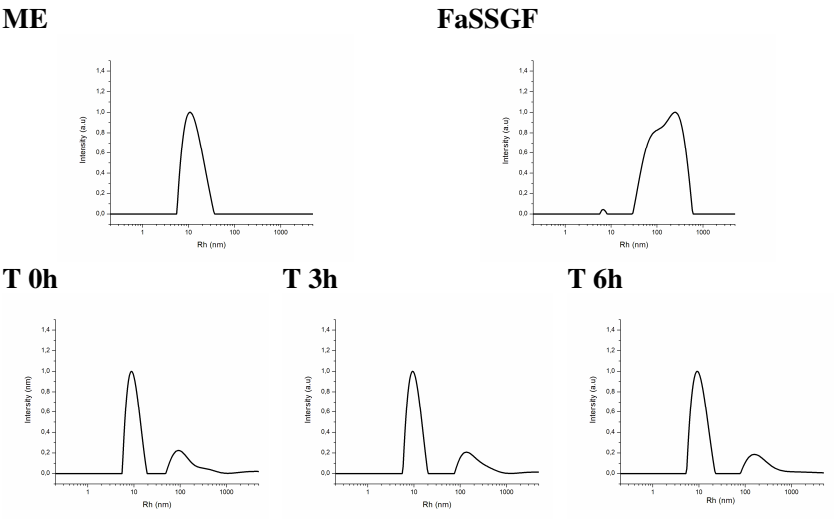

Figure 3. Particle size distribution of PEG660-stearate/SbPC/CO microemulsion after 0, 3 and 6 hours of incubation in FaSSGF.

Effect of the simulated intestinal media on droplet size and size distribution of the microemulsion

Different media for simulating the intestinal fluid have been described in the literature. In this paper we evaluated the effect of three types of intestinal media (SIF, FaSSIF and FeSSIF) with or without addition of the enzyme pancreatin on the particle size of PEG660-stearate/SbPC/CO microemulsion. The Table 4 and Figure 4 demonstrate the results obtained after the incubation of the microemulsion in the intestinal fluids without pancreatin. The analysis of the pure simulated intestinal fluid demonstrates the presence of particles exhibiting hydrodynamic radii of around 80nm for FaSSIF and around 5 and 200 nm for FeSSIF, which corresponds to the presence of the surfactant sodium taurocholate and lecithin in their composition. When the microemulsion was incubated in these media, a peak in approximately 10 nm was observed, which corresponds to the mean hydrodynamic radii of the microemulsion droplets. In the presence of

SIF, only a reduction in the width of this peak was observed after 24 h of incubation. No changes in the size distribution were visualized when the microemulsion was incubated in FaSSIF. When the microemulsion was incubated in FeSSIF, a little shift of the microemulsion peak towards higher values (~15 nm) and the appearance of a peak in around 1 µm were observed.

Table 4. Hydrodynamic radius (R*H*) of PEG660-stearate/SbPC/CO microemulsion following 6 h incubation in simulated intestinal fluid (SIF) and fasted and fed stated simulated intestinal fluid (FaSSIF and FeSSIF) without pancreatin.

Time (h)	**SIF**	**FaSSIF**	**FeSSIF**
	R_H *(nm)*	R_H *(nm)*	R_H *(nm)*
0	9.2±0.3	9.4±0.2	7.4±0.4
1	9.5±0.9	9.1±0.1	10.2±0.3
2	9.7±0.2	9.3±0.1	10.8±0.3
3	10.2±0.1	9.0±0.7	11.4±0.4
4	10.0±0.4	9.5±0.5	11.2±1.9
6	11.3±2.3	10.2±0.2	12.0±1.5
24	10.2±0.1	9.4±0.2	11.4±0.4

Apparently little changes in the particle size distribution were observed after incubation of the PEG660-stearate/SbPC/CO microemulsion after 24 h. The peak corresponding to the particle size distribution of the microemulsion remained unchanged during the experiment, indicating that the formulation is also stable in these media.

On the other hand, the light scattering analysis of the PEG660-stearate/SbPC/CO pure microemulsion in the presence of simulated intestinal fluid containing pancreatin exhibited different scattering profiles (Figures 5, 6 and 7).

The scattering profile of SIF with pancreatin showed a broad peak, ranging from 50 to 1000 nm (Figure 5). Following the incubation of the microemulsion in this medium (time point 0), the peak corresponding to the microemulsion hydrodynamic radii was observed. However, after one hour of incubation, this peak disappeared concomitantly to the appearance of others peaks at around 50 nm and 1µm, which probably corresponds to the lipid degradation by the lipase and formation of micelles and/or vesicles. After 24 h of incubation, peaks at 100 nm and 1µm were observed.

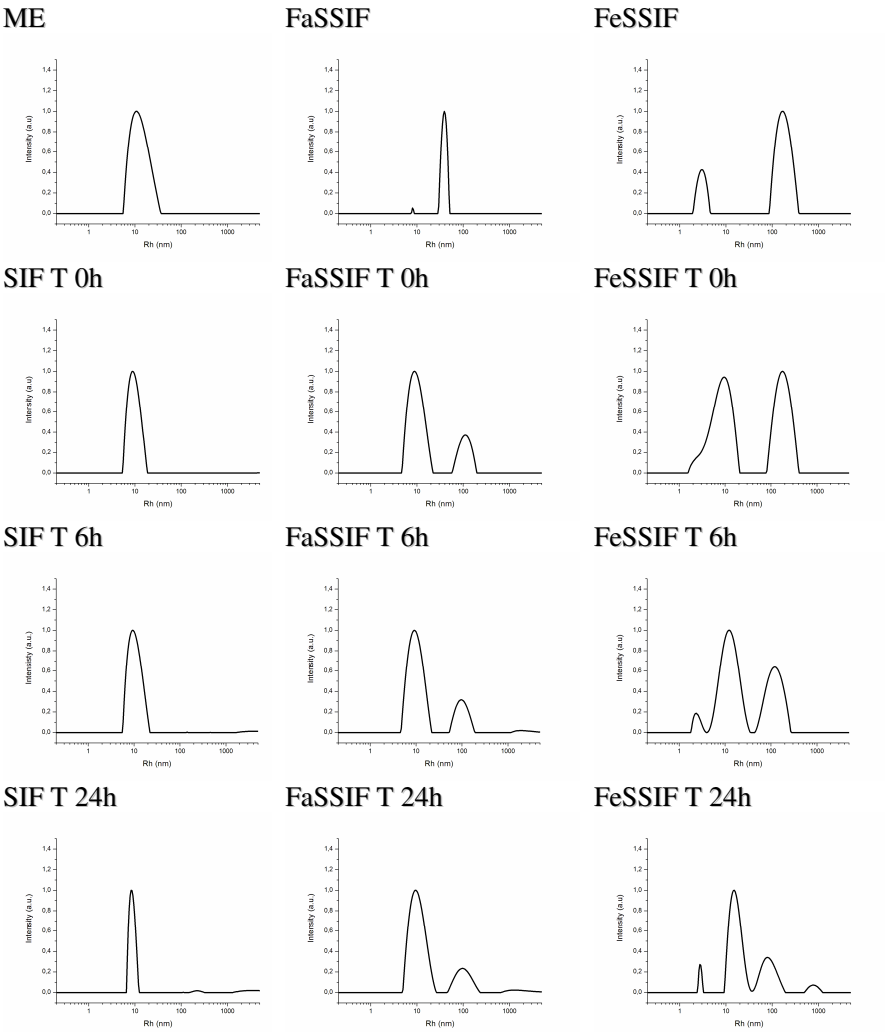

Figure 4. Particle size distribution of PEG660-stearate/SbPC/CO microemulsion following 0, 6, and 24 h of incubation in simulated intestinal fluid (SIF), and fasted (FaSSIF) and fed state simulated intestinal fluid (FeSSIF).

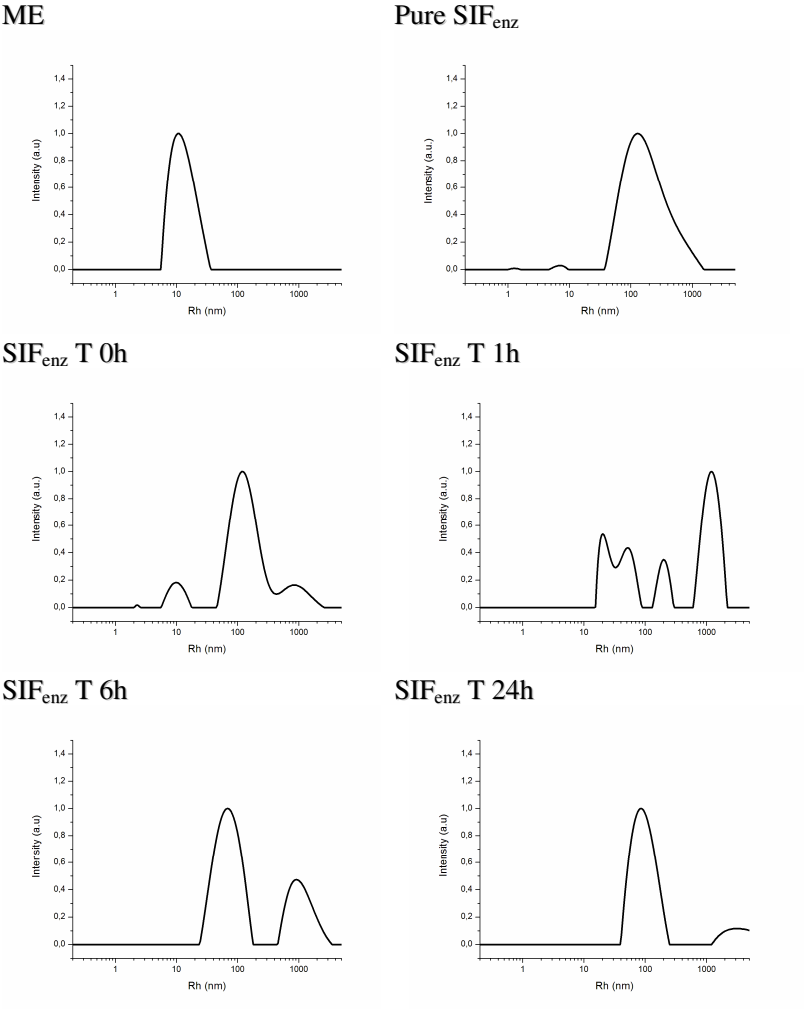

Figure 5. Particle size distribution of PEG660-stearate/SbPC/CO microemulsion after 0, 1, 6, and 24 h of incubation in simulated intestinal fluid with pancreatin (SIF_{enz}).

The analysis realized in FaSSIF containing pancreatin (Figure 6) also showed a large peak between 50-1000nm. The PEG-stearate ME peak was observed only in time point 0 and during the experiment this peak disappears. During the experiment others peaks were observed in 50, 100 and 800 nm, showing the degradation of the formulation and formation of vesicles/micelles or aggregates. The same pattern was observed when FeSSIF with pancreatin was assayed (Figure 7), but in this case, after 24h a large peak between 10 and 800nm was visualized, indicating the presence of various structures with different sizes.

Discussion

The first barrier that the drug crosses after oral administration is constituted by the physicochemical environment of the gastrointestinal tract. As the lipids undergo a complex series of events in the GI environment, their use as drug carriers requires a profoundly exploration of the impact of the digestion of lipids used to prepared formulations on the solubilization and absorption of drug molecules (CHAKRABORTY *et al*., 2009).

The digestive phase of lipid-based formulations initiates with the physical breakdown of the lipid. This is accompanied with hydrolysis of the fatty acid glyceryl esters (TG) by the enzyme lipase. Each TG molecule is digested to generate two molecules of fatty acids (FAs) and one molecule of monoglycerides (MGs). Being partially ionized, FAs and MGs are also potent emulsifiers which promote binding of the lipase to the emulsion surface. However, *in vivo* lipolysis is a dynamic process, which conducts to the successive formation of different colloidal species as multillamellar and unilamellar vesicles, and mixed micelles. The colloidal species produced are then taken up by passive diffusion, facilitated diffusion, and active transport through the enterocyte membrane (PORTER *et al*., 2007; CHAKRABORTY *et al.,* 2009).

Biorelevant dissolution media containing amphiphilic components of bile, for example, bile salts (sodium taurocholate) and phospholipids (lecithin) have been proposed for the testing of oral formulations of poorly soluble drugs because the secretion of bile may have a significant effect on the *in vivo* dissolution and transport of drugs in the small intestine (ILARDIA-ARANA *et al*., 2006).

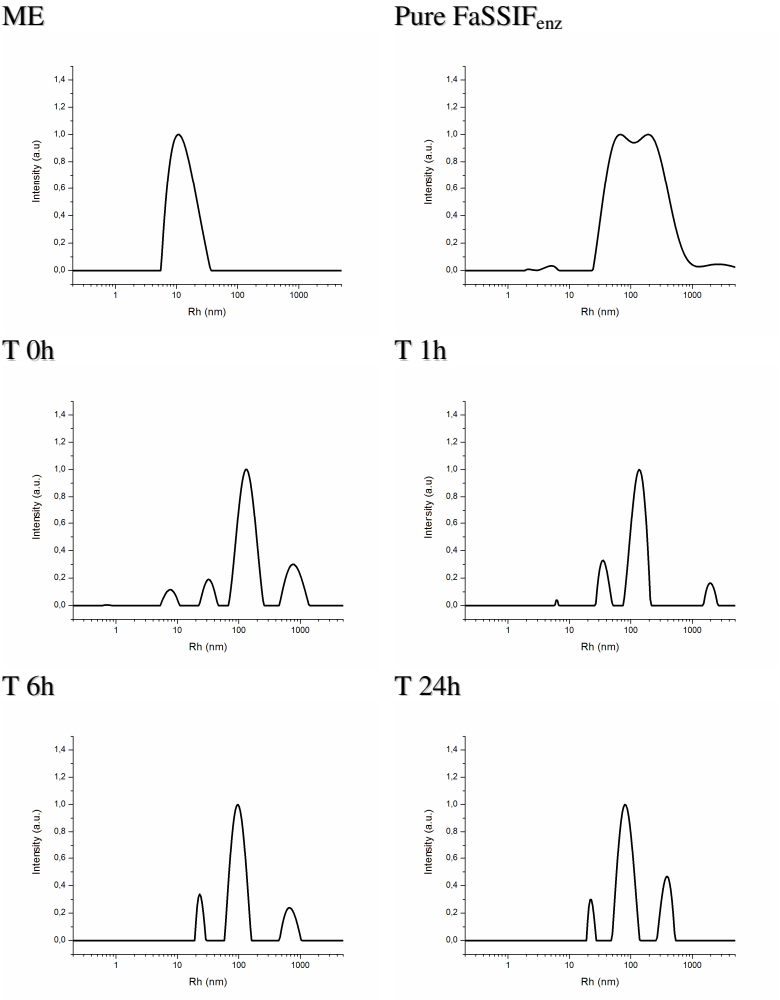

Figure 6. Particle size distribution of PEG660-stearate/SbPC/CO microemulsion after 0, 1, 6, and 24 h of incubation in fasted stated simulated intestinal fluid with pancreatin (FaSSIF$_{enz}$).

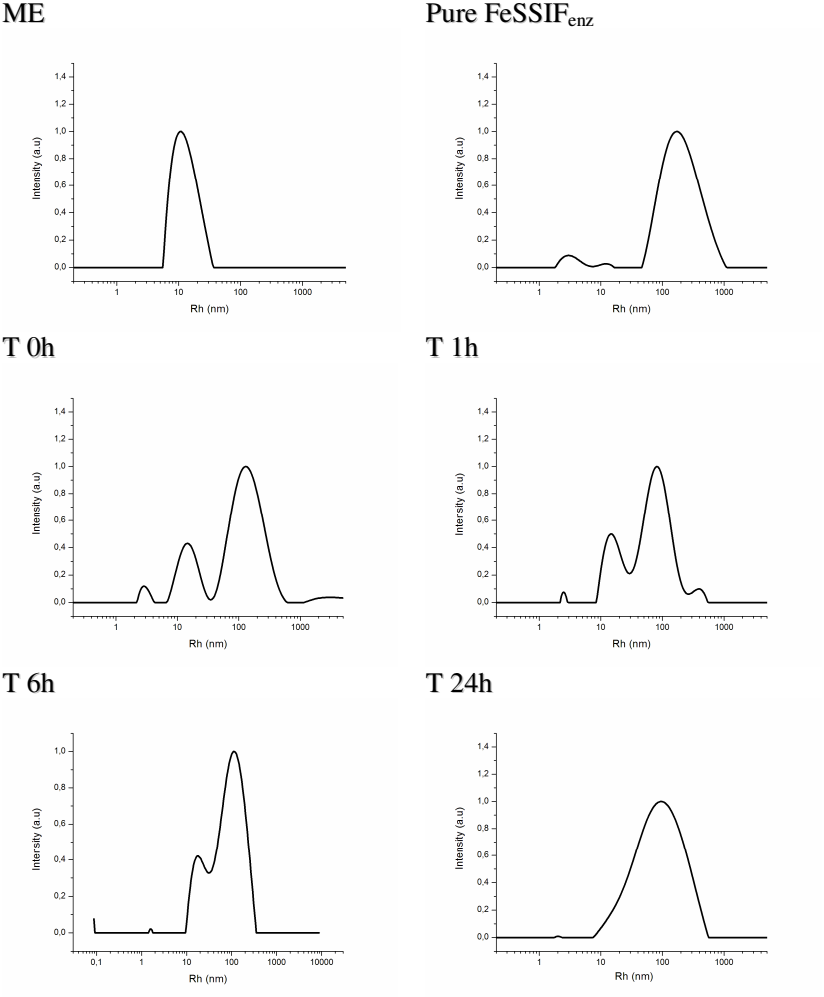

Figure 7. Particle size distribution of PEG660-stearate/SbPC/CO microemulsion after 0, 1, 6, and 24 h of incubation in fed stated simulated intestinal fluid with pancreatin (FeSSIF$_{enz}$).

The simulated gastric fluid has a pH of 1.2 and contains pepsin, a digestive protease. As demonstrated in Table 3 and Figure 2 and 3, the PEG660-stearate/SbPC/CO microemulsion was stable in gastric media for 6h and its size was conserved. Some studies have demonstrated the influence of the particle surface on gastrointestinal stability. In the presence of a polyoxyethylene (PEG) coating the stability of the PLA-based nanoparticle suspension in acidic conditions was improved when compared with uncoated nanoparticles (GARCÍA-FUENTES *et al.,* 2003; SAHU *et al.,* 2008). Similar results were obtained with lipid nanoparticles (GARCÍA-FUENTES *et al.,* 2003) and lipid nanocapsules prepared with polyethoxylated surfactants (ROGER *et al*., 2009).

After, we evaluated the effect of the different intestinal fluids, with or without pancreatin, on the particle size of PEG660-stearate/SbPC/CO microemulsion. When the experiments were carried out in the medium without the enzyme, no significant changes in the particle size distribution was observed after 24 h. However, when the pancreatin was added, the peak corresponding to the microemulsion was only visualized in time point 0. Pancreatin is a mixture of several digestive enzymes produced by the exocrine cells of the pancreas. Pancreatin contains the pancreatic enzymes trypsin, amylase and lipase. The trypsin found in pancreatin works to hydrolyze proteins into oligopeptides; amylase hydrolyzes starches into oligosaccharides and the disaccharide maltose; and lipase hydrolyzes triglycerides into fatty acids and glycerols. The lipid component used to prepare the microemulsion was castor oil, which is a vegetable oil obtained from the castor bean. It is a triglyceride in which approximately ninety percent of fatty acid chains are ricinoleic acid, which is a monounsaturated, 18-carbon fatty acid (long chain triacylglyceride). Therefore, the changes observed in the particle size distribution obtained by DLS can be attributed to the enzymatic digestion of castor oil with concomitantly formation of several aggregates of lipid and surfactants. However, morphological studies by TEM or Cryo-TEM are still need to characterize the structure of these aggregates.

References

Embleton, J., Pouton, J. Structure and function of gastro-intestinal lipases. **Advanced Drug Delivery Reviews**, v.25, p.15-32, 1997.

Porter, C.J.H., Pouton, C.W., Cuine, J.F., Charman, W.N. Enhancing intestinal drug solubilisation using lipid-based delivery systems. **Advanced Drug Delivery Reviews**, v. 60, p. 673–691, 2008.

Porter, C.J., Trevaskis, N.L., Charman, W.N. Lipids and lipid-based formulations: optimizing the oral delivery of lipophilic drugs. Nat Rev**. Drug Discovery,** v.6, p. 231–248, 2007.

Chakraborty, S.; Shukla, D.; Mishra, B.; Singh S. Lipid – An emerging platform for oral delivery of drugs with poor bioavailability. **European Journal of Pharmaceutics and Biopharmaceutics**, v. 73, p. 1–15, 2009.

Gao, Y. et al. Formulation optimization and in situ absorption in rat intestinal tract of quercetin-loaded microemulsion. **Colloids and Surfaces B: Biointerfaces**, v. 71, n. 2, p. 306–314, 2009.

Porter, C., Charman, W. In vitro assessment of oral lipid based formulations. **Advanced drug Delivery Reviews**, v. 50, p. S127-147, 2001.

Roger E; Lagarce, F.; Benoit, J.-P. The gastrointestinal stability of lipid nanocapsules. **International Journal of Pharmaceutics**, v. 379, p. 260–265, 2009.

Rogério, A. P., Dora, C. L., Andrade, E. L., Chaves, J. S.. Silva, L. F. C., Lemos-Senna, E., Calixto, J. B. Effect of quercetin-loaded microemulsion in the eosinophilic inflammatory process in an experimental airway allergic inflammation. **Biochemical Pharmacology**, 61 (4): 288-297, 2010.

Fatouros, D, Deen, D., Arleth, L., Bergenstahl, B., Nielsen, F., Pedersen, J., Mullertz, A. Structural Development of Self Nano Emulsifying Drug Delivery Systems (SNEDDS) during In Vitro Lipid Digestion Monitored by Small-angle X-ray Scattering. **Pharmaceutical Research**, 2007b, v. 24 (10), p.1844-1853.

Fatouros, D.G.; Deen, R.G.; Arleth, L.; Bergenstahl, B.; Nielsen, F.S.; Pedersen, J.S.; Mullertz, A. Structural Development of Self Nano Emulsifying Drug Delivery Systems (SNEDDS) During In Vitro Lipid Digestion Monitored by Small-angle X-ray Scattering. **Pharmaceutical Research**, v.24, n.10, 2007b.

Ilardia-Arana, D., Kristensen, H., Mullertz A. Biorelevant Dissolution Media: Aggregation of Amphiphiles and Solubility of Estradiol. **Journal of Pharmaceutical Sciences**, v. 95 (2), 2006.

García-Fuentes, M., Torres, D., Alonso, M.J. Design of lipid nanoparticles for the oral delivery of hydrophilic macromolecules**. Colloids Surf. B: Biointerfaces**. 2003, v. 27, p. 159–168.

Sahu, A., Bora, U., Kasoju, N., Goswami, P. Synthesis of novel biodegradable and self-assembling methoxy poly(ethylene glycol)-palmitate nanocarrier for curcumin delivery to cancer cells. **Acta Biomater.** 2008, v.4, p. 1752–1761.

Discussão Geral

A quercetina (3, 3´, 4', 5, 7-pentahidroxi-flavona) é um polifenol pertencente à classe dos flavonóides que está presente na nossa dieta em uma ampla variedade de plantas e alimentos, como cebolas, uvas, maçãs, cerejas, brócolis, e produtos derivados destes como sucos, chás e vinhos (HERTOG *et al*., 1995; BOOTS *et al.,* 2008). Em função das suas propriedades farmacológicas, é um dos flavonóides mais estudados, pois apresenta atividade contra uma série de doenças, tais como, câncer, doenças neurodegenerativas, diabetes, disfunções cardiovasculares, doenças inflamatórias, entre outras (GALVEZ *et al.,* 1993; FORMICA e REGELSON, 1995; SHOSKES, 1998; MIDDLETON, *et al.,* 2000; BOOTS *et al*., 2008). No entanto, a quercetina não apresenta uso clínico em decorrência da sua baixa solubilidade nos fluidos do trato gastrintestinal e extenso metabolismo no intestino e no fígado, fazendo com que a concentração sanguínea da sua forma inalterada não seja detectada após administração oral (GUGLER *et al*.,1975, WALLLE *et al.,* 2004; SOOBRATTEE *et al*., 2005; COMALADA *et. al*., 2005; MOON *et al*., 2008). Neste sentido, um grande número de pesquisas tem buscado estratégias farmacotécnicas que aumentem a solubilidade e estabilidade da quercetina ao longo do TGI, de modo a aumentar a sua biodisponibilidade oral.

Dentre as estratégias usadas para aumentar a absorção de fármacos pela via oral destacam-se a utilização de formulações lipídicas, pois permitem aumentar a solubilidade de fármacos hidrofóbicos em espécies coloidais produzidas após digestão dos lipídios, além de interferir nos processos de absorção e metabolismo no interior dos enterócitos. Em especial os carreadores lipídicos nanoestruturados possuem a vantagem de apresentar os fármacos em um estado altamente disperso, com elevada superfície de contato para absorção. A elevada área interfacial ainda acelera a ação das lipases e, conseqüentemente, a liberação do fármaco e/ou geração de micelas e vesículas (CHAKRABORTY *et al*., 2009). Os nanocarreadores lipídicos podem ser constituídos de lipídios sólidos ou líquidos, ou por misturas destes, levando à formação de sistemas matriciais ou reservatórios que exibem uma ampla faixa de tamanhos de partículas, ainda que na faixa nanométrica (HAUSS, 2007).

Assim, a primeira parte deste trabalho consistiu em obter nanocarreadores lipídicos contendo quercetina por meio da técnica de difusão do solvente a quente. Um estudo de formulação foi realizado com o intuito de avaliar o efeito da composição da formulação sobre a capacidade de incorporar a quercetina e de controlar a liberação desta

substância ativa. Para tal foram utilizados a triestearina (TS), um lipídio sólido a temperatura ambiente, o óleo de rícino (CO) ou a mistura desses dois lipídios, em diferentes proporções, para a obtenção das partículas. Além disso, o estearato de polietilenoglicol 660 (estearato de PEG) e o Poloxamer 188 foram testados em diferentes concentrações como surfactantes da fase aquosa e a lecitina de soja hidrogenada, como surfactante lipofílico. Em função da composição das formulações, ou seja, tipo e concentração de lipídio e de surfactante hidrofílico, nanopartículas lipídicas sólidas (NLS), carreadores lipídicos nanoestruturados (CLN), nanoemulsões (NE) e microemulsões (ME) foram obtidas.

As suspensões coloidais foram avaliadas quanto as suas características macroscópicas e quanto ao tamanho de partícula e potencial zeta. Todas as formulações preparadas com poloxamer 188 tiveram aparência leitosa, independente do tipo de material lipídico empregado. Utilizando baixas concentrações, a mesma característica foi observada para os nanocarreadores preparados com estearato de PEG, no entanto, quando 1% (p/V) desse surfactante foi adicionado na fase aquosa da formulação e somente o óleo de rícino foi empregado como lipídio, a formação de um sistema transparente e isotrópico, característico de microemulsões foi verificada. O diâmetro médio das partículas das suspensões coloidais variou em função do tipo e da concentração de surfactante, assim como da proporção de lipídio sólido/liquido utilizada. O aumento da proporção de CO na fase oleosa de 0 a 100% levou a uma diminuição no tamanho de partícula de 298 a 130 nm, quando poloxamer 188 foi utilizado e sistemas coloidais monodispersos foram obtidos (PDI<0,25). Com a utilização de estearato de PEG, sistemas monodispersos foram obtidos a baixas concentrações (0,1% p/V), no entanto o aumento da concentração para 0,5 e 0,75% levou a formação de sistemas polidispersos, provavelmente pelo aparecimento de outros tipos de agregados do tensoativo. Por outro lado, quando 1% de estearato de PEG e somente óleo de rícino foram empregados, um sistema monodisperso com tamanho de partícula de 22 nm foi obtido, corroborando com a hipótese da formação de um sistema microemulsionado.

A capacidade dos sistemas carreadores lipídicos em incorporar a quercetina foi avaliada e comparada, por meio dos parâmetros de teor de fármaco e de eficiência de encapsulação. Para tal, um método analítico de cromatografia líquida de alta eficiência foi desenvolvido e validado. A eficiência de encapsulação foi maior de 99% para todas as formulações testadas, demonstrando que a maior parte do fármaco

encontra-se associado ao nanocarreador. Os valores de teor de fármaco foram afetados pela composição das formulações variando de 17,8 a 236,5 µg/mL, sendo que a incorporação de QU aumentou com o aumento da concentração de óleo de rícino na formulação. Além disso, o surfactante utilizado também influenciou na capacidade de encapsulação do composto. Todas as partículas preparadas com estearato de PEG apresentaram maior capacidade de incorporação de QU quando comparadas com aquelas obtidas com uso do Poloxamer 188. Isto foi atribuído a maior incorporação da quercetina na camada de surfactante/cosurfactante formada na interface da partícula (LIN e KIM; 2002). Entre os tipos de carreadores, as NLS demonstraram uma menor capacidade de incorporar a quercetina. De fato, as NLSs têm demonstrado uma limitada capacidade de incorporar fármacos, seja devido à baixa solubilidade das substâncias na fase oleosa fundida, seja devido à formação de um cristal perfeito, após a solidificação das partículas, constituído de arranjos de moléculas de lipídio altamente organizados, com poucas imperfeições que limitam o espaço para a acomodação das moléculas ou cristais de fármaco (WESTESEN *et al*., 1997; WISSING *et al*., 2004; GARCIA-FUENTES, *et al.,* 2005). O efeito da mistura dos dois lipídios (CLN) causou um aumento na incorporação de QU, atingindo um valor máximo quando somente óleo de rícino foi utilizado (NE). Relatos da literatura atribuem este efeito à modificação da estrutura interna da partícula pela adição de óleo de rícino, permitindo a acomodação do fármaco entre as cadeias das moléculas dos lipídios e à maior capacidade de solubilização do óleo, em relação ao lipídio sólido (WESTESEN *et al*., 1997; GARCIA-FUENTES *et al.,* 2005). Igualmente, o efeito da quantidade inicial de QU adicionada às formulações sobre a capacidade de solubilização deste composto na microemulsão foi avaliado. Os resultados mostraram que a adição de 10 mg de QU levaram à obtenção de dispersões apresentando um aumento de cerca de 1,300 vezes na concentração do mesmo, quando comparado a sua solubilidade aquosa (0,33µg/mL), sem o aparecimento de precipitados na formulação. Assim, esta quantidade inicial QU foi considerada ideal e mantida nos estudos posteriores.

As análises de potencial zeta indicaram a obtenção de partículas de carga negativa, decorrente da presença da lecitina, sendo observada uma redução nos valores de carga superficial nas microemulsões, atingindo valores próximos à neutralidade, provavelmente devido ao mascaramento da carga negativa pelas cadeias de polietilenoglicol presentes no surfactante. Para uma completa estabilização eletrostática valores de potencial zeta de ±30 mV são requeridos. Entretanto, o baixo

valor de potencial zeta verificado para as microemulsões não significou uma baixa estabilidade do sistema, pois a utilização do estearato de PEG proporcionou a estabilização estérica da preparação.

Os perfis de liberação da QU exibiram uma cinética bifásica, consistindo de uma liberação rápida nas primeiras 8 horas, seguida de uma liberação sustentada durante 24 horas, em alguns casos. Quando Poloxamer 188 1 % (p/V) foi empregado como surfactante, não foram observadas diferenças no perfil de liberação da QU entre as diferentes formulações. Entretanto, a liberação do fármaco e difusão através da membrana de diálise foi mais lenta que aquela obtida para QU livre, indicando que as partículas foram capazes de controlar a liberação em alguma extensão. Por outro lado, quando estearato de PEG 0,1% (p/V) foi empregado, a liberação de quercetina a partir das NLSs (TS:CO 100:0) e dos CLNs (TS:CO 50:50) foi mais rápida do que da NE (TS:CO 0:100). Os perfis de liberação da quercetina obtidos a partir da NLSs e CLNs foram muito parecidos com aquele obtido para a QU livre, corroborando com a hipótese de que uma fração de QU encontra-se associada à camada de surfactante/cosurfactante localizada na interface o/a das partículas. Por outro lado, a liberação de QU a partir da NE pode ser controlada em alguma extensão, ocorrendo provavelmente por um mecanismo de difusão do fármaco dissolvido no óleo até meio de liberação. Uma cinética de liberação similar foi obtida para a liberação da microemulsão de QU. No entanto, para completa compreensão deste fenômeno, propriedades estruturais das partículas precisavam ser estudadas.

Desta forma, o terceiro capítulo desta tese teve o objetivo de caracterizar físico-química e estruturalmente as suspensões coloidais de nanocarreadores lipídicos descritas no capítulo 2, que mostraram resultados promissores. Inicialmente, um estudo foi realizado com o objetivo de avaliar o efeito da concentração do surfactante na formação de emulsões nanométricas óleo em água (o/a), usando o óleo de rícino como fase oleosa e estearato de PEG e lecitina de soja hidrogenada como surfactante e co-surfactante, respectivamente. O efeito da concentração do estearato de PEG 660 sobre o tamanho e estrutura das partículas, assim como sobre a capacidade destes sistemas de solubilizar a quercetina, foi avaliado. Para isso, técnicas de espectroscopia de absorção no ultravioleta, espalhamento de luz dinâmico (DLS), potencial zeta, espalhamento de raios-x a baixos ângulos (SAXS), microscopia de luz polarizada, microscopia de transmissão (TEM) e crio-microscopia de transmissão (cryo-TEM) foram empregadas.

As medidas de espalhamento de luz demonstraram que o tamanho e distribuição granulométrica das emulsões nanométricas foram fortemente afetados pela concentração de estearato de PEG, sendo que quanto maior sua concentração, menor foram os tamanhos de partículas obtidos. No entanto, esse tamanho não reduziu continuamente, sendo necessária uma concentração crítica de estearato de PEG (2,5 p/p; proporção surfactante:óleo de aproximadamente 5:1) para que fossem obtidas dispersões coloidais transparentes, apresentando distribuição monodispersa de tamanhos de partícula de aproximadamente 20 nm e excelente estabilidade.

A hipótese da formação de uma microemulsão quando a concentração final de estearato de polietilenoglicol foi de 2,5 % (p/p) foi confirmada pelos estudos de microscopia de luz polarizada e cryo-TEM, os quais evidenciaram a formação de um sistema isotrópico de partículas esféricas. Além disso, a redução do tamanho de partícula de 140 para 20nm permitiu o aumento do teor de quercetina de 3 a 10 vezes, dependendo da quantidade de QU inicialmente adicionada às formulações. Os resultados obtidos por SAXS indicam que a estrutura da partícula é do tipo núcleo-casca com raio hidrodinâmico de 11,6 nm, o que está de acordo com os resultados obtidos pela técnica de espalhamento de luz dinâmico e com as características observadas por cryo-TEM.

O mecanismo de formação da microemulsão foi associado à rápida difusão do solvente orgânico para a fase aquosa e ao uso do aquecimento numa temperatura superior à temperatura de inversão de fases do estearato de PEG (~80º C), a qual foi essencial para promover a microemulsificação do óleo e obter dispersões coloidais transparentes.

A segunda parte do capítulo 3 refere-se à caracterização estrutural dos outros sistemas nanocarreadores lipídicos desenvolvidos, NLS, CLN e NE. O estudo de formulação abordado no capítulo 2 demonstrou que diferentes tipos de nanocarreadores lipídicos foram obtidos pela técnica de difusão do solvente a quente e que estes sistemas exibiram diferentes capacidades em incorporar a quercetina. No entanto, a maneira pela qual as propriedades estruturais das partículas afetaram a capacidade de incorporação da QU não havia ainda sido esclarecida.

Desta forma, na segunda parte do capítulo 3 consistiu em investigar as características físico-químicas e estruturais desses nanocarreadores. A caracterização apropriada é uma etapa essencial no processo de desenvolvimento de uma nova forma farmacêutica e se torna difícil em função do tamanho reduzido das partículas. Para que a interpretação dos dados obtidos fosse feita de forma correta foi

necessário correlacionar resultados de diferentes métodos de análise, incluindo DLS, calorimetria exploratória diferencial (DSC), difração de raios-x a altos (WAXS) e a baixos ângulos (SAXS). Além disso, análises morfológicas foram realizadas por microscopia de força atômica (AFM), microscopia eletrônica de transmissão (TEM) e crio-microscopia de transmissão (cryo-TEM).

Os resultados de DLS demonstraram que sistemas monodispersos foram obtidos em todos os casos (índice de polidispersão < 0,2). No entanto, diferenças no tamanho médio das partículas foram encontradas, sendo de cerca 340, 220 e 145 nm para as NSLs, CLNs e NEs, respectivamente. Como não foi verificada diferença no tamanho de partícula quando os dois tipos de surfactantes foram empregados, pode-se afirmar que esta redução está relacionada à proporção do CO da formulação, ou seja, quanto maior a concentração de CO, menor o tamanho de partícula.

As análises morfológicas indicaram que a NE apresenta formato esférico. No entanto, partículas com formatos não-esféricos foram visualizadas para as NLSs e CLNs. Sobretudo as NLSs exibiram formato irregular e angular, como um cristal lamelar. O aumento da esfericidade foi observado com a incorporação de óleo de rícino nas formulações. Entretanto, a separação de fases entre os lipídio sólido e líquido foi evidenciada nas micrografias obtidas por TEM e cryo-TEM, indicando que o sistema não é homogêneo. De fato, o ácido ricinoleico, componente majoritário do óleo de rícino, é um ácido graxo monoinsaturado de 18 carbonos, apresentando um grupamento hidroxila no carbono 12, que o torna um pouco polar. Assim, esta característica pode ter contribuído para a separação de fases observada. Nas micrografias obtidas por cryo-TEM a partir dos CLNs foi possível visualizar as camadas moleculares relacionadas de triestearina, estando à distância entre as camadas (~4,5 nm) de acordo com os resultados de obtidos por SAXS.

A triestearina cristaliza em quatro tipos de formas cristalinas, γ, α, β' e β, sendo a forma β a mais estável, e a sua formação depende principalmente das velocidades de resfriamento do lipídio e da agitação (HARTEL, 2001). Neste sentido, a investigação de qual polimorfo é produzido após a recristalização das partículas constitui uma etapa importante, uma vez que a transição entre o polimorfo menos estável para o mais estável pode levar a desestabilização do sistema e expulsão do fármaco incorporado (FREITAS e MÜLLER, 1999). Além disso, diferenças na forma das nanopartículas também sido relacionadas ao

tipo de polimorfo. Usando cryo-TEM, Bunjes e colaboradores (2007) demonstraram que o polimorfo β da triestearina apresenta formato de cristal lamelar e que α-TS forma partículas esféricas multilamelares. No nosso caso, as avaliações morfológicas assim como os resultados de WAXS e DSC indicaram a formação de β-TS nas NLSs e CLNs. Este resultado foi associado à técnica de preparação, cuja lenta etapa de recristalização pode ter favorecido a formação deste polimorfo.

Os resultados do estudo de formulação (capítulo 2) indicaram que o aumento da concentração de óleo de rícino na formulação levou ao aumento do teor de quercetina nas partículas, mas os sistemas só foram capazes de retardar a liberação do composto em alguma extensão. Correlacionando os resultados, podemos concluir que o aumento na incorporação da QU ocorreu devido à maior capacidade do óleo de rícino em solubilizar QU e não a desestruturação do arranjo molecular do lipídio sólido na matriz, como sugerido por outros autores (WISSING, *et al*., 2004; SCHAFER-KORTING e MEHNERT, 2005). Esta separação de fases também desfavoreceu o controle da liberação da quercetina.

Dos sistemas nanocarreadores desenvolvidos, a microemulsão de quercetina (QU-ME) foi a formulação que apresentou melhores resultados em relação à capacidade de incorporação do composto e estabilidade do sistema. Desta forma, essa formulação foi testada nos ensaios de atividade farmacológica *in vivo*. Primeiramente foi testada a atividade antiinflamatória da quercetina administrada por via oral, em modelo experimental de asma alérgica em camundongos. Os animais foram tratados com a quercetina em suspensão, com a quercetina microemulsionada em duas diferentes doses (3 e 10 mg/kg) e com dexametasona, a partir do 18º ao 22º dia após a primeira imunização com ovalbumina. Alguns estudos têm demonstrado que em certas doenças alérgicas, a expressão de alguns genes que codificam citocinas e moléculas de adesão é controlada pelo fator de transcrição NF-κB (ANRATHER *et al.,* 1997; YANG *et al*., 1998; ATREYA *et al*., 2008). Em especial, a asma alérgica é freqüentemente acompanhada por elevados níveis de imunoglobulina E (IgE) e associada com o aumento da produção intrapulmonar de certas interleucinas, especialmente a IL-4, IL-5 e IL-13, que por sua vez direcionam seletivamente o recrutamento de eosinófilos. Assim, após o tratamento, os animais foram sacrificados e o fluido bronquioalveolar (BALF) foi obtido e analisado. Os resultados evidenciaram a redução do recrutamento de eosinófilos no BALF dos animais tratados com a QU-ME de uma maneira dose

dependente, o que não ocorreu após a administração deste composto em suspensão. A QU-ME também reduziu significativamente os níveis de IL-4 e IL5, mas não interferiu nos níveis de outros parâmetros da inflamação como CCL11, IFN-□ e LTB_4. Adicionalmente, o tratamento oral da quercetina na forma microemulsionada inibiu a ativação do fator de transcrição nuclear (NF-kB), a expressão de P-selectina e a produção de muco nos pulmões.

Com o intuito de pesquisar a presença de quercetina e/ou seus metabólitos, o sangue de ratos foi analisado por CLAE-EM, após tratamento com quercetina livre (em suspensão) e QU-ME. Neste estudo, um metabólito da quercetina foi detectado somente nas amostras obtidas após extração do plasma dos animais tratados com QU-ME. Estes resultados indicaram que a incorporação de quercetina nas microemulsões aumentou significantemente a absorção oral deste composto e, conseqüentemente, seu efeito farmacológico foi alcançado neste modelo experimental.

Em um segundo estudo de investigação da atividade farmacológica, a atividade antitumoral da quercetina microemulsionada foi avaliada em modelo de melanoma subcutâneo murino B16F10. Como alguns estudos têm demonstrado efeito sinérgico entre polifenóis e quimioterápicos (CIPAK *et al.,* 2003), a combinação da quercetina livre e microemulsionada com a cisplatina também foi avaliada. Neste estudo foi verificado que o crescimento do tumor foi significantemente inibido após o tratamento com a QU-ME e com cisplatina, quando comparado com o grupo controle. No entanto, a associação dos dois compostos não apresentou efeito sinérgico. Por outro lado, a administração da quercetina livre e da microemulsão branca (sem quercetina) não foram capazes de reduzir o volume do tumor. Os resultados das análises de toxicidade renal e hepática demonstraram que não houve diferença entre os grupos tratados e o controle negativo, indicando que a administração oral da microemulsão não causa danos a estes órgãos. Desta forma, pode-se sugerir que a incorporação da quercetina na microemulsão foi importante para que a atividade antitumoral deste composto fosse alcançada, uma vez a redução do volume tumoral foi observada somente quando QU-ME foi administrada. Da mesma forma que o estudo anterior, essa eficácia terapêutica parece estar relacionada com o aumento da biodisponibilidade da quercetina quando encapsulada na microemulsão.

Como foram obtidos resultados promissores com a administração oral da microemulsão de quercetina, estudos foram igualmente realizados com o objetivo de investigar a estabilidade da

microemulsão na presença de fluídos gastrintestinais simulados e biorrelevantes, pela técnica de espalhamento de luz. Diferentes tipos de fluidos gastro-intestinais têm sido desenvolvidos com intuito de similar as condições fisiológicas do trato gastrintestinal (TGI). Estas condições variam não apenas em função do estado pré ou pós-prandial, mas também da localização no TGI. Os fluidos biorelevantes contêm componentes anfifílicos da bile, como por exemplo, sais biliares (taurocolato de sódio) e fosfolipídios (lecitina) e têm sido propostos para análise de fármacos pouco solúveis em água, pois a secreção da bile pode afetar o processo de dissolução *in vivo* e, portanto a absorção de fármacos. A maior capacidade de solubilização de fármacos nestes fluidos é atribuída à formação de micelas mistas de taurocolato e lecitina (ILARDIA-ARANA *et al.,* 2006). A digestão de nanocarreadores lipídicos inicia com a quebra física dos lipídios e posterior formações de outros tipos de estruturas coloidais, tais como, micelas, micelas mistas, vesículas e ácidos graxos livres que serão absorvidos pelos enterócitos (PORTER *et al*., 2007; CHAKRABORTY *et al*., 2009).

As análises de DLS após a incubação da ME nos fluidos gástricos demonstrou que o sistema é estável nestes fluidos após 6 h, uma vez que seu tamanho de partícula não foi alterado. Alguns estudos têm demonstrado que a superfície da partícula pode afetar sua estabilidade em fluídos gástricos (GARCÍA-FUENTES *et al.,* 2003; SAHU *et al.,* 2008; ROGER *et al*., 2009). A presença de polietilenoglicol na superfície aumenta a estabilidade de nanocarreadores, pois os surfactantes contendo PEG são estáveis em baixos pHs. Desta forma, a estabilidade da microemulsão nos fluidos gástricos, demonstrada neste trabalho, pode ser relacionada à utilização de estearato de PEG como surfactante hidrofílico da formulação.

Após avaliação do efeito dos fluidos intestinais sobre o tamanho das partículas foi verificado que a microemulsão também é estável nos fluidos intestinais, na ausência da enzima pancreatina, por 24horas. No entanto, na presença da pancreatina, o pico de tamanho de partícula relacionado à microemulsão (~10nm de raio) somente foi verificado no tempo zero do experimento. No decorrer do ensaio, este pico desapareceu e outros picos foram surgindo, sugerindo o aparecimento de outros agregados de lipídios e tensoativos.

A técnica de DLS permitiu avaliar a estabilidade da microemulsão nos diferentes fluidos testados, através da verificação do tamanho das partículas no decorrer do experimento. Além disso, pode ser verificado que estruturas de diferentes tamanhos foram formadas quando a enzima pancreatina foi utilizada nos fluídos intestinais, no

entanto uma avaliação morfológica por cryo-TEM seria necessária para correlacionar os resultados das duas técnicas e verificar quais seriam exatamente essas estruturas.

Conclusões

- Neste trabalho foi demonstrado que o método de difusão do solvente a quente conduz à obtenção de nanocarreadores lipídicos, usando a triestearina e/ou óleo de rícino como lipídios e a lecitina de soja e estearato de polietilenoglicol ou poloxamer 188, como estabilizantes lipo- e hidrofílicos, respectivamente. Diferentes estruturas (nanopartículas lipídicas sólidas, carreadores lipídicos nanoestruturados, nanoemulsões e microemulsões) apresentando diferentes capacidades de incorporação e de controle de liberação da quercetina foram obtidas, dependendo da composição das formulações.
- Métodos para o doseamento da quercetina por CLAE e UV/VIS foram desenvolvidos, mostrando serem específicos, lineares, exatos, precisos e sensíveis para quantificação da QU. O método foi empregado nos estudos de liberação da quercetina a partir dos nanocarreadores.
- O emprego do estearato de polietilenoglicol (Solutol HS 15) permitiu a obtenção de microemulsões, mas uma concentração mínima deste surfactante foi necessária para a obtenção de sistemas transparentes, isotrópicos e monodispersos, de elevada capacidade de solubilização de quercetina.
- A introdução do óleo de rícino nas formulações contendo triestearina conduziu ao aumento do teor de quercetina. Entretanto, o aumento observado foi decorrente da maior solubilidade do fármaco no óleo, uma vez que uma separação de fases foi verificada por meio do emprego de técnicas de microscopia de transmisão, crio-transmissão, microscopia de força atômica e calorimetria exploratória diferencial.
- Dos sistemas estudados a microemulsão apresentou maior potencial para veicular a quercetina, com vistas à administração oral deste fármaco. Uma maior capacidade de incorporação do fármaco foi verificada para na microemulsão, alcançando um aumento na concentração do QU em cerca de 1.300 vezes em relação a sua solubilidade aquosa, quando 10 mg de QU foram inicialmente adicionados à formulação.
- Estudos de estabilidade *in vitro* da microemulsão em meios biorelevantes, monitorado pela técnica de espalhamento de luz dinâmico, demostraram que o sistema é estável em meio gástrico e intestinal sem enzima. Entretanto, em presença da enzima pancreatina o sistema não se mostrou estável, tendo provavelmente ocorrido a digestão enzimática do lipídio e

formação de outras estruturas constituídas de agregados de tensoativos e lipídios.

- Estudos avaliando a atividade antiinflamatória e antitumoral da microemulsão contendo quercetina (QU-ME) foram realizados em modelo experimental de asma alérgica e em modelo de melanoma subcutâneo murino B16F10, respectivamente, em camundongos. Os resultados de atividade farmacológica *in vivo* indicaram que a incorporação de quercetina nas microemulsões aumentou a biodisponibilidade oral deste composto e, conseqüentemente, seu efeito farmacológico foi alcançado nestes modelos experimentais.
- A análise do sangue de ratos tratados com quercetina livre (em suspensão) e QU-ME por HPLC-EM demonstrou que um íon relacionado a algum metabolito de quercetina foi detectado somente nas amostras extraídas dos animais tratados com QU-ME, corroborando com a hipótese do aumento da biodisponibilidade oral do composto quando o mesmo encontra-se na forma microemulsionada.

Referências Bibliográficas

1. AGULLO, G. *et al*. Relationship between flavonoid structure and inhibition of phosphatidylinositol 3-kinase: a comparison with tyrosine kinase and protein kinase C inhibition. **Biochemical Pharmacology**, v. 53, n. 11, p. 1649-1657, jun., 1997.
2. AHERNE, S. A.; O'BRIEN, N. M. Protection by the flavonoids myricetin, quercetin, and rutin against hydrogen peroxide-induced DNA damage in Caco-2 and Hep G2 cells. **Nutrition and Cancer**, v. 34, n. 2, p. 160-166, 1999.
3. AKSOY, S.; KLENER, J.; WEINSHILBOUM, R. M. Catechol-*O*-methyltransferase pharmacogenetics – photoaffinity-labeling and Western-blot analysis of human liver samples. **Pharmacogenetics**, v. 3, p. 116-122, 1993.
4. ANRATHER J, CSIZMADIA V, BROSTJAN C, SOARES MP, BACH FH, WINKLER H. Inhibition of bovine endothelial cell activation in vitro by regulated expression of a transdominant inhibitor of NF-kappa B. **J Clin Invest,** v. 99, p.763–72, 1997
5. ATREYA I, ATREYA R, NEURATH MF. NF-kappaB in inflammatory bowel disease. **J Intern Med.,** n.263, p.591–596, 2008.
6. AURA, A. M. *et al*. Quercetin derivatives are deconjugated and converted to hydroxyphenylacetic acids but not methylated by human fecal flora in vitro. **Journal of Agricultural and Food Chemistry**, v. 50, n. 6, p. 1725-1730, fev., 2002.
7. BANKER, S.G.; RHODES, C.T. *Modern Pharmaceutics*. New York: Marcel Dekker, 1996.
8. BARRAS, A. *et al*. Formulation and characterization of polyphenol-loaded lipid nanocapsules **International Journal of Pharmaceutics**, v. 379, n. 2, p. 270–277, set., 2009.
9. BARRATT, G. M. Therapeutic applications of colloidal drug carriers. **Pharmaceutical Science & Technology Today**, v. 3, n. 5, p. 163-171, maio, 2000.
10. BISCHOFF, S. Quercetin: potentials in the prevention and therapy of disease. **Current Opinion in Clinical Nutrition and Metabolic Care**, v. 11, p. 733-740, 2008.

11. BOERSMA, M. G. *et al*. Regioselectivity of phase II metabolism of luteolin and quercetin by UDP-glucuronosyl transferases. **Chemical Research in Toxicology**, v. 15, n. 5, p. 662-670, maio, 2002.
12. BOOTS, A. W.; HAENEN, G. R.; BAST, A. Health effects of quercetin: From antioxidant to nutraceutical. **European Journal of Pharmacology**, v. 585, n. 2-3, p. 325-337, maio, 2008.
13. BORGHETTI, G. S. *et al*. Characterization of different samples of quercetin in solid-state: indication of polymorphism occurrence. **Pharmazie**, v. 61, n. 9, p. 802-804, set., 2006.
14. BORGHETTI, G. S. *et al*. Quercetin/β-Cyclodextrin Solid Complexes Prepared in Aqueous Solution Followed by Spray-drying or by Physical Mixture. **AAPS PharmSciTech**, v. 10, n. 1, p. 235-242, mar., 2009.
15. BUDAVARI, S. (Ed.). The Merck Index. 12th ed. White House Station: Merck, 1996
16. BUNJES, H., STEINIGER, F., RICHTER W. Visualizing the structure of triglyceride nanoparticles in different crystal modifications. **Langmuir, v.** 23, p. 4005-4011, 2007.
17. CALABRÓ, M.L. et al. Effects of α- and β-ciclodextrin complexation on the physic-chemical properties and antioxidant activity of some 3-hydroxiflavones. **Journal of Pharmaceutical and biomedical analysis**, v.35, p.361-377, 2004.
18. CANADA, A. T.; GIANNELLA, E.; NGUYEN, T. D. and Mason, R. P. (1990) The production of reactive oxygen species by dietary flavonols. **Free Radical Biology & Medicine**, v. 9, n. 5, p. 441-449, 1990.
19. CAO, G.; SOFIC, E.; PRIOR, R. Antioxidant and prooxidant behavior of flavonoids: structure-activity relationships. **Free Radical Biology & Medicine**, v. 22, n. 5, p. 749-760, 1997.
20. CHAKRABORTY, S.; SHUKLA, D.; MISHRA, B.; SINGH S. Lipid – An emerging platform for oral delivery of drugs with poor bioavailability. European **Journal of Pharmaceutics and Biopharmaceutics**, v. 73, p. 1–15, 2009.

21. CHOI, E. J.; CHEE, K. M.; LEE, B. H. Anti- and prooxidant effects of chronic quercetin administration in rats. **European Journal of Pharmacology**, v. 482, n. 1-3, p. 281– 285, dez., 2003.

22. CIPAK, L., RAUKO, P., MIADOKOVA, E., CIPAKOVA, I.,NOVOTNY, L. Effects of flavonoids on cisplatin-induced apoptosis of HL-60 and L1210 leukemia cells. **Leukemia Research**, v. 27, n. 1, p. 65-72, 2003a.

23. COMALADA, M. *et al*. In vivo quercetrin anti-inflammatory effect involves release of quercetin, which inhibits inflammation through down-regulation of the NF-kB pathway. **European Journal of Immunology**, v., 35, n. 2, p. 584-592, fev., 2005.

24. CONSTANTINIDES, P.P.; CHAUBAL, M.V.; SHORR, R. Advances in lipid nanodispersions for parenteral drug delivery and targeting. **Adv Drug Deliv Rev**, v. 60, p. 757–767, 2008.

25. COUGHTRIE, M. W. H.; SHARP, S.; MAXWELL, K.; INNES, N. P. Biology and function of the reversible sulfation pathway catalysed by human sulfotransferases and sulfatases. **Chemical-Biological Interacts**, v. 109, p. 3-27, 1998.

26. COUVREUR, P.; DUBERNET, C.; PUISIEUX, F. Controlled drug delivery with nanoparticles: current possibilities and future trends. **European Journal of Biopharmaceutics**, v. 41, p. 2-13, 1995.

27. CRESPY, V. *et al*. Comparison of the intestinal absorption of quercetin, phloretin and their glucosides in rats. **The Journal of Nutrition**, v. 131, n.8, p. 2109-2114, ago., 2001.

28. CSOKAY, B.; PRAJDA, N.; WEBER, G.; OLAH, E. Molecular mechanisms in the anti-proliferative action of quercetin. **Life Science**, v. 60, p. 2157-2163, 1997.

29. DAY, A. J. *et al*. Dietary flavonoid and isoflavone glycosides are hydrolysed by the lactase site of lactase phlorizin hydrolase. **FEBS Letters**, v. 468, n. 2-3, p. 166-170, fev. 2000.

30. DAY, A. J.; DUPONT, M. S.; RIDLEY, S.; RHODES, M.; RHODES, M. J.; MORGAN, M. R.; WILLIAMSON, G. Feglycosylation of flavonoid and isoflavonoid glycosides by human

small intestine and liver β-glucosidase activity. **FEBS Letters**, v. 436, p. 71-75, 1998.

31. DUNNICK, J. K.; HAILEY, J. R. Toxicity and carcinogenicity studies of quercetin, a natural component of foods. **Fundamental and Applied Toxicology**, v. 19, n. 3, p. 423-431, out., 1992.

32. FASOLO, D.; BASSANI, V. L.; TEIXEIRA, H. F. Development of topical nanoemulsions containing quercetin and 3-O-methylquercetin. **Pharmazie**, v. 64, n. 11, p. 726-730, nov., 2009.

33. FATOUROS, D.G.; DEEN, R.G.; ARLETH, L.; BERGENSTAHL, B.; NIELSEN, F.S.; PEDERSEN, J.S.; MULLERTZ, A. Structural Development of Self Nano Emulsifying Drug Delivery Systems (SNEDDS) During In Vitro Lipid Digestion Monitored by Small-angle X-ray Scattering**.** **Pharmaceutical Research**, v.24, n.10, 2007b.

34. FORMICA, J. V.; REGELSON, W. Review of the biology of quercetin and related bioflavonoids. **Food and Chemical Toxicology**, v. 33, n. 12, p. 1061-1080, dez., 1995.

35. FREITAS, C.; MÜLLER, R.H. Correlation between long-term stability of solid lipid nanoparticles (SLN(TM)) and crystallinity of the lipid phase. **Eur J Pharm Biopharm**., v. 47, p. 125–32, 1999.

36. FRESCO, P. *et al*. New insights on the anticancer properties of dietary polyphenols. **Medicinal Research Reviews**, v. 26, n. 6, p.747-766, nov., 2006.

37. GALVEZ, J. Antidiarrhoeic activity of *E*uphorbia *hirta* extract and isolation of an active flavonoide constituent. **Planta Med**, v. 59, n. 4, p. 333-336, 1993.

38. GAO, Y. *et al*. Formulation optimization and in situ absorption in rat intestinal tract of quercetin-loaded microemulsion. **Colloids and Surfaces B: Biointerfaces**, v. 71, n. 2, p. 306–314, jul., 2009.

39. GARCÍA-FUENTES, M.; TORRES, D.; ALONSO, M. Design of lipid nanoparticles for the oral delivery of hydrophilic macromolecules. **Colloid Surf. B**., v. 27, p. 159–168, 2003.

40. GHOSH, A. *et al*. Nanoencapsulation of quercetin enhances its dietary efficacy in combating arsenic-induced oxidative damage in liver and brain of rat. **Life Sciences**, v. 84, n. 3-4, p. 75–80, jan., 2009.

41. GRAEFE, E. U.; DERENDORF, J.; VEIT, M. Pharmacokinetics and bioavailability of the flavonol quercetin in human. **International Journal of Clinical Pharmacology Therapy**, v. 37, p. 219-233, 1999.

42. GRAEFE, E. U.; WITTIG, J.; MUELLER, S.; RIETHLING, A-K.; UEHLEKE, B.; DREWELOW, B.; PFORTE, H.; JACOBASCH, G.; DERENDORF, H.; VEIT, M. Pharmacokinetics and bioavailability of quercetin glycosides in humans. **The Journal of Clinical Pharmacology**, v. 41, p. 492-499, 2001.

43. GUGLER, R.; LESCHIK, M.; DENGLER, H. J. Disposition of quercetin in man after single oral and intravenous doses. **European Journal of Clinical Pharmacology**, v. 9, n. 2-3, p. 229–234, 1975.

44. GUPTA, S. *et al*. Designing and testing of an effective oil-in-water microemulsion drug delivery system for in vivo application. **Drug Delivery**, v. 12, n. 5, p. 267-273, set./out., 2005.

45. HARTEL R. **Crystallization in foods**. Aspen Publishers:USA. **2001**. p15-22.

46. HAUSS, D.J. Oral lipid-based formulations. **Adv. Drug Deliv. Rev**., v. 59, p. 667-676, 2007.

47. HERTOG, M. G. *et al*. Flavonoid intake and long-term risk of coronary heart disease and cancer in the seven countries study. **Archives of Internal Medicine**, v. 155, n. 4, p. 381-386, fev., 1995.

48. HEURTAULT, B.; SAULNIER, P.; PECH, B.; PROUST, J.E.; BENOIT, J.P. Physico-chemical stability of colloidal lipid particles. **Biomaterials**, v. 24, p. 4283–4300, 2003.

49. HU, F.Q.; YUAN, H.; ZHANG, H.H.; FANG, M. Preparation of solid lipid nanoparticles with clobetasol propionate by a novel solvent diffusion method in aqueous system and physicochemical characterization. **Int J Pharm**, v. 239, p. 121–128, 2002.

50. IKEGAWA, T., OHTANI, H., KOYABU, N., JUICHI, M., IWASE, Y., ITO, C., FURUKAWA, H., NAITO, M., TSURUO, T.,SAWADA, Y. Inhibition of P-glycoprotein by flavonoid derivatives in adriamycin-resistant human myelogenous leukemia (K562/ADM) cells. **Cancer Letters**, vol. 177, n. 1, p. 89-93, 2002.

51. INAL, M. E.; KAHRAMAN, A. The Protective effect of flavonol quercetin against ultraviolet a induced oxidative stress in rats. **Toxicology**, v. 154, n. 1-3, p. 21-29, nov., 2000.

52. JANISCH, K. M. *et al*. Properties of quercetin conjugates: modulation of LDL oxidation and binding to human serum albumin. **Free Radical Research**, v. 38, n. 8, p. 877-884, ago., 2004.

53. JEONG, J-H.; AN, J. Y.; KWON, Y. T.; RHEE, J. G.; LEE, Y. J. Effects of low dose quercetin: cancer cell-specific inhibition of cell cycle progression. **Journal of Cellular Biochemistry**, v. 106, p. 73-82, 2009.

54. JORES, K. *et al*. Investigations on the structure of solid lipid nanoparticles (SLN) and oil-loaded solid lipid nanoparticles by photon correlation spectroscopy, field-flow fractionation and transmission electron microscopy. **Journal of Controlled Release**, v. 95, n. 2, p. 217-227, mar., 2004.

55. JORES, K.; MEHNERT, W.; MÄDER, K. Physicochemical investigations on solid lipid nanoparticles and on oil-loaded solid lipid nanoparticles: a nuclear magnetic resonance and electron spin resonance study. **Pharmaceutical Research**, v. 20, n. 8, p. 1274-1283, ago., 2003.

56. JULLIAN, C. *et al*. Lorena Moyano, Claudia Yanez, Claudio Olea-Azar. Complexation of quercetin with three kinds of cyclodextrins: An antioxidant study. **Spectrochimica Acta. Part A, Molecular and Biomolecular Spectroscopy**, v. 67, n. 1, p. 230–234, maio, 2007.

57. KAHRAMAN, A., *et al*. The antioxidative and antihistaminic properties of quercetin in ethanol induced gastric lesions. **Toxicology,** v. 183, p. 133-42, 2003

58. KALE, R. *et al*. Decreased B16F10 melanoma growth and impaired tumour vascularization in BDF1 mice with quercetin-cyclodextrin binary system. **The Journal of Pharmacy and Pharmacology**, v. 58, n. 10, p.1351-1358, out., 2006.

59. KAPISZEWSKA, M.; CIERNIAK, A.; ELAS, M.; LANKOFF, A. Lifespan of etoposide-treated human neutrophils is affected by antioxidant ability of quercetin. **Toxicology *In Vitro*,** v. 21, p. 1020-1030, 2007

60. KIM, D. H.; JUNG, E. A.; SOHNG, I. S.; HAN, J. A.; KIM, T. H.; HAN, M. J. Intestinal bacterial metabolism of flavonoids and its relation to some biological activities. **Archives of Pharmacal Research**, v. 21, p. 17-23, 1998.

61. KING, C. D.; RIOS, G. R.; GREEN, M. D.; TEPHLY, T. R. UDP-glucuronosyltransferases. **Current Drug Metabolism**, v. 1, p. 143-161, 2000.

62. KREILGAARD, M. Influence of microemulsions on cutaneous drug delivery. **Adv Drug Deliv Rev**, v. 54(1), p. S77–S98, 2002.

63. KROON, P. *et al*. How should we assess the effects of exposure to dietary polyphenols in vitro? **The American Journal of Clinical Nutrition**, v. 80, n. 1, p. 15-21, 2004.

64. KUO, I.; CHEN, J.; CHANG, T. K. Effect of Ginkgo biloba extract on rat hepatic microsomal CYP1A activity: role of ginkgolides, bilobalide, and flavonols. **Canadian Journal of Physiology and Pharmacology**, v. 82, n. 1, p. 57-64, jan., 2004.

65. LAMSON, D. W.; BRIGNALL, M. S. Antioxidants and Cancer III: Quercetin. **Alternative Medicine Review**, v. 5, n. 3, p. 196-208, jun., 2000.

66. LEE, E-S. *et al*. The flavonoid quercetin inhibits dimetylnitrosamine-induced liver damage in rats. **Journal of Pharmacy and Pharmacology**, v. 55, n. 8, p. 1169-1174, ago., 2003.

67. LI, H. *et al*. Enhancement of gastrointestinal absorption of quercetin by solid lipid nanoparticles. **Journal of Controlled Release**, v. 133, n. 3, p. 238–244, fev., 2009.

68. LI, H. *et al*. Studies on the preparation of quercetin solid lipid nanoparticles and oral absorption in mice. **Nanoscience**, v. 11, n. 4, p. 306-310, dez., 2006

69. LIM S.J., KIM, C. Formulation parameters determining the physicochemical characteristics of solid lipid nanoparticles loaded with all-trans retinoic acid. **International Journal of Pharmaceutics**, v. 243, p.135-46, 2002.

70. MACGREGOR, J. T.; JURD, L. Mutagenicity of plant flavonoids: structural requirements for mutagenic activity in Salmonella typhimurium. **Mutation Research**, v. 54, n. 3, p. 297-309, dez., 1978.

71. MÄDER, K.; MEHNERT, W. Solid Lipid Nanoparticles - Concepts, procedures and Physicochemical Aspects. In: NASTRUZZI, C. **Lipospheres in Drug Targets and Delivery: Approaches, Methods and Applications**. Boca Raton: CRC PRESS, 2005. p.1-22.

72. MANJUNATH, K., REDDY, J. S., VENKATESWARLU, V. Solid lipid nanoparticles as drug delivery systems. **Methods and Findings in Experimental and Clinical Pharmacology**, v. 27, n. 2, p. 127-144, mar., 2005.

73. MATTER, W. F.; BROWN, R. F.; VLAHOS, C. J. The inhibition of phosphatidylinositol 3-kinase by quercetin and analogs. **Biochemical and Biophysical Research Communication**, v. 186, n. 2, p. 624-631, jul., 1992.

74. MEHNERT, W.; MÄDER, K. Solid lipid nanoparticles: Production, characterization and applications. **Advanced Drug Delivery Reviews**, v. 47, n. 2-3, p. 165-196, abr., 2001.

75. MERTENS-TALCOTT, S. U.,PERCIVAL, S. S. Ellagic acid and quercetin interact synergistically with resveratrol in the induction of apoptosis and cause transient cell cycle arrest in human leukemia cells. **Cancer Letters***,* vol. 218, n. 2, p. 141-151, 2005.

76. METODIEWA, D. *et al*. Quercetin may act as a cytotoxic prooxidant after its metabolic activation to semiquinone and

quinoidal product. **Free Radical Biological & Medicine**, v. 26, n. 1-2, p. 107-116, jan., 1999.

77. MIDDLETON, E. Jr.; KANDASWAMI, C.; THEOHARIDES, T. C. The effects of plant flavonoids on mammalian cells: implications for inflammation, heart disease, and cancer. **Pharmacological Reviews**, v. 52, n. 4, p. 673-751, dez. 2000.

78. MIN, Y.-D.; CHOI, C.-H.; BARK, H.; SON, H.-Y.; PARK, H.-H.; LEE, S.; PARK, J.-W.; PARK, E.-K.; SHIN, H.-I.; KIM, S.-H. Quercetin inhibits expression of inflammatory cytokines through attenuation of NF-κB and p38 MAPK in HMC-1 human mast cell line, **Inflammation Research**, v. 56, p. 210-215, 2007.

79. MOMIC, T. *et al*.. Protolytic equilibria and photodegradation of quercetin in aqueous solution. **Collection of Czechoslovak Chemical Communications**, v. 72, n. 11, p. 1447-1460, nov., 2007.

80. MOON, Y. J. *et al*. Quercetin pharmacokinetics in humans. **Biopharmaceutics & Drug Disposition**, v. 29, n. 4, p. 205-217, maio, 2008.

81. MULHOLLAND, P. J. *et al*. Pre-clinical and clinical study of QC12, a water-soluble, pro-drug of quercetina. **Annals of Oncology**, v. 12, n. 2, p. 245-248, fev., 2001.

82. National Toxicology Program. NTP Technical Report (No. 409) on the Toxicology and Carcinogenesis Studies of Quercetin in F344/N Rats. NIH Publication Nº 91-3140, N. P. N., Ed., **U.S. Department of Health and Human Services**, Public Health Service, National Toxicology Program, Research Triangle Park, N.C U.S.A, 1991.

83. NAZAR, M.F; KHAN, A.M.; SHAH, S.S. Microemulsion System with Improved Loading of Piroxicam: A Study of Microstructure. **AAPS PharmSciTech**, v. 10(4), p. 1286-1294, 2009.

84. NEMETH, K. *et al*. Deglycosylation by small intestinal epithelial cell beta-glucosidases is a critical step in the absorption and metabolism of dietary flavonoid glycosides in humans. **European Journal of Nutrition**, v. 42, n. 1, p. 29-42, jan., 2003.

85. OKAMOTO, T. Safety of quercetin for clinical application. **International Journal of Molecular Medicine**, v. 16, n. 2, p. 275-278, ago., 2005

86. O'LEARY, K. A. *et al*. Metabolism of quercetin-7- and quercetin-3-glucuronides by an in vitro hepatic model: the role of human beta-glucuronidase, sulfotransferase, catechol-O-methyltransferase and multi-resistant protein 2 (MRP2) in flavonoid metabolism. **Biochemical Pharmacology**, v. 65, n. 3, p. 479-491, fev., 2003.

87. OLIVEIRA, E. J.; WATSON, D. G.; GRANT, M. H. Metabolism of quercetin and kaempferol by rat hepatocytes and the identification of flavonoid glycosides in human plasma. **Xenobiotica; the fact of foreign compounds in biological systems**, v. 32, n. 4, p. 279-287, abr., 2002.

88. ONG, C. S.; TRAN, R.; NGUYEN, T. T.; ONG, C. K.; LEE, S. K.; LEE, J. J.; NG, C. P.; LEONG, C.; HUYNH, H. Quercetin-induced growth inhibition and cell death in nasopharyngeal carcinoma cells are associated with increase in Bad and hypophosphorylated retinoblastoma expressions. **Oncology Reports**, v. 11, p. 727-733, 2004.

89. PISKULA, M. K.; TERAO, J. Accumulation of (-)-epicatechin metabolites in rat plasma after oral administration and distribution of conjugation enzymes in rat tissues. **The Journal of Nutrition**, v. 128, n. 7, p. 1172-1178, jul., 1998..

90. PORTER, C.J., TREVASKIS, N.L., CHARMAN, W.N. Lipids and lipid-based formulations: optimizing the oral delivery of lipophilic drugs. **Nat Rev. Drug Discovery,** v.6, p. 231–248, 2007.

91. PORTER, C.J.H., POUTON, C.W., CUINE, J.F., CHARMAN, W.N. Enhancing intestinal drug solubilisation using lipid-based delivery systems. **Advanced Drug Delivery. Reviews,** v. 60, p. 673–691, 2008.

92. PRALHAD, T.; RAJENDRAKUMAR, K. Study of freeze-dried quercetin–cyclodextrin binary systems by DSC, FT-IR, X-ray diffraction and SEM analysis. **Journal of Pharmaceutical and Biomedical Analysis,** v. 34, p. 333–339, 2004.

93. PRIPREM, A. Anxiety and cognitive effects of quercetin liposomes in rats. **Nanomedicine: Nanotechnology, Biology, and Medicine**, v. 4, n. 1, p. 70–78, mar., 2008.
94. PURI *et al.* Lipid-Based Nanoparticles as Pharmaceutical Drug Carriers: From Concepts to Clinic. **Crit Rev Ther Drug Carrier Syst**., v.26, n. 6, p. 523–580, 2009.
95. RICE-EVANS, C. A.; MILLER, N. J.; PAGANGA, G. Structure-antioxidant activity relationships of flavonoids and phenolic acids. **Free Radical Biology & Medicine**, v. 20, n. 7, p. 933-956, 1996.
96. ROGER E; LAGARCE, F.; BENOIT, J.-P. The gastrointestinal stability of lipid nanocapsules. **International Journal of Pharmaceutics**, v. 379, p. 260–265, 2009.
97. ROGERIO, A. P. *et al*. Anti-inflammatory activity of quercetin and isoquercetrin in experimental murine allergic asthma. **Inflammation Research**, v.56, n. 10, p. 402–408, out., 2007.
98. SAHU, A., BORA, U., KASOJU, N., GOSWAMI, P. Synthesis of novel biodegradable and self-assembling methoxy poly(ethylene glycol)-palmitate nanocarrier for curcumin delivery to cancer cells. **Acta Biomater.**, v.4, p. 1752–1761, 2008.
99. SAUPE, A.; RADES, T. Solid lipid nanoparticles. In: MOZAFARI, M. R.. **Nanocarrier technologies: Frontiers of Nanotherapy**, Holanda: Springer, 2006. p. 41-50.
100. SCHAFER-KORTING, M.; MEHNERT, W. Delivery of lipophilic compounds with lipid nanoparticles: Applications in dermatics and for transdermal therapy. In: NASTRUZZI, C. **Lipospheres in Drug Targets and Delivery: Approaches, Methods and Applications**. Boca Raton: CRC PRESS, 2005. p.127-142.
101. SCHIMMER, O.; HÄFELE, F.; KRÜGER, A. The mutagenic potencies of plant extracts containing quercetin in *Salmonella typhimurium* TA98 and TA100. **Mutation Research**,v. 206, n. 2, p. 201-208, out., 1988.
102. SCHNEIDER, H.; BLAUT, M. Anaerobic degradation of flavonoids by *Eubacterium ramulus*. **Archives of Microbiology**, v. 173, p. 71-75, 2000.
103. SCHNEIDER, H.; SCHWIERTZ, A.; COLLINS, M. D.; BLAUT, M. Anaerobic transformation of quercetin-3-glucoside by bacteria

from human intestinal tract. **Archives of Microbiology**, v. 171, p. 81-91, 1999.

104. SCHUBERT M.A., HARMS, M.; MÜLLER-GOYMANN, C. Structural investigations on lipid nanoparticles containing high amounts of lecithin. **European Journal of Pharmaceutical Sciences**, v. 27, p.226-36, 2006.
105. SESINK, A. L. *et al*. Breast cancer resistance protein (Bcrp1/Abcg2) limits net intestinal uptake of quercetin in rats by facilitating apical efflux of glucuronides. **Molecular Pharmacology**, v. 67, n. 6, p. 1999-2006, jun., 2005.
106. SHOSKES, D. A. Effect of bioflavonoids quercetin and curcumin on ischemic renal injury: a new class of renoprotective agents. **Transplantation**, v. 66, n. 2, p. 147-152, jul., 1998.
107. SIEKMANN, B.; WESTESEN, K. Investigation on solid lipid nanoparticles prepared by precipitation in o/w emulsions. **European Journal of Pharmaceutics and Biopharmaceutics**, v. 43, p. 104-109, 1996.
108. SILVA, I. D. *et al*. Chemical features of flavonols affecting their genotoxicity. Potential implications in their use as therapeutical agents. **Chemico-Biological Interactions**, v. 124, n. 1, p. 29-51, jan., 2000.
109. SONG, X. *et al*. Dual agents loaded PLGA nanoparticles: systematic study of particle size and drug entrapment efficiency. **European Journal of Pharmaceutics and Biopharmaceutics**, v. 69, n. 2, p. 445-453, jun., 2008.
110. SOOBRATTEE, M. A. *et al*. Phenolics as potential antioxidant therapeutic agents: mechanism and actions. **Mutation Research**, v. 579, n. 1-2, p. 200-213, nov., 2005.
111. SOUTO, E. B.; MÜLLER, R. H.. Lipid Nanoparticles (Solid Lipid Nanoparticles and Nanostructured Lipid Carriers) for Cosmetic, Dermal, and Transdermal Applications. In: THASSU, D.; DELEERS, M.; PATHAK, Y. **Nanoparticulate drug delivery systems**, Nova York: Informa Healthcare, 2007. v. 166, p. 213-234.

112. STAVRIC, B. Quercetin in our diet: From potent mutagen to probable anticarcinogen. **Clinical Biochemistry**, v. 27, n. 4, p. 245-248, ago., 1994.

113. TALALAY, P. *et al*. Chemoprotection against cancer by phase 2 enzyme induction. **Toxicology Letters**, v. 82-83, p. 173-179, dez., 1995.

114. TAN, W. *et al.* Quercetin, a dietary-derived flavonoid, possesses antiangiogenic potencial. **European Journal of Pharmacology**, v. 459(2), p.255-62, 2003.

115. TONG-UN, T; MUCHIMAPURA, S; PHACHONPAI, W.; WATTANATHORN, J. Nasal Administration of quercetin liposomes modulate cognitive impairment and inhibit acetylcholinesterase activity in hippocampus. **American Journal of Neuroscience**, v.1, n. 1, p. 21-27, 2010.

116. TROTTA, M.; DEBERNARDI, F.; CAPUTO, O. Preparation of solid lipid nanoparticles by a solvent emulsification-diffusion technique. **Int J Pharm**, v. 257, p. 153–160, 2003.

117. VAN ACKER, S. A. *et al*. A quantum chemical explanation of the antioxidant activity of flavonoids. **Chemical Research in Toxicology**, v. 9, n. 8, p. 1305-1312, dez., 1996.

118. VESSAL, M., HEMMATI, M., VASEI, M. Antibiabetic effects of quercetin in streptozocin induced diabetic rats. **Comparative Biochemistry and Physiology part C**, v.135, p.357-64, 2003.

119. VRIJSEN, R.; MICHOTTE, Y.; BOEYE, A. Metabolic activation of quercetin mutagenicity. **Mutation Research**, v. 232, n. 2, p. 243-248, out., 1990.

120. WALGREN, R. A. *et al*. Cellular uptake of dietary flavonoid quercetin 4'-beta-glucoside by sodium-dependent glucose transporter SGLT1. **The Journal of Pharmacology and Experimental Therapeutics**, v. 294, n. 3, p. 837-843, set., 2000.

121. WALGREN, R. A. *et al*. Efflux of dietary flavonoid quercetin 4'-beta-glucoside across human intestinal Caco-2 cell monolayers by apical multidrug resistance-associated protein-2. **The Journal of Pharmacology and Experimental Therapeutics**, v. 294, n. 3, p. 830-836, set., 2000b.

122. WALLE, T. *et al*. Flavonoid glucosides are hydrolyzed and thus activated in the oral cavity in humans. **The Journal Nutrition**, v. 135, n. 1, p. 48-52, jan., 2005.
123. WALSKY, R. L.; GAMAN, E. A.; OBACH, R. S. Examination of 209 drugs for inhibition of cytochrome P450 2C8. **Journal of Clinical Pharmacology**, v. 45, n. 1, p. 68-78, jan., 2005.
124. WANG, J. X.; SUN, X.; ZHANG, Z. R. Enhanced brain targeting by synthesis of 3', 5'–dioctanoyl-5-fluoro-2'-deoxyuridine and incorporation into solid lipid nanoparticles. **European Journal of Pharmaceutics and Biopharmaceutics**, v. 54, n, 3, p. 285-290, nov., 2002.
125. WANG, L.; TABOR, R.; EASTOE, J.; LI, X.; HEENANC, R.K.; DONG, J. Formation and stability of nanoemulsions with mixed ionic–nonionic surfactants. **Phys. Chem. Chem. Phys**., v. 11, p. 9772–9778, 2009.
126. WENZEL E.; SOMOZA V. Metabolism and bioavailability of trans-resveratrol. **Molecular Nutrition & Food Research**, v. 49, n. 5, p. 472- 481, maio, 2005.
127. WISSING, S. A., KAYSER, O., MÜLLER, R. H. Solid lipid nanoparticles for parenteral drug delivery. **Advanced Drug Delivery Reviews**, v. 56, n. 9, p. 1257-1272, maio, 2004.
128. WOLFFRAM, S.; BLÖCK, M.; ADER, P. Quercetin-3-glucoside is transported by the glucose carrier SGLT1 across the brush border membrane of rat small intestine. **The Journal of Nutrition**, v. 132, n. 4, p. 630-635, abr., 2002.
129. WU, T. H. *et al*. Preparation, physicochemical characterization, and antioxidant effects of quercetin nanoparticles **International Journal of Pharmaceutics**, v. 346, n. 1-2, p. 160–168, jan., 2008.
130. YAMAMOTO, N. *et al*. Inhibitory effect of quercetin metabolites and their related derivatives on copper ion-induced lipid peroxidation in human low-density lipoprotein. **Archives of Biochemistry and Biophysics**, v. 372, n. 2, p. 347-354, dez., 1999.
131. YANG L, COHN L, ZHANG DH, HOMER R, RAY A, RAY P. Essential role of nuclear factor kappaB in the induction of eosinophilia in allergic airway inflammation. **J Exp Med.,** n.188, p.1739–1750, 1998.

132. YANG, J. H.; HSIA, T. C.; KUO, H. M.; CHAO, P. D.; CHOU, C. C.; WEI, Y. H.; CHUNG, J. G. Inhibition of lung cancer cell growth by quercetin glucuronides via G2/M arrest and induction of apoptosis. **Drug Metabolism and Disposition**, v. 34, p. 296-304, 2006.
133. YOSHIZUMI, M.; TSUCHIYA, K.; KIRIMA, K.; KYAW, M.; SUZAKI, Y.; TAMAKI, T. Quercetin inhibits Shc- and phosphatidylinositol 3-kinase-mediated c-Jun N-terminal kinase activation by angiotensin II in cultured rat aortic smooth muscle cells. **Molecular Pharmacology**, v. 60, p. 656-665, 2001.
134. YUAN, Z. P. *et al*. Liposomal Quercetin efficiently suppresses growth of solid tumors in murine models. **Clinical Cancer Research**, v. 12, n. 10, p. 3193-3199, maio, 2006.
135. ZHANG, Y. *et al*. A major inducer of anticarcinogenic protective enzymes from broccoli: isolation and elucidation of structure. **Proceedings of The National Academy of Sciences of The United States of America**, v. 89, n. 6, p. 2399-2403, mar., 1992.
136. ZUANAZZI, J., MONTANHA, J. Flavonóides. In: SIMÕES, C., et al. (Org.) **Farmacognosia: da planta ao medicamento**. 5. Ed.. Porto Alegre/Florianópolis: Editora Universidade da UFRGS/Editora da UFSC, 2003. Cap. 23, p.577-614.

Anexos

ANEXO 1. VALIDAÇÃO DAS TÉCNICAS DE CLAE E ESPECTROSCOPIA UV/VIS

TABLE 1. Summary of the results obtained after linear regression analysis of the calibration curve data.

	UV spectrophotometry	HPLC
Concentration range (µg mL^{-1})	1 - 20	0.25 -10
Equation of the straight line	y = 0.066x+0.0036	y = 95880.15x–5543.04
r^2	0.9990	0.9996
F_{cal}	7759.67	51307.5
LOD (µg mL^{-1})	0.459	0.036
LOQ (µg mL^{-1})	1.393	0.109

UV method: $F_{cal} > F_{crit} = 6.46$; $P = 0.05$. HPLC method: $F_{cal} > F_{crit} = 3.18$; $P = 0.05$.

TABLE 2. Recovery of quercetin standard solution added to lipid nanocarrier colloidal suspensions.

Sample	Theoretical QU concentration (μg mL^{-1})	Experimental QU concentration (μg mL^{-1})		Quercetin Recovery (%)		RSD[a] (%)	
		UV/VIS	HPLC	UV/VIS	HPLC	UV/VIS	HPLC
Solutol HS15							
QU-SLN	2.8	2.81	2.82	100.3	100.8	2.04	0.71
	4.0	4.01	3.96	100.3	99.2	1.58	0.78
	5.2	5.20	5.19	99.8	99.8	1.07	0.54
QU-ME	2.8	2.79	2.87	99.7	102.7	2.47	0.78
	4.0	4.02	3.94	100.4	98.6	1.03	0.75
	5.2	5.16	5.21	98.9	100.3	1.45	0.83
Lutrol F68							
QU-SLN	2.8	2.78	2.85	99.5	101.9	2.81	0.54
	4.0	4.00	3.94	100.1	98.6	0.82	0.16
	5.2	5.17	5.15	99.2	99.0	1.24	0.26
QU-NE	2.8	2.78	2.84	99.1	101.4	1.51	1.41
	4.0	4.03	3.92	100.7	98.1	0.98	1.04
	5.2	5.19	5.14	99.6	98.8	1.57	0.61

[a] RSD = Relative standard deviation. QU-SLN refers to quercetin-loaded lipid nanoparticles, QU-ME refers to quercetin-loaded microemulsiom, and QU-NE refers to quercetin-loaded nanoemulsions.

TABLE 3. Results obtained in the precision evaluation of the UV and HPLC methods.

Sample	Day no.	Quercetin Recovered (%)		RSD[a] (%)	
		UV/VIS	**HPLC**	**UV/VIS**	**HPLC**
Solutol HS15	Inter-day				
QU-SLN	Day 1 (n=3)	100.1	98.4	0.99	0.78
	Day 2 (n=3)	99.3	99.7	1.23	0.67
	Day 3 (n=3)	101.8	99.6	4.13	1.26
	Intra-day (n=6)	99.7	98.6	1.45	1.44
QU-ME	Inter-day				
	Day 1 (n=3)	99.3	97.8	1.95	0.75
	Day 2 (n=3)	99.2	97.9	1.34	0.15
	Day 3 (n=3)	99.7	97.5	2.17	1.6
	Intra-day (n=6)	99.5	97.7	2.36	0.29
Lutrol F68	Inter-day				
QU-SLN	Day 1 (n=3)	101.2	99.7	2.05	0.73
	Day 2 (n=3)	97.4	98.0	1.62	0.47
	Day 3 (n=3)	97.1	97.8	4.06	0.16
	Intra-day (n=6)	97.2	98.6	4.10	1.2
QU-NE	Inter-day				
	Day 1 (n=3)	99.7	98.0	2.17	0.62
	Day 2 (n=3)	102.1	98.0	1.65	0.39
	Day 3 (n=3)	99.3	97.3	1.95	1.03
	Intra-day (n=6)	102.4	98.0	4.48	0.39

[a] RSD = Relative standard deviation. QU-SLN refers to quercetin-loaded lipid nanoparticles, QU-ME refers to quercetin-loaded microemulsiom, and QU-NE refers to quercetin-loaded nanoemulsions.

TABLE 4. Results obtained from the study of robustness of the HPLC method.

Variable	Value	Quercetin content[a] (µg/mL)	RSD[a] (%)
Column temperature (ºC)	35	4.04	0.65
	40	4.00	1.16
	45	4.04	0.39
Mobile phase composition (1% phosphoric acid : methanol)	45:55	4.00	1.16
	50:50	4.02	0.80
	60:40	4.07	0.38
pH of the mobile phase	2.0	4.07	0.51
	2.3	4.00	1.16
	2.7	4.06	0.50

[a] Mean of three replicates

ANEXO 2.

Anti-inflammatory effect of quercetin-loaded microemulsion in the airways allergic inflammatory model in mice

Supplementary Data:

Fig. S1

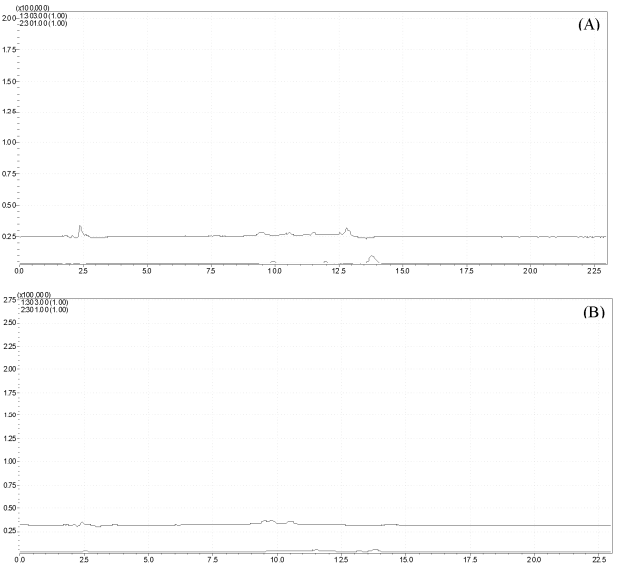

Figure S1 Legend: HPLC-MS chromatograms (TIC x Tr): (A) vehicle; (B) QU-SP (10 mg/kg). Mobile phase consisted of a gradient solvent system of aqueous formic acid 0.2% (A) and acetonitrile (B). The elution profile was, 0 to 4 min: 9 to 20% B (linear); 4 to 9 min: 20 to 100% B (linear); 9 to 14 min: 100 to 20 % B min (linear); 14 to 18: 20 to 9 % B (linear); 18 to 23: 9 % B (isocratic). The flow rate was 200 µl/min. ESI source operated in SIM mode (negative ionization: *m/z* 301, positive ionization: *m/z* 303).